Bianca Kerschbaumer BSc

EVALUATION OF CYP505 VARIANTS FOR THE PREPARATION OF DRUG METABOLITES: BRIDGING FROM ANALYTICAL TO PREPARATIVE SCALE

MASTER`S THESIS

to achieve the university degree of

Diplom-Ingenieurin

Master`s thesis programme: Biotechnology

submitted to

Graz University of Technology

Supervisor

Univ.-Prof. Dr.rer.nat. Robert Kourist

Institute of Molecular Biotechnology

Co-Supervisor: Dipl.-Ing. Dr.techn. Margit Winkler

Institute of Molecular Biotechnology/Acib GmbH

Graz, July 2018

AFFIDAVIT

I declare that I have authored this thesis independently, that I have not used other than the declared sources/resources, and that I have explicitly indicated all materials which has been quoted either literally or by content from the sources used. The next document uploaded to TUGRAZonline is identical to the present master's thesis.

Date	Signature

ACKNOWLEDGMENTS

I would like to express my sincere gratitude towards all persons who supported me in creating this thesis.

A special thank goes to the Austrian Center of Industrial Biotechnology (ACIB GmbH) for the opportunity to write my thesis there and to my supervisor Dipl.-Ing. Dr. techn. Margit Winkler (ACIB GmbH) who arranged the basic framework for this thesis and supported me in all phases of my work. Thank you for your guidance and patience and the opportunity to integrate my own ideas. Additionally, I want to thank Univ.-Prof. Dr.rer.nat. Robert Kourist, head of the Institute of Molecular Biotechnology (Graz, University of Technology) for undertaking the function as my official supervisor. Further on, I want to thank and Ao. Univ.-Prof. Mag. rer. nat. Dr. rer. nat. Anton Glieder (bisy e.U.) for valuable conceptions concerning this thesis. Finally, I want to thank Thorsten Bachler, BSc and Dipl.-Ing. Melissa Horvat for all their patience and willingness to help as well as all colleagues who have welcomed me with warmth and hospitality in their team.

This work received funding from the EU project ROBOX (grant agreement n° 635734) under EU's H2020 Programme Research and Innovation actions H2020-LEIT BIO-2014-1 and from the Austrian BMWFJ, BMVIT, SFG, Standortagentur Tirol and ZIT through the Austrian FFG-COMET- Funding Program. Disclaimer: This publication reflects the author's view and the Agency is not responsible for any use that may be made of the information it contains.

ROBOX

This project is funded by the European Union (grant agreement 635734) under EU's Horizon 2020 Programme Research and Innovation actions H2020-LEIT BIO-2014-1

acib

ABSTRACT

A naturally high regio- and stereoselectivity and the ability to insert a single oxygen atom into complex structures make cytochrome P450 enzymes valuable biocatalysts. In recent years, improvements by protein engineering and process development gave CYPs more relevance in industrial applications and drug development - especially in respect to the production of drug metabolites.

In this work, wild-type and variants of fungal bifunctional CYP505X from *Aspergillus fumigatus* as well as CYP505A30 from *Myceliophthora thermophila* were investigated. The performance of the enzymes was evaluated in form of whole cell biocatalysts using two different microbial host systems*: Escherichia coli* and *Komagataella phaffii (Pichia pastoris)*. The formulation of the biocatalysts was studied in view of activity, stability and robustness. Optimization of the working protocol was done regarding cultivation and lyophilization of the biocatalyst preparation as well as biotransformation parameters. After optimization, activity towards 22 active pharmaceutical ingredients (APIs) was tested.

Finally, four whole-cell bioconversions were selected to implement biooxidations on preparative scale. A CYP505X variant with five mutations expressed in *P. pastoris* was used to convert ibuprofen and chlorzoxazone. In a total reaction volume of 500 ml, 69% conversion of chlorzoxazone to 6-hydroxychlorzoxazone was reached after 7 hours. 147 mg of metabolite were recovered by using silica gel chromatography, corresponding to 48% isolated yield. Structural characterization was done by NMR. Ibuprofen was oxidized to 3 metabolites reaching a total conversion of 81% after 22 hours. The metabolites were isolated by RP18 HPLC fractionation and characterized by NMR. By now, two of the three metabolites were unambiguously identified as 1-hydroxyibuprofen and 2-hydroxyibuprofen. CYP505A30 wild-type and a triple mutant in *E. coli* were used to oxidize ibuprofen. According to the chromatograms and HPLC/MS data, the metabolites resemble the chemical structures of CYP505X metabolites, however, experimental proof by NMR needs still to be furnished.

KURZFASSUNG

Die natürliche Regio- und Stereoselektivität von Cytochrome P450 Enzymen sowie die Eigenschaft, ein einzelnes Sauerstoffatom in komplexe Strukturen einfügen zu können, macht diese Enzyme zu wertvollen Biokatalysatoren. Vor allem durch Verbesserungen im Bereich Protein Engineering und Prozessentwicklung, wurde CYPs in den letzten Jahren mehr Aufmerksamkeit in industriellen Anwendungen und der Entwicklung von Medikamenten zuteil – ganz besonders hinsichtlich der Herstellung von Wirkstoffmetaboliten.

In dieser Arbeit wurden sowohl der Wildtyp und Varianten von pilzlichem, bifunktionalen CYP505X aus *Aspergillus fumigatus* als auch CYP505A30 aus *Myceliophthora thermophila* untersucht. Die Leistung der Enzyme wurde in Form von Ganzzellbiokatalyse unter der Verwendung von zwei Wirtssystemen untersucht: *Escherichia coli* and *Komagataella phaffii* (*Pichia pastoris*). Die Erscheinungsform der Biokatalysatoren wurde hinsichtlich Aktivität, Stabilität und Robustheit untersucht. Das Arbeitsprotokolls wurde hinsichtlich Kultivierung, Lyophilisierung der Biokatalysatoren sowie deren Herstellung und Biotransformationsparameter, optimiert. Danach wurde die Aktivität gegenüber 22 aktiven pharmazeutischen Inhaltsstoffen (APIs) getestet.

Zum Schluss wurden vier Ganzzellen-Biooxidations-Ansätze ausgewählt, um Experimente im präparativen Maßstab durchzuführen. Eine fünffach mutierte CYP505X Variante in *P. pastoris* wurde als Biokatalysator für Chlorzoxazon und Ibuprofen gewählt. Im Gesamtreaktionsvolumen von 500 ml wurden nach 7 h 69% Umsetzung von Chlorzoxazon zu 6-Hydroxychlorzoxazon erreicht. 147 mg des Metabolits wurden durch Silicagel-Chromatographie gewonnen. Dies entspricht 48% isolierte Ausbeute. Die chemische Struktur des Metaboliten wurde mittels NMR verifiziert. Ibuprofen wurde nach einer Reaktionszeit von 22 h zu 81% umgesetzt und insgesamt zu 3 Metaboliten oxidiert. Die Metabolite wurden mittels PR18 HPLC Fraktionierung isoliert und mit mittels NMR charakterisiert. Bis jetzt konnten zwei der 3 Metabolite eindeutig als 1-hydroxyibuprofen und 2-hydroxyibuprofen identifiziert werden. Die Wildtypvariante sowie eine 3-fach Mutante von CYP505A30 in *E. coli* wurden ebenfalls verwendet, um Ibuprofen zu oxidieren. Anhand der Chromatogramme und HPLC/MS Analyse dürften die Metabolite die gleichen Strukturen aufweisen, wie jene, die von CYP505X produziert wurden. Dies muss noch experimentell durch NMR Analyse nachgewiesen werden.

TABLE OF CONTENTS

Affidavit I

Acknowledgments II

Abstract III

Kurzfassung IV

Table of Contents V

1 Objectives 1

2 Introduction 3

2.1 Cytochrome P450 enzymes - Discovery 5

2.2 Cytochrome P450 enzymes – Nomenclature and structure 5

2.2.1 Nomenclature 5

2.2.2 Structure 6

2.3 Cytochrome P450 enzymes – Reaction mechanism and classification 8

2.3.1 Reaction mechanism – Catalytic cycle 8

2.3.2 Classification 9

2.3.3 Class VIII 9

2.4 Expression hosts 12

2.4.1 *Escherichia coli* 12

2.4.2 *Komagataella phaffii* (*Pichia pastoris*) 13

2.5 Whole-cell biocatalysis 14

2.6 Aims in regards of previous results 15

3 Materials and Methods 18

3.1 Substrates 18

3.2 Class VIII CYP prodrucing strains 22

3.3 RUG - purified enzymes 22

3.4 Parameter optimization 23

3.4.1 Section CYP505X 23

3.4.2 Section CYP505A30 – Whole cells 25
3.4.3 Chemical cell disruption with BugBuster® Kit 26
3.4.4 Determination of total protein concentration via BCA protein assay ... 27
3.4.5 Determination of P450 expression levels 27
3.4.6 Analysis by HPLC/MS 28
3.4.7 Analysis by GC/MS 28
3.4.8 Analysis by GC/FID 29
3.4.9 Determination of oxidative activity via GC/MS analysis 30
3.4.10 Calculations of kinetic parameters 31
3.4.11 Preparative scale reactions 31
4 Results and Discussion 35
4.1 Direct comparison of CYP505x in *E. coli* and *P. pastoris* 35
4.1.1 cell wet-weight vs. cell dry-weight 35
4.1.2 conversion of chlorzoxazone (CX): 1 *E. coli* cell vs. 1 *P. pastoris* cell .. 36
4.2 Expression levels of CYP variants in *E. coli* 37
4.3 Influence of washing and co-factor recycling 40
4.4 Impact of $NADP^+$ 42
4.5 Determination of apparent initial rate activity of CYP505X in *P. pastoris* ... 44
4.6 Influence of reaction buffer and GDH feeding – *P. pastoris* 46
4.7 Optimal OD_{600} for biooxidation with *P. pastoris* cells 47
4.8 Optimal chlorzoxazone concentration for CYP505X 50
4.9 Cell free exctract (CFE) for API oxidations 52
4.9.1 Buffer optimization and GDH feeding 52
4.9.2 Activity of CYP505X towards APIs: a comparison of CFE and whole cell biocatalyst 55
4.10 Activity of CYP505X towards fatty acids and aliphatic compounds 60
4.11 API oxidation by CYP505A30 63

4.11.1 Preliminary evaluation of CYP505A30: 63
activity of purified CYP and CYP in whole cells towards lauric acid, chlorzoxazone and ibuprofen 63
4.11.2 Activity of CYP505A30 towards APIs: 64
a comparison of whole cell biocatalyst and purified enzyme 64
4.12 Preperative scale API biooxidations 71
4.12.1 Ibuprofen biooxidation by CYP505X 5xmut (A21) in *P. pastoris* 72
4.12.2 Chlorzoxazone biooxidation BY CYP505X 5xmut (A21) in *P. pastoris* .. 74
4.12.3 Ibuprofen biooxidation by CYP505A30 WT in *E. coli*..... 75
4.12.4 Ibuprofen biooxidation by CYP505A30 5xmut in *E. coli* 77
5 Conclusion and Future Perspectives 78
6 References V
List of figures XII
List of tables XV
7 Appendix XVII
7.1 *E. coli* SOP XVII
7.2 *P. pastoris SOP* XXXII
7.3 HPLC-methods XLVI

1 OBJECTIVES

The major aim of this thesis was the optimization and characterization of CYP505X both in the prokaryotic host *Escherichia coli* and the eukaryotic host *Komagataella phaffii,* respectively. The formulation of the biocatalysts needed to be studied in view of activity, stability and robustness. The optimization included the investigation of cultivation and lyophilization parameters to obtain highly active biocatalyst preparations as well as the biotransformation parameters. Characterization included the monitoring of oxidative reactions on several drug molecules. After successful evaluation and comparison, the constituted biotransformation conditions were tested in terms of applicability for a further CYP505 variant: CYP505A30.

In case of eukaryotic strains, the results created the basis of a Standard Operation Procedure (SOP) for CYP producing whole-cell *Komagataella phaffii* biocatalysts.

The second goal was the implementation of the best oxidative biocatalysts for preparative scale reactions with following metabolite isolation and characterization to show the applicability of the developed biocatalysts for drug metabolite synthesis.

Figure 1 gives an overview of this thesis.

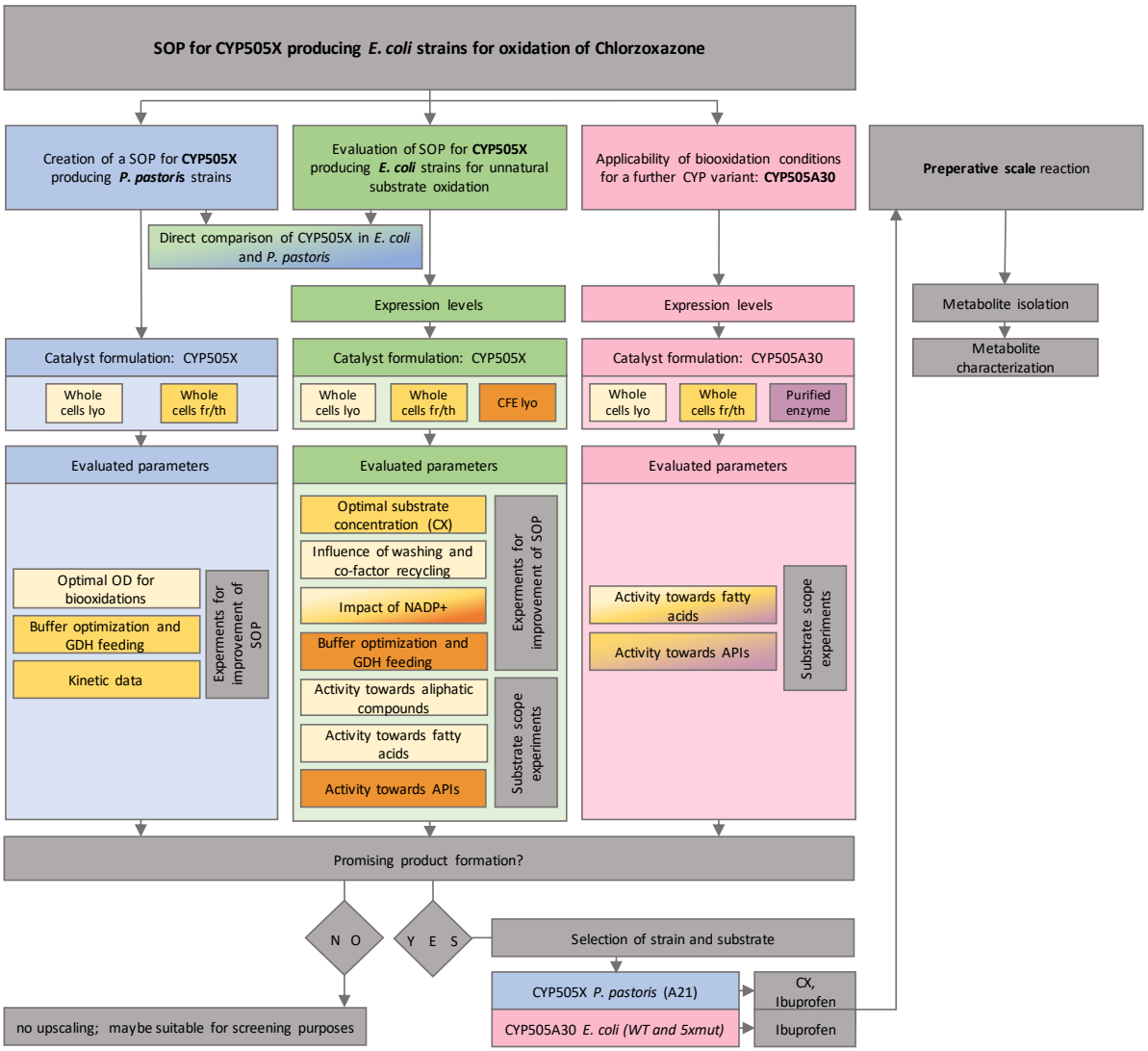

Figure 1: Overview of tasks performed. The SOP "Preparation and use of CYP505 expressed in *E. coli* for the oxidation of small molecules" created the basis for the following experiments. The green path includes experiments performed in order to optimize the current standard protocol for CYP505X expressed in *E. coli* and following substrate scope examinations (green path). Based on the protocol and results of the *E. coli* experiments, a SOP for CYP505X expressing *Komagataella phaffii (Pichia pastoris)* strains was created and further evaluated (blue path). The pink path shows experiments that aimed to test the applicability of the determined biooxidation conditions in the SOP on a different CYP variant: CYP505A30. After successful improvement the most promising conditions were identified and used for implementation of preparative scale reactions. Finally, the metabolites were isolated and characterized.

2 INTRODUCTION

In recent years, the use of cytochrome P450 enzymes (CYPs) in industrial applications gained more and more attention, as high regio- and stereoselectivities are required to produce drug metabolites [1, 2], fine chemicals, pharmaceuticals and food ingredients [2].

In drug development, not only the drug as such, but also the impact of its metabolites on the organism are of great importance to make sure that adverse drug reactions (ADRs) are avoided. For this kind of studies, a certain amount of pure metabolites is needed [3, 4].

To find a working point to produce such metabolites, the pathway of natural drug metabolism, chemical modifications as well as involved enzymes are essential. The metabolic breakdown mechanism of drugs can be divided into three phases. During phase I reactive or polar groups are introduced to the drug. Corresponding reactions are mainly oxidation, reduction or hydrolysis. Typical enzymes that carry out oxidations are cytochrome P450 monooxygenases, flavin containing monooxygenases, alcohol- and aldehyde dehydrogenases or monoamine oxidases. Esterases, amidases and epoxide hydrolases are commonly responsible for hydrolysis. In phase II, these modified structures are conjugated to polar compounds such as glutathione, sulfate, glycine or glucuronic acid. These reactions are typically carried out by different types of transferases. In phase III, additional modification may take place to finally facilitate the excretion of the substance [5].

Chemical synthesis of such metabolites is challenging. Drug molecules are often complex structures with multiple functional groups. Direct introduction of an oxygen atom into a complex organic structure is complicated and calls for protection/deprotection strategies [6]. Consequently, it requires a high amount of resources and is time consuming since multiple step reactions are often required to gain the desired product. Typically, these reactions are working under harsh conditions including very high or very low temperatures, extreme pH values and the use of hazardous substances. Summarizing, the chemical synthesis of drug metabolites as well as subsequent purification of the product implies high efforts and high costs [7]. This is, why the use of CYPs attracted attention particularly in the pharma industry.

CYPs are able to act as monooxygenases and therefore can introduce a single oxygen atom into non-activated C - H bonds while the second oxygen atom is reduced to water [8]. Moreover, they show a high regio- and stereoselectivity naturally, work under mild conditions and can be further engineered to improve capabilities for industrial applications [9–11].

Even if there is an enormous potential in the concept of using CYPs for industrial processes, there are still several disadvantages, which make further optimization necessary. Typical drawbacks that should be eradicated encompass low activities, limited stability and the need for one or more electron transfer partners. When working with whole-cell systems, further challenges like undesired side reactions may occur. Furthermore, poor substrate uptake as well as product or substrate toxicity may limit the desired reaction [8].

2.1 CYTOCHROME P450 ENZYMES - DISCOVERY

In the 1940s, A. Claude and colleagues discovered a novel subcellular fraction and called them microsomes [12]. This attracted many researchers in the field of biochemistry and in the following couple of years, some important enzymes were discovered, among them the "oxygenase" [13]. When M. Klingenberg studied the spectral properties of microsomes derived from rat liver in 1955, he found a new microsome-binding pigment that showed an absorption maximum at 450 nm when complexed with carbon monoxide in its reduced state. In 1958, Klingenberg published the results of his research of the "microsomal carbon monoxide-binding pigment" which included that the pigment was highly predisposed to solubilization steps and its characteristic absorption maximum at 450 nm [14]. R. Sato and T. Omura found out and proved the heme protein nature of the "microsomal carbon monoxide-binding pigment" and named it P-450 [15–18]. At the same time, H.S. Mason and colleagues Y. Hashimoto and T. Yamano detected an allegedly iron complex when studying electron paramagnetic resonance (EPR) spectra of the subcellular fractions from animal tissues and named it "*microsomal Fex*". They published their finding in 1962. Later they found out, that their findings concerning "microsomal Fex" were identical with findings concerning P-450 [19, 20].

2.2 CYTOCHROME P450 ENZYMES – NOMENCLATURE AND STRUCTURE

2.2.1 NOMENCLATURE

Cytochrome P450 enzymes, also known as P450s or CYPs, are a group of heme-proteins that show enzymatic activity and appear in all kingdoms of life.

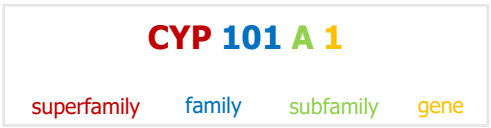

Figure 2: Illustration of CYP designation on the example of CYP101A1 from *Pseudomonas putida*

Figure 2 illustrates the system of P450 nomenclature using the example of CYP101A1. CYPs are named and classified by starting with the root symbol CYP which identifies the superfamily. A number, which indicates to which family they belong, a capital letter, to identify the subfamily and a second number, that refers to the individual gene, are

added (Figure 2). Enzymes that show at least 40% amino acid similarity are dedicated to the same family, whereas 55% similarity are required for the assignment to the same subfamily [21–23]. Even if this nomenclature process can be seen as universal rule, there are some exceptions, especially referring to CYPs from plant origin [22].

The first crystal structure of P450 identified was $P450_{cam}$, also known as CYP101A1 from *Pseudomonas putida* in 1987, followed by the structure of $P450_{BM-3}$, also known as CYP102A1 derived from *Bacillus megaterium* in 1993 [24]. Nowadays, more than 21000 different (putative) P450 sequences have been identified and since 1987, numerous P450 structures have been solved [8]. Currently, the Protein Data Bank (PDB) lists 914 entries that involve a P450 name. Thereof, 548 belong to the taxonomic group bacteria, 352 to eukaryota and 14 to archaea [25].

2.2.2 STRUCTURE

P450s generally show a size between 40 and 60 kDa [26] and by now it can be safely stated, that the general P450 structure is quite conserved, even if the exact position of several structural elements shows a great variability between the different CYP forms [27]. Strictly conserved amino acids are rare in P450 sequences but these few residues play key roles in preservation of structure and catalytic function of the protein. One of the key amino acids is a cysteine (Cys) residue with its thiolate group, which is needed near the heme for interaction with iron.

The conserved secondary structures of a P450 enzyme are found directly near the heme group. In principle, the greater the distance from the heme, the more structural variance is possible. Thus, structural elements that are distant from the heme, can differ enormously [26, 28]. As an example for the overall P450 architecture, Figure 3 shows the structure of $P450_{cam}$ with the most important and also most conserved structural elements highlighted. The most highly conserved elements can be found in a four-helix bundle (three parallel helices D, L, I and one antiprarallel helix E). Helix I and L contriubute to the covalent binding of the heme to an immutable cysteine in the kink of the I helix (cys-pocket) [29, 30].

An exceptional structural characteristic of CYPs is the ability to adapt to a broad spectrum of substrates without losing P450 characteristic properties such as the overall P450 fold, electron transfer and O_2 activation mechanism. So far, the reasons why

CYPs accept such a variety of substrates are not understood in its whole extent. Nonetheless, several features are well known. One feature is, that the substrate is located in a way, that the atom to be hydroxylated shows a distance of 4-5 Å to the heme iron. This is true for most of CYPs. As a consequence, specific protein-substrate interactions that ensure the correct orientation of the substrate facilitate regio- und stereoselective hydroxylation [28]. More information about the reaction mechanism is given in chapter 2.3.1.

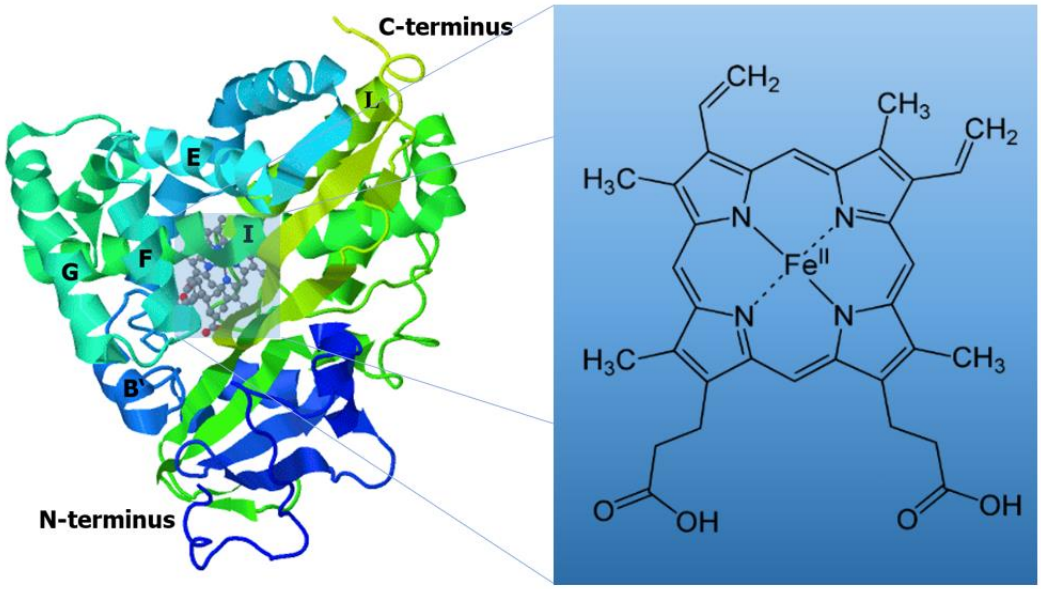

Figure 3: The structure of $P450_{cam}$ indicating the most important elements: Image of CYP structure taken and adjusted from [31] and named according to T.L. Poulos and E.F. Johnson – Structures of Cytochrome P450 Enzymes [28]. Additionally, the structure and arrangement of the heme iron is shown in the protein and separately (highlighted in blue).

Besides the overall conserved structure of P450s, those regions that control substrate acceptance can deviate from each other fundamentally. In particular, the B' helix (Figure 3) can adopt totally different angles in distinct CYPs. Different orientation of the B' helix leads to an alteration in the local environment and therefore to an altered substrate selectivity [28]. Further, the "F and G domain", which covers the active site,is involved in substrate acceptance. The domain is formed by the F helix, the F/G loop and the G helix [29, 30].

2.3 CYTOCHROME P450 ENZYMES – REACTION MECHANISM AND CLASSIFICATION

2.3.1 REACTION MECHANISM – CATALYTIC CYCLE

Cytochrome P450 enzymes mainly act as monooxygenases, a subclass of class 1 enzymes - oxidoreductases, by inserting a single oxygen atom in non-activated C-H bonds at ambient conditions while reducing the second oxygen to water (Equation 1). In general, hydroxylation is the preferred catalyzed reaction, but also other oxidations can occur on a broad spectrum of different substrates [8].

Equation 1: General reaction equation of a CYP catalyzed reaction

$$\mathbf{NAD(P)H + RH + O_2 + H^+ \rightarrow R\text{-}OH + NAD(P)^+ + H_2O}$$

It is generally accepted that the major steps in P450 catalyzed substrate hydroxylation are those shown in Figure 4.

The catalytic cycle of P450s starts with the binding of the substrate to the heme moiety. The ferric heme iron (Fe^{3+}) is transformed to its ferrous state (Fe^{2+}) due to the transfer of the first electron triggered by cytochrome P450 reductase (CPR). Now, molecular oxygen can be bound and the reduced ferrous dioxy complex (Fe^{2+}–O_2) is formed. The delivery of the second electron and of a proton leads to a hydroperoxyl complex (Fe^{3+}–OOH, compound 0). A further protonation and heterolytic cleavage of the O - O bond leads to the formation of a water molecule and a ferryl – oxo intermediate with a porphyrin with a p radical cation (Fe^{4}+=O, compound I). In the next step - the product formation step – the substrate is oxygenated by compound I. Triggered by the dissociation of

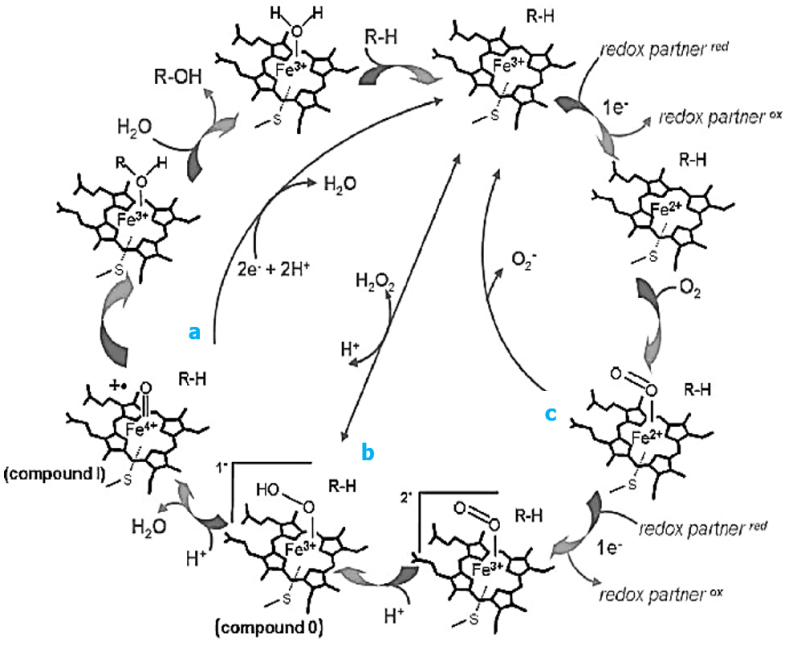

Figure 4: Schematic representation of the catalytic cycle of P450 enzymes. Taken from Munro *et al.* [30].

the hydroxylated product (R-OH), the final step comprises the re-binding of a water molecule to the restored initial ferric heme (Fe^{3+}).

Additionally, non-productive pathways leading to a collapse of the oxy intermediates in the cycle are also described. They are known as "oxidase shunt- "(Figure 4a), "peroxide shunt- "(Figure 4b), and "autoxidation shunt"- pathway" (Figure 4c), where the catalytic cycle is shortened. These reactions take place regularly under physiological conditions and are known as uncoupling reactions [32–35].

2.3.2 CLASSIFICATION

Due to the need of electron transfer partners, P450s are classified according to their electron transport system. Over a long period of time, only two classes were known [36]. However, as more and more CYPs have been characterized, 10 classes have been defined until today. In this work, CYPs belonging to class VIII were used exclusively and therefore, this class will be described in more detail. All 10 classes are extensively described in the review of F. Hannemann *et al.* [37].

2.3.3 CLASS VIII

Due to their structural setup, P450 belonging to class VIII have the exceptional ability to act in a catalytically self-sufficient manner. In contrast to other classes, they comprise an *N*-terminal heme domain (the actual P450) which is fused to a eukaryotic like *C*-terminal diflavin reductase partner (cytochrome P450 reductase, CPR) in a single polypeptide chain (Figure 5). The CPR domain contains the prosthetic groups flavin adenine dinucleotide (FAD) and flavin mononucleotide (FMN) and transfers electrons from NADPH to the heme [32, 37, 38, 38].

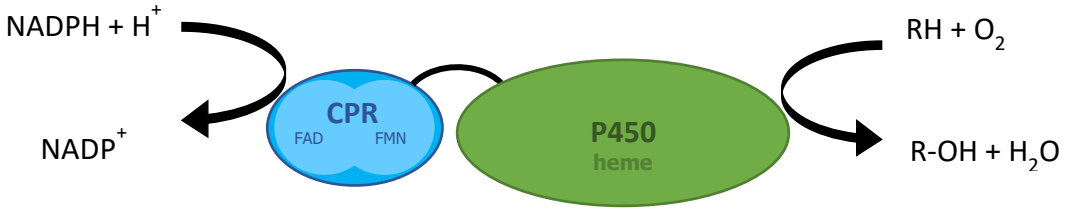

Figure 5: Schematic representation of P450 enzyme system - class VIII: (adapted from F. Hannemann *et al.* [29])

2.3.3.1 Cytochrome $P450_{BM-3}$ (CYP102A1)

$P450_{BM-3}$ (CYP102A1), which is the archetype of the class VIII cytochrome P450 enzyme family, is one of the best studied enzymes in the P450 category. It was firstly described

by Nahri and Fulco in 1986 [39, 40]. They studied a purified soluble CYP from *B. megaterium* and found that in contrast to all other known CYPs at that time, this enzyme was able to catalyze the entire oxygenation reaction of fatty acids by only adding a substrate, nicotinamide adenine dinucleotide phosphate (NADPH) and oxygen. Further, they observed that the enzyme was present as a large, single polypeptide [41].

Therefore, $P450_{BM-3}$ is considered as a self-sufficient monooxygenase showing a total molecular weight of about 117 kDa. Among other saturated fatty acids, pentadecanoic acid (C15:0) appeared to be the favorized substrate. With respect to saturated fatty acids, P450 activity depends on the chain length. $P450_{BM-3}$ shows highest activity towards C12 to C20 fatty acids [42]. Activity decreases for both, shorter and longer fatty acids [43]. Furthermore, other long- and mid-chain aliphatic compounds like fatty amides, alcohols and unsaturated fatty acids are accepted as substrates. Unsaturated compounds can also be epoxidized [44].

In contrast to many P450 enzymes that appear membrane-bound, $P450_{BM-3}$ is soluble. Therefore, recombinant expression is more efficient and handling is more convenient. Furthermore, it is highly active. These are reasons why it has been intensively studied and engineered for a broadened substrate acceptance and why researchers tried to find homologues of this special enzyme in other organisms [39].

In 2012, genome databases offered more than 50 homologues to CYP102A1 in bacteria (CYP102) and fungi (CYP505), respectively [45]. Today, a CYP102A1-based (accession number: P14779) BLAST search via Uniprot gives 1581 hits. Thereof, 81 hits show >90% similarity and 1460 hits show >50% similarity to CYP102A1.

2.3.3.2 Cytochrome P450 - CYP505

In 2012, about 2500 species of fungal P450 enzymes were annotated and dedicated to about 400 families [46]. The first isolated CYP505 was $P450_{foxy}$ (CYP505A1) which originates from *Fusarium oxysporium* [47]. In this work, two enzymes of the CYP505 family (CYP505X and CYP505A30) are investigated and therefore are described in more detail in the following subchapters.

2.3.3.3 CYP505X

CYP505X belongs to class VIII and originates from *Aspergillus fumigatus*. Beside the genes for other P450s, this filamentous fungi possesses, like several other filamentous fungi, the CYP505 family [48].

CYP505X enzymes were described to be fatty acid hydroxylases even if their full physiological function is not yet revealed. A possible evolutionary scenario is the development of CYP505 in fungi by horizontal gene transfer from CYP102A1 ($CYP450_{BM-3}$) [47]. Using the BLAST tool in the Uniprot database reveals 35% identity between CYP102A1 (P14779.2) and CYP505X (EAL92660.1).

In 2009, Weis *et al.* tested several self-sufficient CYPs derived from different organisms. During their research, CYP505X showed high stability during catalyst preparation and subsequent biocatalytic applications. Furthermore, it remained active in the presence of 10 and 20 % dimethyl sulfoxide (DMSO) (>95 % of initial activity). By contrast, the activity dropped to 80-90 % when ethanol was used as a solvent [49].

In the present work, 10 variants of CYP505X from *A. fumigatus* expressed in *E. coli* and two variants expressed in *K. phaffii* were investigated: the CYP505X wild-type and 9 further variants harboring special mutations designed by A. Glieder (TU Graz & bisy e.U.) in course of the master project of J.P.R. Eichmann. Most of these variants were designed towards steroid acceptance (Table 4: M5-M10 and M14). The others were designed to convert substrates in order to produce valuable precursors for chemical synthesis of pharmaceutical ingredients (Table 4: M3, M4) or the pharmaceutical ingredient itself (Table 4: M11) [31]. Therefore, the predicted acceptance towards unnatural substrates as well as acceptance of fatty acids of the variants were investigated more deeply in course of this thesis.

2.3.3.4 CYP505A30

The eukaryotic CYP505A30 from the moderately thermophilic fungus *Myceliophthora thermophila* is a self-sufficient P450 enzyme and belongs to class VIII as well. As far as structure and catalytic activity are concerned, it shows high similarities to its bacterial and fungal counterparts: $P450_{BM-3}$ (36 % similarity to primary sequence) and $P450_{foxy}$ (57 % similarity to primary sequence). Further it shows a similarity of 51 % to CYP505X (Uniprot BLAST Tool: query ID: EAL92660.1 (CYP505X); subject ID: FASTA

Sequence of G2QDZ3_MYCTT (CYP505A30)). The current understanding is that CYP505A30 prefers C10 to C20 straight chain fatty acids where tridecanoic acid (C13:0) is most favored. Despite the structural analogy to $P450_{BM-3}$ and its affinity to fatty acid substrates, CYP505A30 shows a different regioselectivity. Although both prefer ω-1 hydroxylation compared to ω-2 and ω-3 hydroxylation, the amount of the three products in the final product mixture differs. Beside ω-1 hydroxylated product, $P450_{BM-3}$ produces considerable amounts of ω-2 and ω-3 hydroxylated products. In contrast, CYP505A30 shows a significant higher affinity to the ω-1 hydroxylated product and only produces low amounts of ω-2 and ω-3 hydroxylated products [39, 50].

In this thesis, 3 variants of CYP505A30 were investigated: CYP505A30 wild-type, a triple mutant that equals the BM-3 triple mutant described by Van Vugt-Lussenburg *et al.* and a variant that harbors 5 mutations. The BM-3 triple mutant was created by site-directed mutagenesis with the aim to convert various drug-like compounds. The quintuple mutant was created by random mutagenesis of the triple mutant with the aim to increase the catalytic activity towards drug compounds [51, 52].

Since the corresponding mutations were introduced to the CYP505A30 scaffold, it is assumed that the resulting enzyme variants may accept drug-like compounds as substrates. Consequently, another thought was that they show lower activity towards fatty acids. In course of this thesis this hypothesis was tested.

2.4 EXPRESSION HOSTS

2.4.1 *ESCHERICHIA COLI*

For the expression of recombinant proteins, a variety of hosts is available. Often *E. coli* strains are used, since they show several advantages compared to other expression systems and are also commercially available in numerous variants to cover a broad spectrum of requirements [53]. Some advantages are the easy handling, short doubling times, low costs for the experimental setup as well as for the following long-term implementation. Further, *E. coli* can be used for laboratory scale experiments as well as in industrial scale cultures [54]. Nonetheless, *E. coli* has also some disadvantages. As a prokaryote, *E. coli* is not able to do posttranslational modifications like for example *N*-linked or *O*-linked glycosylation as well as phosphorylation and is

also not able to form disulfide bonds. This can be a major problem in respect to correct protein folding and functionality of a recombinant protein [55].

For the heterologous expression of P450 enzymes, *E. coli* has, however, a particular advantage over other organisms: the lack of endogenous CYP and CPR genes leads to reduced background and facilitates characterization of the foreign enzymes [56].

In this project, *E. coli* BL21 (DE3) and K12 DH5α-T1 were used for the expression of CYP505X. *E. coli* BL21 is known to reach high expression levels due to a lack of proteolytic proteins. *E. coli* DH5α is a typical strain for plasmid propagation. However, it has been shown that strong induction of protein expression sometimes leads to the formation of improperly folded protein and, that slow expression can facilitate folding and leads to higher activities. *E. coli* DH5α was used in this project in addition to BL21 as for difficult expression targets it might lead to more functional protein even if expression levels are lower. CYP505X expressing *E. coli* strains (DH5α and BL21 (DE3)) were developed in a previous project [31].[1] CYP505A30 expressing *E. coli* strains (BL21 (DE3)) and a CYP102A1 expressing *E. coli* strain (NEB10-beta) were obtained from project partners.[2]

2.4.2 *KOMAGATAELLA PHAFFII* (*PICHIA PASTORIS*)

Pichia pastoris, recently re-classified as *Komagataella phaffii,* is a methylotrophic yeast and can therefore use methanol as its only carbon source. Due to its analogy to the probably best studied yeast *Saccharomyces cerevisiae,* a variety of easy to use tools for protein expression and cultivation has been developed. [57]. Furthermore, protein expression can be regulated by expressing the desired gene under the control of strong inducible promoters like for example the *AOX1* promoter [58]. As a eukaryote, *Pichia pastoris* can do typical posttranslational modifications such as disulfide bond formation or glycosylation which might be important for correct folding and stability. In addition, *P. pastoris* is capable to secrete high levels of recombinant proteins into the supernatant under certain circumstances, allowing for easy purification and analysis [59]. In contrast to *E. coli*, *P. pastoris* contains endogenous CYPs. Yet, this is not

[1] Glieder, A. University of Technology Graz, bisy e.U.
[2] Fürst, M. & Fraaije, M. University of Groningen

considered as a problem since endogenous P450s only appear in low levels and are hardly detectable by CO-difference spectroscopy [60].

For the expression of CYP505X the host strain *P. pastoris* BG11 Mut^S, which originates from CBS7435, was used. In BG11 Mut^S the *AOX1* gene is deleted, which leads to a slower methanol utilization (i.e. Mut^S) phenotype. *P. pastoris* BG11 Mut^S was developed in house previously [61].

2.5 WHOLE-CELL BIOCATALYSIS

In whole-cell biocatalysis, two major modes can be distinguished: biotransformation and fermentation processes. The term biotransformation is used, when production of biomass and bioconversion phase are separated, whereas fermentation processes describe product formation from growth substrates during the natural metabolism of the host cells. In the latter case, different metabolic intermediate products can be formed, which hamper subsequent downstream processing steps [62].

Recent improvements in biocatalysis drew attention to the field of whole-cell biocatalysis for industrial applications. Chemical synthesis of fine chemicals, pharmaceutical ingredients, etc. often requires environmentally unfriendly reagents and harsh reaction conditions. Using natural biocatalysts can be favorable since they typically show high regio- and stereoselectivity, work under mild conditions and are further commonly regarded as environmentally friendly [62, 63]. Further, the use of whole-cell systems instead of crude, purified or immobilized enzymes offers some exceptional advantages. Whole-cell catalysts represent the cheapest form of catalyst possible since purification of the enzyme is not necessary and additional costs for immobilization are omitted. Further, whole cells are advantageous for reactions that depend on costly co-factors since they are available in the host cell itself. The regeneration of the co-factor using sacrificial co-substrates is also commonly applied. Another advantage is that reactions can be performed in conventional as well as unconventional media, as the enzymes are in a protected environment provided by the cellular chassis itself [64]. Regarding large scale applications, downstream processing is an important issue. Compared to free enzymes in solution, whole-cell biocatalysts allow easier separation and purification of the product which results in lower costs and higher process efficiency [62].

Despite all these positive aspects that make whole-cell biocatalysis lucrative for industrial processes, there are also some disadvantages that need to be addressed. Even if the stability is higher in whole-cell systems compared to isolated enzymes, catalyst stability and recovery may still be limiting and need further improvement.

The appearance of metabolic side products in whole cell biotransformations is another challenge, which can be, however, tackled by strain engineering. Regarding substrate availability, the cell walls and membranes can act as a mass transport barrier and prevent the substrate partly or even totally from entering the cell [62–64]. Here, permeabilization strategies may give improvements. Additionally, the upscaling of a biocatalytic process can be challenging due to possible genetic instabilities such as loss of plasmids [65]. Integration of the expression cassette into the host genome can be used to circumvent this problem. Additional common challenges in processes with enzymes are that product formation does not work as desired due to a possible substrate- or product inhibition. However, such problems might be solved by enzyme engineering [62–64].

Regarding substrate hydroxylation using CYPs for industrial scale, whole-cell biocatalysis embodies a great opportunity, especially due to their need of a co-factor. Today, more and more well studied systems are available which can serve as basis for individual adaption of expression of the respective CYP [66].

2.6 AIMS IN REGARDS OF PREVIOUS RESULTS

This thesis focuses mainly on optimizations regarding stability and activity of CYP505X in regards of cultivation and whole cell conversions as well as substrate acceptance of available CYP expressing strains variants used for whole cell biooxidation of small molecule compounds such as active pharmaceutical ingredients (APIs). Based on the results of previous studies, the most promising strains and CYP variants have been selected for further investigation.

Table 1 and Table 2 give an overview of previously tested CYP variants expressed in different host strains and their activity towards tested substrates. In addition, CYP505A30 producing strains from collaboration partners from the University of Groningen (group of Marco Fraaije) were also tested to elucidate their substrate scope.

Table 1: Overview of CYP variants expressed in *E. coli* and their activity towards 30 selected substrates: N=negative T=trace values [%]: <1% 1-10% 11-25% 26-40% 41-50% multiple values represent multiple products

	cyp505 2.1 M1	cyp505 4.1 M2	cyp505 5.1 M3	cyp505 7.1 M4	cyp505 9.1 M5	cyp505 11.1 M6	cyp505 13.1 M7	cyp505 15.1 M8	cyp505 18.1 M9	cyp505 19.1 M10	cyp505 21.1 M11
Benzydamin	N	N	N	N	N	N	N	N	N	N	N
Caffein	N	N	N	N	N	N	N	N	N	N	N
Capsaicin	59 26	43 29	7	9 11	6 20 2	6 16 4 2	4 6	5	12 28 10 3	15 33 14 2	5 7 3 2
Chlorzoxazone	7	2	N	N	T	10	T	T	25	16	N
Clopidogrel	N	N	N	N	N	N	T	N	5	2	N
Dextrometorphan	N	N	T	T	T	T	T	T	N	T	T
Diclofenac	N	N	N	N	N	N	N	N	N	N	N
Estriol	N	N	N	N	1	N	N	N	2	N	N
Ethionamide	N	N	N	N	N	N	T	T	N	T	N
Famciclovir	N	N	N	N	N	N	N	N	<1	<1	N
Flumesulam	N	N	N	N	N	N	N	N	N	N	N
Harmine	N	N	N	N	N	N	N	N	N	N	N
Hydrocortisol	N	N	N	N	N	N	N	N	N	N	N
Ibuprofen	N	N	<1	<1	<1	1	1	1	8 7	13 6	1
Lidocain	N	N	N	N	N	N	N	N	N	N	N
Metoprolol	N	N	N	N	N	N	N	N	1	<1	N
Moclobemide	N	N	N	N	N	N	N	N	N	N	N
Naphthol	N	N	N	12	N	N	N	N	6	2	N
Naproxen	N	N	N	N	N	N	N	N	N	N	N
Nebivolol	N	N	N	N	N	N	N	N	N	N	N
Phenacetin	N	N	N	N	N	N	N	N	N	N	N
Piperine	N	N	N	N	N	<1	<1	N	<1	N	N
Progesterone	N	N	N	N	N	N	N	N	6 6	4 7	N
Propranolol	N	N	N	N	N	N	N	N	N	N	N
Quinazoline	N	N	N	N	N	N	N	N	N	N	N
Salbutamol	N	N	N	N	N	N	N	N	N	N	N
Testosterone	N	N	N	N	N	N	N	N	N	N	N
Tolbutamide	N	N	N	N	<1	N	N	<1	1	2	N
Trifluoperazine	N	N	N	N	N	N	N	N	N	N	N
Vardenafil	N	N	N	N	N	N	N	N	N	N	N

Table 2: Overview of CYP variants expressed in *K. phaffii* and their activity towards 30 selected substrates: N=negative ☐ T=trace ☐ values [%]: <1% ☐ 1-10% ☐ 11-25% ☐ 26-40% ☐ 41-50% ☐ multiple values represent multiple products ☐; * multiple peaks in MS, no peak in UV, CYPs shaded in gray were not further evaluated in this thesis

	CBS7435_wt	BSYBG11_mutS	BSYBG10_wt	BSYBG11_mutS	CBS7435_Wt	CBS7435_mutS	Bg10_Wt	Bg10_mutS	CBS7435_mutS	Bg10_Wt	Bg10_Wt
	cyp505 M12 P2	cyp505 M12 A15	cyp505 M13 P6	cyp505 M14 A21	CYPfoxy-M1 P7	CYPfoxy-M1 P8	CYPfoxy-M1 P9	CYPfoxy-M1 P10	CYPfoxy-M2 P11	CYPfoxy-M2 P12	CYPfoxy-M2 P13
	wt	wt	wt	4xmut	wt	wt	wt	wt	wt	wt	wt
Benzydamin	N	N	N	N	N	N	N	N	N	N	N
Caffein	N	N	N	N	N	N	N	N	N	N	N
Capsaicin	61 13 0	84 12 0	63 9 0	38 12 11	N	N	N	N	N	N	N
Chlorzoxazone	16	36	45	32	N	N	N	N	N	N	N
Clopidogrel	N	N	N	24	N	N	N	N	N	N	N
Dextrometorphan	N	N	N	N	N	N	N	N	N	N	N
Diclofenac	N	N	N	N	N	N	N	N	N	N	N
Estriol	48*	36*	26*	8*	N	N	N	N	N	N	N
Ethionamide	1	19	19	39	2	1	3	2	3	3	3
Famciclovir	N	N	N	<1	~14% deacetylation						
Flumetsulam	N	N	N	N	N	N	N	N	N	N	N
Harmine	N	N	N	<1	N	N	N	N	N	N	N
Hydrocortisol	N	N	N	N	N	N	N	N	N	N	N
Ibuprofen	5 2 6	13 6 7	28 9 31	24 0 28	N	N	N	N	N	N	N
Lidocain	N	N	N	N	N	N	N	N	N	N	N
Metoprolol	N	T	2	3	N	N	N	N	N	N	N
Moclobemide	N	N	N	N	N	N	N	N	N	N	N
Naphthol	6	11	18	21	N	N	N	N	N	N	N
Naproxen	N	N	N	N	N	N	N	N	N	N	N
Nebivolol	<1	7	6	6	N	N	N	N	N	N	N
Phenacetin	N	3	N	5	N	N	N	N	N	N	N
Piperine	N	N	N	<1	N	N	N	N	N	N	N
Progesterone	8 0 0	7 0 0	1 0 0	0 13 6	N	N	N	N	N	N	N
Propranolol	N	N	N	N	N	N	N	N	N	N	N
Quinazoline	N	N	N	N	N	N	N	N	N	N	N
Salbutamol	N	N	N	N	N	N	N	N	N	N	N
Testosterone	N	N	N	N	N	N	N	N	N	N	N
Tolbutamide	N	N	5 1	5 1	N	N	N	N	N	N	N
Trifluoperazine	N	N	N	1	N	N	N	N	N	N	N
Vardenafil	N	N	N	N	N	N	N	N	N	N	N

3 MATERIALS AND METHODS

Material information that is not listed in the material and method section is available in the attached SOPs "Preparation and use of CYP505 expressed in *E. coli* for the oxidation of small molecules" and "Preparation and use of CYP505 expressed in *Pichia pastoris* (*Komagataella phaffii*) for the oxidation of small molecules" (cf. appendix 7.1 and 7.2).

3.1 SUBSTRATES

Table 3 shows an alphabetic listing of the substrates used in this study.

Table 3: Alphabetic listing of all tested substrates with their respective supplier and relevant specifications

Name **Provider** **Item Number**	**Abbr.**[3]	**Formula** **MW [g/mol]**	**Structure**
Benzydamine-Hydrochloride Sigma-Aldrich B5524-5G	BEN	$C_{19}H_{23}N_3O \cdot HCl$ 345.87	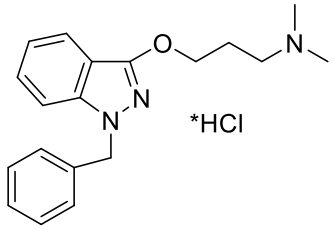
Caffeine Sigma-Aldrich C0750	CAF	$C_8H_{10}N_4O_2$ 194.19	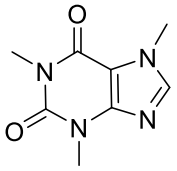
Capsaicin Sigma-Aldrich M2028	CPS	$C_{18}H_{27}NO_3$ 305.42	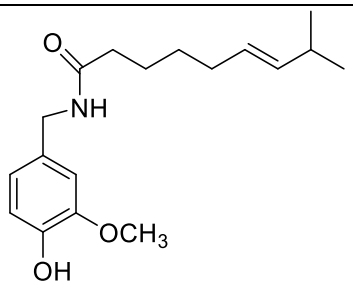
Chlorzoxazone Sigma-Aldrich C4397-25G	CX	$C_7H_4ClNO_2$ 169.57	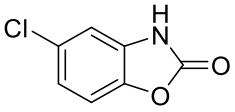

[3] Abbreviations (Abbr.): as such used to facilitate naming within this project

Name **Provider** **Item Number**	**Abbr.[3]**	**Formula** **MW [g/mol]**	**Structure**
Clopidogrel Bisulfate Sigma-Aldrich PHR1431-1G	CLO	$C_{16}H_{16}ClNO_2S \cdot H_2SO_4$ 419.90	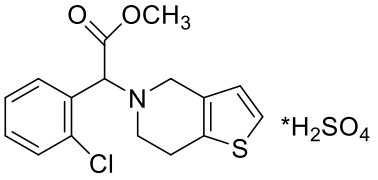
Dextromethorphan Hydrobromide Monohydrate Sigma-Aldrich 81091-10G-F	DEX	$C_{18}H_{25}NO \cdot HBr \cdot H_2O$ 370.32	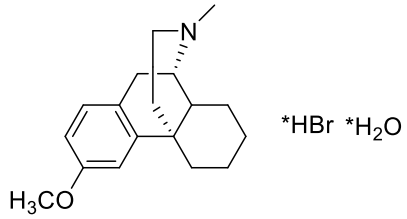
Diclofenac sodium salt Sigma-Aldrich D6899-10G	DIC	$C_{14}H_{10}Cl_2NNaO_2$ 318.13	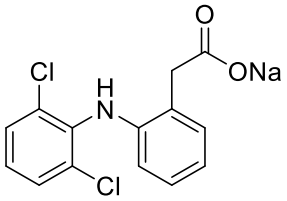
Estriol TCI Deutschland GmbH E0218	EST	$C_{18}H_{24}O_3$ 288.39	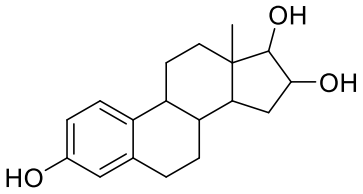
Famciclovir TCI Deutschland GmbH F0842	FAM	$C_{14}H_{19}N_5O_4$ 321.34	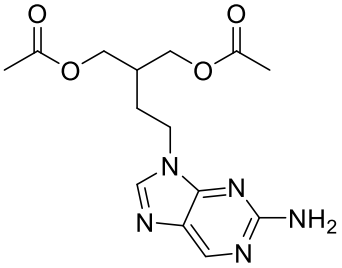
Harmine Fluka (Sigma-Aldrich) 51400 (Product annulled)	HAR	$C_{13}H_{12}N_2O$ 212.25	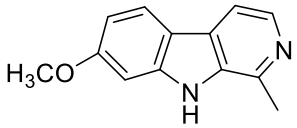
Hydrocortisone Sigma Aldrich H-0888	HYD	$C_{21}H_{30}O_5$ 362.46	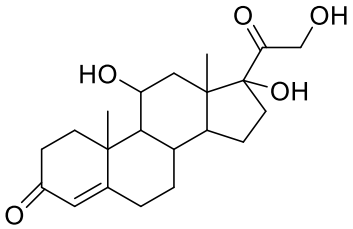
Ibuprofen TCI Deutschland GmbH I0415	IBU	$C_{13}H_{18}O_2$ 206.29	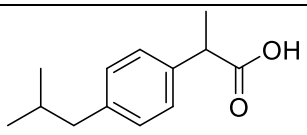

Name **Provider** **Item Number**	**Abbr.[3]**	**Formula** **MW [g/mol]**	**Structure**
Lauric acid Sigma Aldrich W261408	LA	$CH_3(CH_2)_{10}COOH$ 200.32	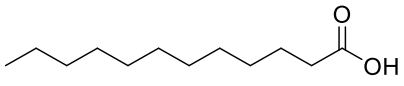
Lidocaine Sigma-Aldrich L7757	LID	$C_{14}H_{22}N_2O$ 234.34	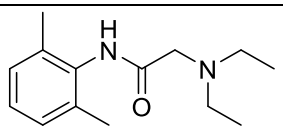
Moclobemide AvaChem Scientific 1638	MOC	$C_{13}H_{17}ClN_2O_2$ 268.74	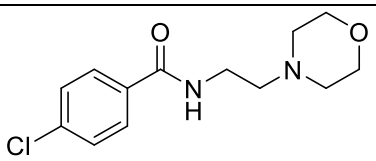
2-Naphthol Sigma-Aldrich 185507	NAP	$C_{10}H_7OH$ 144.17	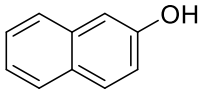
Phenacetin Sigma-Aldrich 77440	PHE	$CH_3CONHC_6H_4OC_2H_5$ 179.22	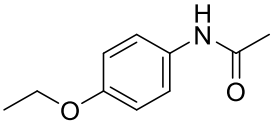
Piperine Sigma-Aldrich P49007	PIP	$C_{17}H_{19}NO_3$ 285.34	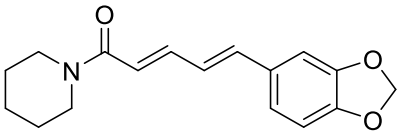
Progesterone Sigma-Aldrich P8783	PRO	$C_{21}H_{30}O_2$ 314.46	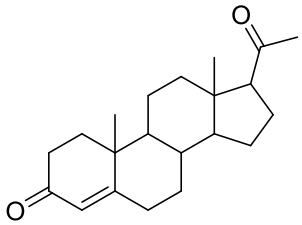
(±)-Propranolol hydrochloride Sigma-Aldrich P0884	PPL	$C_{16}H_{21}NO_2 \cdot HCl$ 295.80	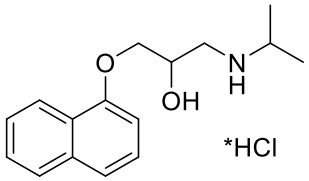
Salbutamol hemisulfate salt Sigma-Aldrich 46732	SAL	$C_{13}H_{21}NO_3 \cdot 0.5H_2SO_4$ 288.35	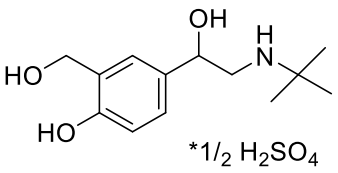

Name **Provider** **Item Number**	**Abbr.[3]**	**Formula** **MW [g/mol]**	**Structure**
Testosterone Sigma-Aldrich 86500	TES	$C_{19}H_{28}O_2$ 288.42	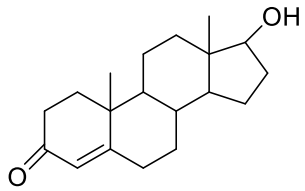
Tolbutamide Sigma-Aldrich T0891	TOL	$C_{12}H_{18}N_2O_3S$ 270.35	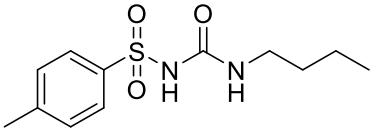
Undecatriene 10%TEC Givaudan N/A	UD	$C_{11}H_{18}$ 150.26	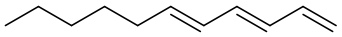
10-Undecenoic acid Sigma Aldrich 124672	UA	$CH_2=CH(CH_2)_8COOH$ 184.28	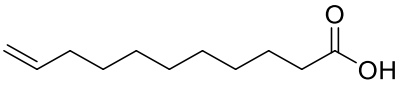

3.2 CLASS VIII CYP PRODRUCING STRAINS

Table 4 lists CYP variants and strains used within this thesis.

Table 4: List of self-sufficient CYP variants with their respective expression host and relevant specifications

Term	Strain	Construct	Plasmid	Origin of gene	Mutations
BSYEJE 2.1	*E. coli* DH5α	CYP505-M1	pMS470	*A. fumigatus*	wild-type
BSYEJE 4.1	*E. coli* DH5α	CYP505-M2	pMS470	*A. fumigatus*	A192Q
BSYEJE 5.1	*E. coli* BL21	CYP505-M3	pMS470	*A. fumigatus*	A286V/I242V
BSYEJE 7.1	*E. coli* BL21	CYP505-M4	pMS470	*A. fumigatus*	F90V/I242L
BSYEJE 9.1	*E. coli* BL21	CYP505-M5	pMS470	*A. fumigatus*	F90A
BSYEJE 11.1	*E. coli* BL21	CYP505-M6	pMS470	*A. fumigatus*	V85N/F90A
BSYEJE 13.1	*E. coli* BL21	CYP505-M7	pMS470	*A. fumigatus*	F90A/L334W
BSYEJE 15.1	*E. coli* BL21	CYP505-M8	pMS470	*A. fumigatus*	W50I/R52I/F54I/ F90A
BSYEJE 18.1	*E. coli* DH5α	CYP505-M9	pMS470	*A. fumigatus*	W50Y/R52F/I81L/ V85M/F90A
BSYEJE 19.1	*E. coli* BL21	CYP505-M10	pMS470	*A. fumigatus*	W50Y/R52F/V85M/F90A
BSYEJE 21.1	*E. coli* BL21	CYP505-M11	pMS470	*A. fumigatus*	W50L/E67G/G84I/ V85W/F90V/D147G/A192Q
BSYBG11_mutS A15	*K. phaffii*	CYP505-M12	pPpT4	*A. fumigatus*	wild-type
BSYBG11_mutS A21	*K. phaffii*	CYP505-M14	pPpT4	*A. fumigatus*	W50Y/R52F/I81L/ V85M/F90A
RUG BL21 empty	*E. coli* BL21 (DE3)	none	none	none	none
RUG BL21 WT (*M.t.*)	*E. coli* BL21 (DE3)	His-Tt-CYP505A30 -WT	pET28a	*M. thermophila*	wild-type
RUG BL 21 3xmut (*M.t.*)	*E. coli* BL21 (DE3)	His-Tt- CYP505A30 -3xmut	pET28a	*M. thermophila*	R47L/F87V/L188Q
RUG BL21 5xmut (*M.t.*)	*E. coli* BL21 (DE3)	His-Tt-CYP505A30 -5xmut	pET28a	*M. thermophila*	R47L/F87V/ L188Q/ E267V/ G415S
RUG NEB10β empty	*E. coli* NEB 10-beta	none	none	none	none
RUG NEB10β WT (*BM3*)	*E. coli* NEB 10-beta	His-CYP102A1-WT	pBAD	*B. megaterium*	wild-type

3.3 RUG - PURIFIED ENZYMES

Table 5 lists purified CYP variants obtained from University of Groningen.

Table 5: List of purified CYP505A30 variants showing all relevant specifications

Term	Appearance	Produced in	Construct	Origin of gene	Mutations
RUG P450 WT (*M.t.*)	Purified enzyme	*E. coli* BL21 (DE3)	His-Tt-CYP505A30 -WT	*M. thermophila*	wild-type
RUG P450 3xmut (*M.t.*)	Purified enzyme	*E. coli* BL21 (DE3)	His-Tt- CYP505A30 -3xmut	*M. thermophila*	R47L/F87V/L188Q
RUG P450 5xmut (*M.t.*)	Purified enzyme	*E. coli* BL21 (DE3)	His-Tt-CYP505A30 -5xmut	*M. thermophila*	R47L/F87V/ L188Q/ E267V/ G415S
RUG P450 BM3 WT (*B.M.*)	Purified enzyme	*E. coli* NEB 10-beta	His-CYP102A1-WT	*B. megaterium*	wild-type

3.4 PARAMETER OPTIMIZATION

For a better understanding of the multistep protocol and possible points of investigation, Figure 6 gives an overview of the general work flow. It starts with strain cultivation and CYP expression, followed by cell harvest and preparation for storage, biotransformation including workup and analysis of results.

Figure 6: Overview of the general workflow

3.4.1 SECTION CYP505X

Generally, experiments that included CYP505X expressing strains and following bioconversion of small molecule compounds such as active pharmaceutical ingredients (APIs) were performed according to the standard operation procedure (SOP) **"Preparation and use of CYP505 expressed in *E. coli* for the oxidation of small molecules"** (appendix 7.1) and **"Preparation and use of CYP505 expressed in *P. pastoris* for the oxidation of small molecules"** (appendix 7.2). In order to investigate experimental parameters for further evaluation and optimization of the SOP, different parameters of the experiment have been varied separately. Deviations are quoted as follows (numbering and subdivision refers to the numbering in the respective SOP, see 7.1 and 7.2):

4.6 Procedure

1. Preculture: no deviations

2. Main culture: no deviations

3. Cell harvest:

- **e1.** supernatant discarded and the pellet resuspended in 10-20 ml PS buffer (8.5%) pH 7.4
- **e2.** supernatant discarded and the pellet resuspended in 10-20 ml PS buffer (1%) pH 7.4
- **e3.** supernatant discarded and the pellet resuspended in 10-20 ml ddH_2O

e4. supernatant discarded and the pellet resuspended in 10-20 ml PT (1%) buffer

g1. **cell disruption:**

5 ml cell suspension was sonified using a BRANSON microTip probe (tapered microtip 3.2 mm for 13 mm horn (VWR, item no.: 142-3746) equipped with interchangeable tips, for 13 mm horn, flat, tapped (VWR, item no.: 142-3751)) for at least ten times for 30 s; between disruption cycles the sample was cooled for a minimum of 1 min on ice.

settings: duty cycle: 70-80; output control: 5; pulser: on

or alternatively:

g2. **cell disruption:**

20 ml cell suspension was sonified using a BRANSON microTip probe (disruptor horn, Ø 13 mm (VWR, item no.: BRAN101-147-037)) for 6 min on ice

settings: duty cycle: 70-80, output control 80%

h. centrifuged at 22000 rpm at 4°C for 20 min

i. collected supernatant and pipetted portions into 24-well plates (used volume: equal to OD_{600} =100/well)

4. Lyophilization and storage

b1. Stored cell pellet without lyophilization at -20°C.

5. Determination of oxidative activity (Biotransformation)

a1. cells resuspended in PS buffer (1%) pH 7.4

a2. cells resuspended in ddH_2O

a3. cells resuspended in PT (1%) buffer

d1. – h1. a mastermix was prepared containing all ingredients except the substrate

d2. sodium citrate omitted

d3. glucose omitted

d4. $NADP^+$ omitted

k1. incubated at 28 – 30°C at 120 rpm in orbital shaker for 16 h or between 0 – 90 h (for time course experiments)

3.4.2 SECTION CYP505A30 – WHOLE CELLS

Generally, experiments conducted with CYP505A30 expressing strains and following bioconversion of small molecule compounds, such as active pharmaceutical ingredients (APIs) were performed according to the following protocol:

1. Glycerol stocks were streaked out on LB agar plates

Preparation of LB-Agar plates:

10 g	Tryptone
10 g	Sodium Chloride (NaCl) (Carl Roth, Item no.: 9265.1)
5 g	Yeast Extract
15 g	Bacto™ Agar (BD Life Sciences, item no.: 214030)

add 1000 ml ddH_2O

Media components were weighted out, dissolved in approximately 800 ml of deionized water and autoclaved. After autoclaving, the broth was filled up with double distilled water to a final volume of 1000 ml. After cooling the medium to 50 – 60°C, antibiotics were added as follows:

- LB-Amp: 300 µl of 100 mg/ml Ampicillin stock solution in 300 ml LB-medium
- LB-Kan: 500 µl of 50 mg/ml Kanamycin stock solution in 500 ml LB-medium
- LB w w/o AB: 200 ml LB-medium without antibiotic

Afterwards, the plates were poured and stored at 4°C.

2. A single colony was picked to inoculate a 5 ml overnight culture in a 50 ml Greiner flask. Culture was grown at 37°C and at 120 rpm.

3. The overnight culture was diluted 1:100 in a main culture of a total volume of 300 mL in a sterile 2 l non-baffled Erlenmeyer flask (max. 15% filled volume of flask volume must be used). Main culture was grown at 37°C and at 120 rpm.

4. At a OD_{600} value of 0.7 – 1.0 the main culture was induced with IPTG (1 mM final concentration) and grown for around 16 h at 24°C at 120 rpm.

For expression of P450 variants in *E. coli* BL21, kanamycin (Carl Roth, item no.: T832.1) was used as selection marker and TB medium contained 0.5 mM 5-aminolevulinic acid (Carl Roth, item no.: 8451.3).

For expression of P450 variants in *E. coli* NEB10-beta, ampicillin was used as selection marker and TB medium contained additionally 0.02% D-(-) arabinose (Sigma Aldrich, item no.: 10850-25G) and no 5-aminolevulinic acid.

The empty vector controls were grown in TB media which comprised all components that were needed for their P450 expressing equivalents except antibiotics.

Cells were harvested and prepared for following bioconversion according to the SOP **"Preparation and use of CYP505 expressed in *E. coli* for the oxidation of small molecules"** (see appendix 7.1).

Deviations are quoted as follows:

4. Lyophilization and storage

b1. Cell pellet was stored without lyophilization at -20°C.

5. Determination of oxidative activity (Biotransformation)

a1. cells were resuspended in the correct amount of PS buffer (8.5%) pH 7.4 to a total of 825 µl

3.4.3 CHEMICAL CELL DISRUPTION WITH BUGBUSTER® KIT

E. coli cells were disrupted using the BugBuster® 10X Protein Extraction Reagent (Merck Millipore, item no.: 70921). The cell suspensions were diluted with H_2O to a total volume of 1 ml (OD_{600}=100) and centrifuged for 10 min at max. speed in a table top centrifuge. The supernatant was removed and the pellets were resuspended in 450 µl to 550 µl (equals 5 ml disruption reagent per 1 g wet cell paste) 1X BugBuster/100 mM PPi buffer (pH 7.4). 1 µl 50% Benzonase/water (equals 1µl Benzonase per 1 ml 1X Bugbuster extraction reagent) was added to the resuspended cells and the suspensions were incubated for 20 min at 750 rpm at room temperature.

Afterwards, the suspensions were centrifuged for 20 min at maximum speed and room temperature and the supernatant containing the soluble proteins was transferred to a new reaction tube.

3.4.4 DETERMINATION OF TOTAL PROTEIN CONCENTRATION VIA BCA PROTEIN ASSAY

Bicinchoninic acid (BCA) Assay was performed in a 96-well microplate (Greiner Bio-One; item no.: 655101) using the Pierce™ BCA Protein Assay Kit (Thermo Fisher Scientific, Catalog number: 23227) according to the protocol provided by the manufacturer. To make sure, that the total protein concentration of each samples was in the working range of the assay (20 – 2000 µg/ml) an estimation of the total protein concentration was made by using a Thermo Scientific™ NanoDrop 2000c full-spectrum UV-Vis spectrophotometers. If necessary, the samples were diluted properly.

3.4.5 DETERMINATION OF P450 EXPRESSION LEVELS

CYP expression levels were investigated by loading 10 µg (total protein) on a NuPAGE™ 4-12% Bis-Tris Protein Gel (Invitrogen, Catalog number: NP0321BOX or Catalog number: NP0323BOX or) and the use of NuPAGE MOPS SDS Running Buffer (20X) (Thermo Fisher Scientific, Catalog number: NP0001) which was diluted to 1X with ddH_2O. Proteins were separated for 45 – 70 min (running time increases with salt content in sample) and 200 V.

Preparation of Samples:

Pellet: A sample of the pellet was transferred to a fresh, pre-weighed 1.5 ml reaction vessel. Per 1 mg of pellet, 10 µl of 6 M Urea were added. Samples were agitated on a vortex mixer, until the pellet was totally dissolved. Finally, the samples were centrifuged for 5 min at maximum speed in a table top centrifuge. 6.5 µl of the supernatant were added to 6.5 µl of ddH_2O, 5 µl of 5X loading dye and 2 µl of 10X reducing agent (= 20 µl total volume).

Cell Free Extract:

CFE samples were diluted in ddH_2O to a final concentration of 20 µg in 13 µl. These 13 µl of CFE were added to 6.5 µl of ddH_2O, 5 µl of 5X loading dye and 2 µl of 10X reducing agent (= 20 µl total volume).

Samples were denatured at 95°C for 10 min and centrifuged for a few seconds, before loading 10 µl of each sample onto the gel. Additionally, 4 µl PageRuler Prestained Protein Ladder (Thermo Scientific, Catalog number: 26616) was used as protein standard.

After protein separation, gels were stained with Coomassie Brilliant Blue staining solution (15-20 min). Unspecific staining was removed with Destaining solution (heated in microwave 15 - 20 sec, 15 – 20 min 750 rpm at r.t.; repeated at least 3 times).

Preparation of Coomassie Brilliant Blue Staining solution:

2.5 g Coomassie Brilliant Blue G-250 (Carl Roth, Catalog number: 9598.2)
75 ml Acetic acid (Carl Roth, Catalog number: 6755.2)
500 ml $EtOH_{absolute}$ (VWR Chemicals, Catalog number: 20821.330)

fill up to 1000 ml with ddH_2O (Fresenius Kabi, D21.100)

Preparation of Destaining solution:

75 ml Acetic acid (product information: as mentioned above)
200 ml $EtOH_{absolute}$ (product information: as mentioned above)

fill up to 1000 ml with ddH_2O

3.4.6 ANALYSIS BY HPLC/MS

Conversion of APIs was measured by HPLC/MS

The HPLC measurements were performed with a Kinetex 50x4.6 mm; 2.6µ C18; 100 Å column equipped with a SecurityGuard™ Ulltra Cartridge (AJ0-8775). The mobile phases were 0.1 % aqueous formic acid and acetonitrile (ACN). All relevant method parameters for the investigated substrates are listed in detail in the appendix (see 7.3).

3.4.7 ANALYSIS BY GC/MS

Conversion of lauric acid and 10-undecenoic acid was measured by GC/MS.

The samples were analysed on a Shimadzu Standard Gas Chromatograph – Mass Spectrometer GCMS-QP2010 SE equipped with a Phenomenex Zebron™ ZB-5MSi

Column (Thickness: 0.25 µm, Length: 30.0 m, Inside Diameter: 0.25 mm Max Usable Temp: 360°C) and a Shimadzu AOC-20i/s Autoinjector. The settings for analysis are listed as follows:

Sampler: # of rinses with solvent (Pre-run) = 5; # of rinses with solvent (post-run) = 5; # of rinses with sample = 3; plunger speed (suction): middle; viscosity comp. time: 0.2 sec; plunger speed (injection): high, Syringe Insertion Speed: high; Injection mode: "0: Normal"

GC: column oven temp.: 70 °C; injection temp.: 250 °C; injection mode: split; sampling time: 1 min; carrier gas: He; pressure: 73.9 kPa; total flow: 5.3 ml/min; column flow: 1.16 ml/min; linear velocity: 39.5 cm/sec; purge flow: 3.0 ml/min; split ratio: 1.0; temperature program: 70 °C - hold 4 min, 15 °C/min to 300 °C – hold 5 min: total program time: 24.33 min;

MS: ion source temp.: 250 °C, interface temp.: 320 °C, solvent cut time: 3.5 min; detector voltage: relative to the tuning result – 0 kV; micro scan width: 0 µ; threshold: 0; start time: 3.50 min; end time: 24.33 min, acq. mode: scan; event time: 0.13 sec; scan speed: 5000; start m/z: 30.00; end m/z 500.00;

RT: Tetradecane (internal standard): 9.87 min
RT: Lauric acid and metabolites: 11.06 and 12.85 min
RT: 10-undecenoic acid and metabolites: 10.36 and 11.68 min

3.4.8 ANALYSIS BY GC/FID

Conversion of undecatriene was measured by GC-FID.

The samples were analysed on a GC/FID from Agilent equipped with Agilent 1220732 DB-1701 column, 30m, 252µ, 0.25µ, with a flow rate of 1ml/min. Gradient: 1min at 100°C, 10°C/min to 250°C, hold 3 min. UT isomers: RT=3.61 and 3.90 min, respectively.

3.4.9 DETERMINATION OF OXIDATIVE ACTIVITY VIA GC/MS ANALYSIS

3.4.9.1 CYP505X and CYP505A30 whole cell Biotransformations

Bioconversion was done according to the SOP section 5 "Determination of oxidative activity (Biotransformation). After 16h, the reactions were stopped and prepared for GS-MS analysis according to the following protocol:

600 µl reaction mix of a total of 1,000 µl reactions volume were transferred to a 2 ml reaction tube. The reaction was stopped by adding 200 µl 3 M HCl. For extraction, 400 µl 0.01% tetradecane/ethyl acetate was added, followed by mixing for 10 min on a G-560 Vortex Genie-2 Lab Shaker Mixer (Scientific Industries, Inc. model: G-560E) at maximum speed. Next, the samples were centrifuged for 15 min and 15,000 rpm at 4 °C. The upper phase was removed (approx. 300 µl) and transferred to a fresh 2 ml reaction tube containing a spatula tip full sodium sulfate. The extraction step was repeated once und the volumes of the extractions were pooled. Then the samples were mixed shortly and 200 µl of the solution were transferred to 2 ml glass vials, sealed with a membrane containing lid and analyzed via GC-MS immediately.

3.4.9.2 Purified CYP505A30 enzymes

The reaction mixture contained the following components (calculation for a total reaction volume of 1 mL):

2-10 µM CYP505A30
5 µl glucose dehydrogenase (GDH) stock (10 mg/ml)
10 µl glucose stock (1 M)
50 µl $NADP^+$ stock (1mM)

---

add up to a volume of 950 µl with 50 mM Tris/HCl pH 7.5
start reaction by addition of 50 µl substrate stock (100 mM in DMSO)

Reaction was run at 30°C and 120 rpm for 16-17 h. To prevent dissipation of purified enzyme either 600 µl or 75 µl were taken as total reaction volume. Stopping and extraction as well as preparation for GC-MS analysis were done as described above. All volumes of needed reagents were taken relatively to the defined amount.

3.4.10 CALCULATIONS OF KINETIC PARAMETERS

The following formula was used for the calculation:

$$\text{Conversion in mM} = \frac{\text{Conversion [\%]} \cdot 5}{100}$$

To calculate the conversion in mM/h, measuring points that followed a linear trend were identified. A trendline was drawn as a tangent to the fitted dynamical curve, which was defined by these measuring points and the coefficient of determination was determined. The presumption of an intersection point at 0/0 could be made, since no substrate was converted at point in time 0. The slope (k) of the regression line described the reaction rate in mM/h. To determine K_M and V_{max}, the enzyme kinetics tool in SigmaPlot (version 14.0)[4] was used.

3.4.11 PREPARATIVE SCALE REACTIONS

3.4.11.1 Bioconversion

Cells were cultivated (according to the respective SOP) and then stored in form of wet cell pellet at -80°C. A total reaction volume of 500 ml was used. In case of Ibuprofen, 501.5 mg (dissolved in 25ml DMSO) were used to introduce the substrate into the reaction, in case of chlorzoxazone 442.5 mg (dissolved in 25ml DMSO) were used, representing a total concentration of 5 mM in the final reaction volume. Reaction conditions were chosen according to the respective SOPs. All parameters were linearly upscaled to a final reaction volume of 500 ml (instead of 1ml for *E. coli* and instead of 200 µl in case of *P. pastoris*). Each reaction was performed in two 2L baffled flasks, each containing 250 ml of the reaction suspension. Throughout the reaction (30°C, 120 rpm) samples were collected as follows: 500 µl were withdrawn and the reaction terminated by adding 500 µl ACN/MeOH. Samples were mixed for 10 min at rt and 700 rpm and centrifuged for 5 min at maximum speed in a tabletop centrifuge. 200 µL of the supernatant were transferred into wells of polypropylene microtiter plates and analyzed as described in the SOPs. As soon as no significant increase in product formation could be detected anymore, the flasks were removed from the shaker, the

[4] https://systatsoftware.com/products/sigmaplot/installation-procedures-for-sigmaplot-all-licenses/instructions-how-to-update-a-30-day-trial-to-a-full-license-version-of-sigmaplot/

reaction mixture of the two flasks was pooled in one bottle and frozen and stored at -20 °C until further treatment.

3.4.11.2 Extraction

Samples were removed from the freezer in the evening and placed at +4 °C. The next day, extraction was performed as follows:

Reaction mixture was homogenized by brief shaking. Afterwards, it was separated to equal amounts and transferred to two PPCO centrifuge tubes. 100 ml of EtOAc were added per tube, the tube closed with a lid, and vigorously shaken for 5 min manually. Then, the upper phase was transferred to o 1000 ml round bottom flask. The procedure was repeated 3 times in total.

3.4.11.3 Concentration of sample by removal of EtOAc

The 1000 ml round bottom flask, containing the extraction sample, was placed on a rotary evaporator (Heidolph Instruments GmbH & Co. KG, Laborota 4000 efficient) equipped with a VACUUBRAND diaphragm pump (PC 2001 VARIO). Cooling was performed by coil passing tap water. Rotary evaporation was conducted by heating the water bath up to 40-42°C. Pressure was reduced to about 200 mbar. After approximately 1 hour, the organic solvent was removed. Samples were stored at 4°C for further analysis.

3.4.11.4 Isolation of Metabolites

3.4.11.4.1 Chlorzoxazone

After workup, isolation by preparative HPLC was evaluated but proved time consuming and inefficient in comparison to silica gel chromatography [49]. 6-OH-CX was therefore isolated from the raw product by silica gel chromatography (Anna K. Migglautsch[5]). Specifically: a silica gel column with 600 ml cyclohexane/ethyl acetate (3:1) and 600 ml cyclohexane/ethyl acetate (2:1) as eluent was used for purification. The weight of the crude product was 815 mg. Fractions were identified by thin layer chromatography (eluent: cyclohexane/ethyl acetate (2:1), detection: by UV and cerium ammonium molybdate stain (CAM)). Product containing fractions were pooled, concentrated in vacuo and analyzed by 1 and 2D NMR (Anna K. Migglautsch[5]).

[5] Anna Katharina Migglautsch, Institute of Organic Chemistry, Graz University of Technology

3.4.11.4.2 Ibuprofen

After extraction (cf. 3.4.11.2) and concentration of the remaining sample (cf. 3.4.11.3), 1.5 ml ACN/MeOH (ratio 1:1) was added to the oily material, resulting in a total volume of 3 ml. After workup, isolation by preparative HPLC was performed on an Agilent Series 1200 HPLC system. Figure 7 gives an overview of the used modules, solvents and column.

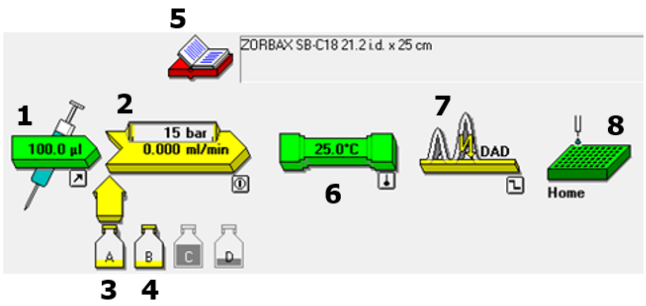

1 G1367A well plate autosampler
2 G1311A quaternary pump
3 Solvent A: 0.1% formic acid/dH_2O
4 Solvent B: Acetonitrile (ACN)
5 ZORBAX SB-C18 21.2 x 25 cm column (Agilent Technologies, part number: 877250-102
6 G1316A column thermostat
7 G1315B diode array detector (DAD)
8 G1364C automatic fraction collector

Figure 7: HPLC system diagram showing used modules and their specifications

For sufficient peak separation and following collecting of the fractions, the crude sample was further diluted 1:10 with ACN/MeOH (ratio 1:1). Table 6 gives information about the used method settings.

Table 6: preparative HPLC method specifications for ibuprofen

Ibuprofen		BKE_IBU_UV_ROBOX_PREP_TEST1.M		
Injection volume		100 µl		
Flow		4 ml/min		
Solvents		**A**	**B**	
		H_2O - 0.1 % formic acid	acetonitrile (ACN)	
Solvent gradient		**Time [min]**	**ACN %**	
		0.00	0	
		1.00	25	
		15.00	100	
		17.00	100	
		20.00	25	
		30.00	0	
Column		ZORBAX SB-C18 21.2 x 25 cm		
Precolumn		none		
Column temperature		25°C		
Substrate		Ibuprofen (206.29 g/mol)		
Product(s)		OH-Ibu (223 g/mol)		
Detection	**Trace**	**UV**		
	Signal	239 nm		
Retention time substrate		27.33 min		
Retention time product(s)		20.31 min	20.67 min	21.70 min

Fractions were collected as depicted in Figure 8. Afterwards, the respective fractions were pooled, transferred to a 50 ml reaction tube, frozen at -80°C for at least three hours and lyophilized. The remaining powder was analyzed by 1 and 2D NMR (Hansjörg Weber[6]).

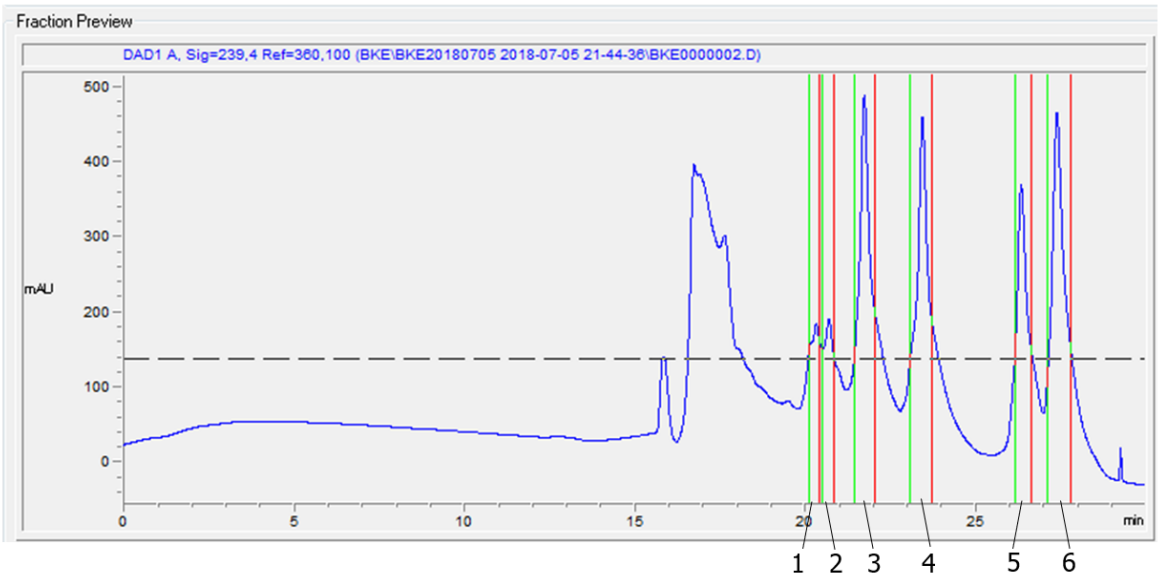

Figure 8: Fraction preview of CYP505X mediated ibuprofen bioconversion in *P. pastoris* on preparative scale; detector: diode array detector (DAD), fractions were labeled from 1 to 6; settings of fraction collector: start of collection after 20.10 min, trigger mode: peak based, maximum peak duration: 0.70 min, threshold 137.918 mAU (indicated by dashed line), up slope 0.10 mAU/s, down slope 5 mAU/s, start of a single fraction collection: indicated by green line, stop of a single fraction collection: indicated by red line

[6] Hansjörg Weber, Institute of Organic Chemistry, Graz University of Technology

4 RESULTS AND DISCUSSION

To evaluate activity of enzymes towards new substrates, a fast, efficient and reliable screening method is appreciated. In the following chapters, a standard operation procedure (SOP) for CYP505X producing strains was evaluated and partly optimized for both eukaryotic and prokaryotic CYP production strains. After successful evaluation and comparison, the constituted biotransformation conditions were tested in terms of applicability to another CYP505 variant: CYP505A30.

Finally, the evaluated procedure was used to implement preparative scale reactions for selected substrates. The products were isolated and analyzed to determine whether the metabolites are chemically identical to human drug metabolites.

4.1 DIRECT COMPARISON OF CYP505X IN *E. COLI* AND *P. PASTORIS*

4.1.1 CELL WET-WEIGHT VS. CELL DRY-WEIGHT

One research question was, whether and how biooxidation results of *E. coli* and *P. pastoris* CYP expressing strains can be compared. According to the SOPs, cell material equaling OD_{600} 100 should be used for biooxidations with *E. coli* and OD 50 for biooxidations with *P. pastoris*. For direct comparison of *P. pastoris* and *E. coli* cells, the cell wet-weight (CWW) and cell dry-weight (CDW) of cells corresponding to 100 OD units of 5 different *E. coli* and 4 different *P. pastoris* batches were determined in 10 replicates each. Therefore, already lyophilized cells (100 OD units each) were rehydrated, washed and resuspended in water, to a total amount of 1 ml. The suspension was transferred to pre-weighed reaction tubes and centrifuged. The

Table 7: Summary of WCW and DCW determination.

Strain	batch	CWW [mg]	CDW [mg]
***E. coli* 2.1**	**4.10.17**	65.80 ± 7.66	18.62 ± 8.71
***E. coli* 2.1**	**11.10.17**	74.99 ± 5.79	16.93 ± 3.49
***E. coli* 2.1**	**25.10.17**	90.30 ± 4.39	23.89 ± 2.52
***E. coli* 18.1**	**4.10.17**	67.08 ± 7.80	17.50 ± 3.82
***E. coli* 18.1**	**25.10.17**	69.89 ± 3.82	14.99 ± 3.01
***P. pastoris* A15**	**15.9.17**	61.10 ± 6.69	12.39 ± 0.61
***P. pastoris* A15**	**19.10.17**	58.85 ± 1.36	14.31 ± 0.84
***P. pastoris* A21**	**15.9.17**	54.92 ± 1.88	12.80 ± 0.33
***P. pastoris* A21**	**19.10.17**	86.14 ± 1.60	20.88 ± 0.18

supernatant was discarded, and the weight of the wet cell paste was determined. Afterwards, the cells were lyophilized again and the cell dry weight was determined. For control, the cell powder was resuspended again and the OD measured. The determined OD was within 20% deviation from the expected OD of 100. Weights of both *E. coli* and *P. pastoris* were within the same range (Table 7). Considering these results, a direct comparison between *P. pastoris* strains and *E. coli* strains expressing CYP505 variants seems valid, assuming both are used at the same cell density. For direct comparison of CYP505X variants, it was decided to use OD 100 in all the experiments although it is stated to use OD 50 in the *Pichia pastoris* SOP (cf. appendix 7.2)

4.1.2 CONVERSION OF CHLORZOXAZONE (CX): 1 *E. COLI* CELL VS. 1 *P. PASTORIS* CELL

Since *E. coli* cells and *P. pastoris* cells differ in size considerably, we were interested in, how many *P. pastoris* cells and *E. coli* cells equal an OD_{600}, respectively. Therefore, it was assumed that *P. pastoris* and *S. cerevisiae* show similar cell numbers. Data from literature was used [67]. For *E. coli*, data provided by Agilent Technologies was used [68]. Further, the conversion of chlorzoxazone to 6-OH chlorzoxazone (cf. results 4.3) conducted by one *E. coli* cell compared to one *P. pastoris* cell was calculated (Table 8).

Table 8: Theoretical calculation of number of *P. pastoris* cells and number of *E. coli* cells (OD_{600}=100/ml) and theoretical conversion of chlorzoxazone to 6-OH-chlorzoxazone conducted by one cell

P. pastoris		***E. coli***	
OD_{600}	**# of cells**	**OD_{600}**	**# of cells**
0.341	$16.625*10^6$	1	$8*10^8$
100	$4.9*10^9$	100	$8*10^{10}$
1 ml of reaction volume contained 0.845 mg of chlorzoxazone (≡5 mM)			
CX conversion (CYP505X wild-type) A15 **(OD_{600}=100)**		**CX conversion** (CYP505X wild-type) 2.1 **(OD_{600}=100)**	
7.5 %	63.38 µg	9.4 %	79.43 µg
CX conversion (CYP505X wild-type) A15 **(per cell)**		**CX conversion** (CYP505X wild-type) A15 **(per cell)**	
$1.62*10^{-8}$ µg		$7.92*10^{-10}$ µg	

According to the data given in Table 8, in a reaction volume of 1 ml (OD_{600}=100) were $8*10^{10}$ *E. coli* cells and $4.9*10^9$ *P. pastoris* cells representing 16.3 times the amount of *E. coli* cells compared to *P. pastoris* cells. Based on the data given in 4.3, one *E. coli*

cell could convert $7.92*10^{-10}$ µg of CX while one *P. pastoris* cell could convert $7.92*10^{10}$ µg. Based on these calculations, one *P. pastoris* cell converted 20.5 times the amount of CX compared to one *E. coli* cell.

Even, if these assumptions are theoretical values (since the actual number of cells was not experimentally verified by counting), they underline the importance of accurate data analysis and consideration of the used biocatalyst. By now, it seems, that activity of CYP505X in *P. pastoris* is higher compared to *E. coli*. However, for further statements regarding activity of CYP505X in *E. coli* and *P. pastoris*, expression levels should be determined and compared. In this thesis, only the expression levels in *E. coli* were investigated and all gained data were referred to OD_{600}=100 in 1 ml of reaction volume for comparison.

4.2 EXPRESSION LEVELS OF CYP VARIANTS IN *E. COLI*

Data was based on endpoint measurements that showed the conversion of CX in a given time. Overall oxidative efficiency of the whole cell biocatalysts, which is the sum of expression level, mutant activity, substrate/product transport and cofactor recycling efficiency. CO difference spectra indicated that BL21 gives higher amounts of active CYP than DH5α [28]. To evaluate, if the amount of soluble CYP corresponds to the CO difference spectra, the proteins were visualized. The aim was also, to understand if differing conversions by CYP variants were a result of expression level or can be attributed to the respective mutations. Figure 9a shows CYP505A30 variants and CYP102A1 expressed in BL21 and NEB10 beta, respectively. Further, the respective purified enzymes were used as positive control (Figure 9b). The expected size of CYP505A30 is 120 kDa. 10 µg of cell free extract (CFE) as well as purified enzyme were used. A fraction of the corresponding cell pellet was visualized on the gel to determine the amount of insoluble CYP (improperly folded/inclusion bodies).

The size and intensity of the bands (Figure 9a) indicate that all variants of CYP505A30 are expressed equally. As expected, the empty vector control (BL21 (DE3) empty v.CO CFE and BL21 (DE) empty v. CO Pellet) did not show a band at the expected 120-123 kDa position. Since no band was apparent at the expected height, CYP102A1 seemed not to be expressed at all (NEB10-beta WT (CYP102A1 (*B. megaterium*) CFE and CYP102A1 (*B. megaterium*) Pellet). The empty vector control appeared as expected

(NEB10-beta empty v. CO CFE and NEB10-beta empty v. CO Pellet). The bands for the purified enzymes (Figure 9b) appeared at the expected position. However, the size of the bands indicated that the supposed amount of 10 µg purified enzymes has been overestimated. Since we had no detailed information of the exact concentration of the purified enzymes, the concentration was estimated by using UV/VIS spectrophotometer only. The protein concentration in the cell free extracts was determined using the BCA Assay was performed to get a more accurate result.

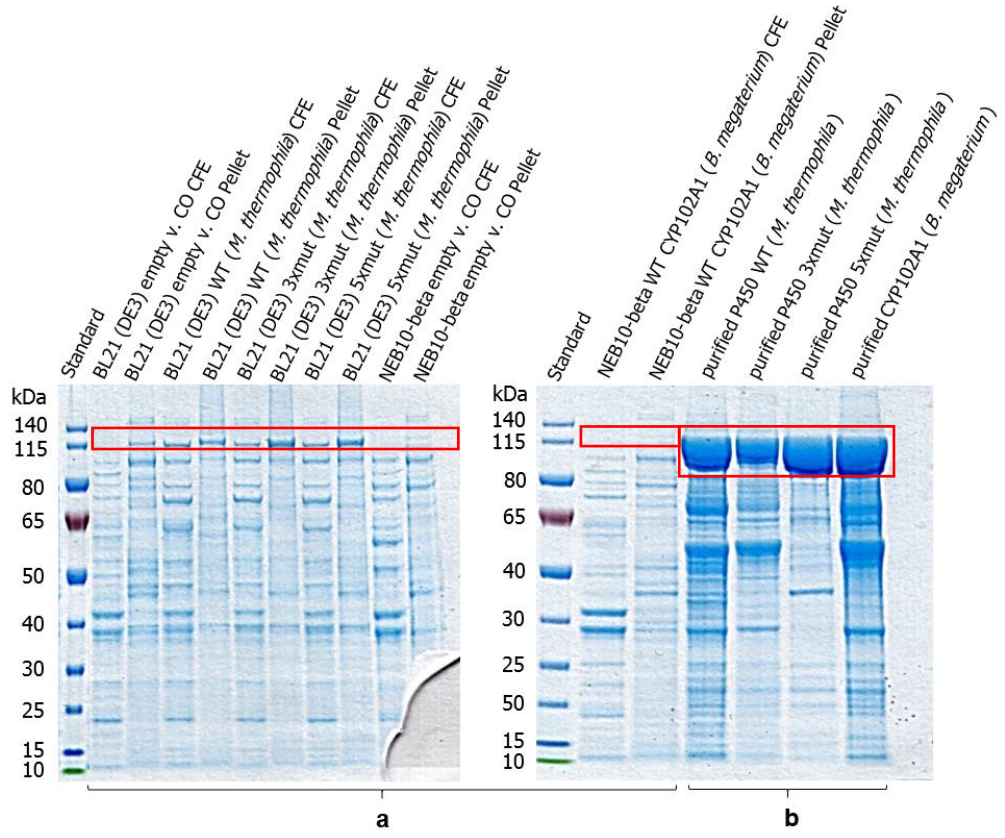

Figure 9: NUPAGE of CYP 505 variants: (a) cell disruption: sonication. (b) purified enzymes. 10 µg protein loaded; expected size: 120-123 kDa (as indicated by the red box); empty v. CO = empty vector control

Figure 10a shows CYP505X variants expressed in *E. coli* DH5α (18.1 and 2.1) and BL21 (all other variants) from one culture and disruption round. Figure 10b shows CYP102A1 expressed in NEB10-beta. Figure 10c shows CYP505X variants 19.1 and 7.1 expressed in BL21 from one culture and disruption round compared to CYP505X variants 18.1 and 2.1 expressed in DH5α from one culture and disruption round (Figure 10d). All mutants except 18.1 and 2.1 (Figure 10a) showed approximately the same level of

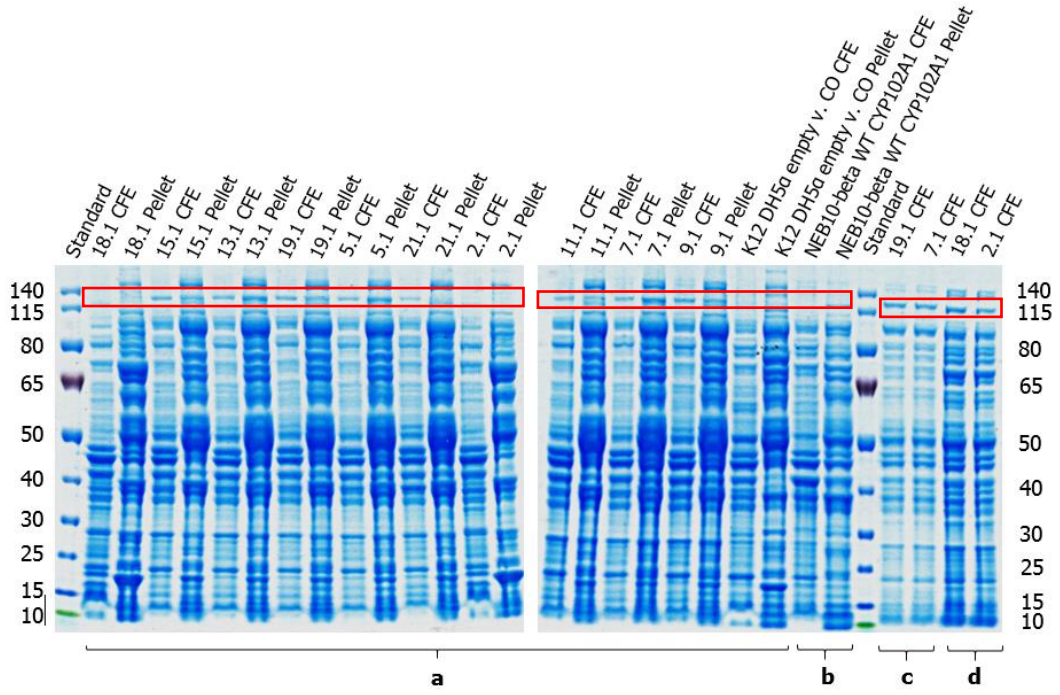

Figure 10: NUPAGE of CYP505 variants: (a) and (b) cell disruption: BugBuster. (c) and (d) cell disruption: sonication. 10 µg protein loaded; expected size: 120-123 kDa (as indicated by the red box); empty v. CO = empty vector control

soluble expression. For both, a weak band which appears lower compared to all other CYP bands can be seen. The most likely reason for this may be that 18.1 and 2.1 are expressed in K12 DHα strains and all others are BL21 (DE3) strains, which are known to reach a higher expression level compared to DH5α. Another consideration may be, that the disruption method is the reason for the lighter appearing bands for 18.1 and 2.1 is, that the pattern of the bands appears differently for the same mutants when using BugBuster® (Figure 10a 18.1 CFE and 2.1 CFE) or sonication (Figure 10d 18.1 CFE and 2.1 CFE). Expression of CYP102A1 in NEB10-beta was investigated again since in the first batch (Figure 9a) no band could be detected at 123 kDa. For this batch (Figure 10b), a weak band could be seen in the pellet fraction (NEB10-beta WT CYP102A1 Pellet). Variant 19.1 and 7.1 (Figure 10c) were disrupted with the small sonication probe (see 3.4.1 g1) and 18.1 and 2.1 (Figure 10d) were disrupted with the large sonication probe (see 3.4.1 g2) Since the disruption efficiencies seemed inconsistent, CYP505X content was analyzed by NuPAGE. The bands representing the enzyme appeared similar in size and intensity. Here should be mentioned that for loading 10 µg of total protein approximately seven times the amount of protein received from 2.1 and ten times the amount of protein received from 18.1 were needed compared to 7.1 and 19.1, which is important for further data evaluation (see 4.9.2).

Summarized, all variants except 18.1 and 2.1 - which were expressed in DH5α - were expressed in similar amounts in *E. coli* BL21. As similar expression levels have been verified among all CYP505 expressing strains except for 18.1 and 2.1, direct

comparison of their overall oxidative efficiency was considered appropriate. When comparing 18.1 and 2.1 results with other mutants, it must be mentioned that CYP expression level is lower. Finally, all CYP505 variants are also present in significant amounts in the insoluble fraction. Co-expression of chaperones GroEL/GroES may give an improvement [49].

4.3 INFLUENCE OF WASHING AND CO-FACTOR RECYCLING

In a preliminary experiment, cell suspension was frozen and thawed. To investigate, whether CYP505X leaked to the supernatant from lysed cells, the thawed suspension was centrifuged and both, the biooxidation activity of the supernatant and the pellet were determined separately. The pellet was therefore suspended in fresh buffer. The results showed, that CYP505X activity was solely present in the pellet and that the activity had even increased upon the replacement of the freezing buffer (Results T. Bachler). The effect was attributed to the removal of inhibiting compounds. To investigate whether washing of lyophilized cells also has a positive effect on product formation, biooxidation of CX over a period of 16 h was investigated. Further, components which were intended to facilitate NADPH recycling in the standard procedure were omitted. Figure 11 shows all ingredients needed for a CYP505 driven biooxidation in whole cells as stated in the SOP (cf. 7.1).

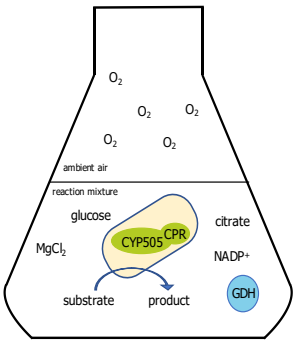

Figure 11: Schematic representation of the reaction setup for a CYP505 driven whole cell biooxidation in *E. coli* according to the SOP (cf. 7.1)

Any simplification of the protocol would decrease the price in a potential commercial application of our catalysts and only additives with a significantly positive effect on the biooxidation efficiency are justified from the cost-perspective.

Table 9 and Figure 12 show the results for CYP505X variants 18.1 and 2.1 expressed in *E. coli*. Table 10 and Figure 13 show the results for the respective CYP505X variants A15 and A21 expressed in *P. pastoris*.

In general, using standard conditions according to the SOP (cf. 7.1) turned out to be the best condition for CYP variants expressed in *E. coli*. An increase product formation could be detected for the 5x mutant expressed in *E. coli* (18.1) when using standard conditions according to the SOP and additional washing (≈18% washed, ≈13% without washing) (Table 9). For the same variants in *Pichia pastoris*, a minor improvement could be detected for the wild-type when using standard conditions and additional washing (≈15% washed, ≈ 9% without washing). Here should be mentioned that the standard deviation was about 1.9% for the washed fraction and therefore the calculated improvement was considered as minor. No enhanced product formation could be seen for all other conditions (Table 10).

Although washing of cells seemed to show some increase in product titer, the overall enhancement of substrate conversion was little. Therefore, the additional washing steps were not incorporated into the standard protocol.

Table 9: (right) CX Bioconversion *E. coli* - Effect of washing rehydrated, lyophilized cells and effect of glucose and citrate: w (washed), S (standard conditions), -C (without citrate), -g (without glucose)

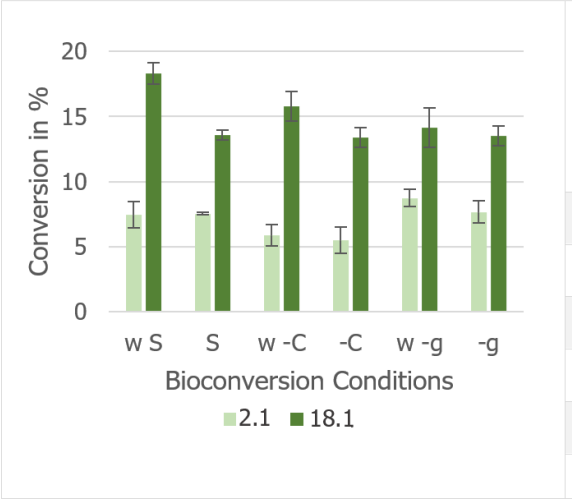

washed	Glucose 10mM	Citrate 50mM	*E. coli* 2.1 CYP505X WT Conv. %	*E. coli* 18.1 CYP505X 5xmut Conv. %
+	+	+	7.5±1.0	18.3±0.8
-	+	+	7.5±0.1	13.6±0.4
+	+	-	5.9±0.8	15.8±1.1
-	+	-	5.5±1.0	13.4±0.8
+	-	+	8.7±0.7	14.2±1.5
-	-	+	7.7±0.9	13.5±0.8

Figure 12: (left) CX Bioconversion *E. coli* - Effect of washing rehydrated, lyophilized cells and effect of glucose and citrate: w (washed), S (standard conditions), -C (without citrate), -g (without glucose)

Table 10: (left) CX Bioconversion *P. pastoris* - Effect of washing rehydrated, lyophilized cells and effect of glucose and citrate: w (washed), S (standard conditions), -C (without citrate), -g (without glucose)

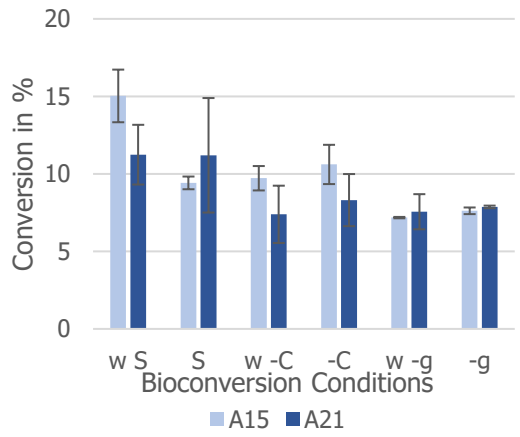

washed	Glucose 10mM	Citrate 50mM	*P. pastoris* A15 CYP505X WT Conv. %	*P. pastoris* A21 CYP505X 5xmut Conv. %
+	+	+	15.0±1.7	11.2±1.9
-	+	+	9.4±0.4	11.2±3.7
+	+	-	9.7±0.8	7.4±1.8
-	+	-	10.6±1.3	8.3±1.7
+	-	+	7.2±0.1	7.6±1.1
-	-	+	7.6±0.2	7.9±0.1

Figure 13: (right) CX Bioconversion *P. pastoris* - Effect of washing rehydrated, lyophilized cells and effect of glucose and citrate: w (washed), S (standard conditions), -C (without citrate), -g (without glucose)

Even if the omitting of some components of the cofactor recycling system (glucose and citrate) resulted in a diminished product formation, the overall outcome was higher than expected since NADPH is needed for the main reaction. Here should be mentioned that co factor recycling is not obligatory when working with whole cell systems since cells provide NADPH through their natural metabolism, which is also fueled by the added glucose. Nonetheless, oversaturation of all components of the co factor recycling system prevents depletion of NADPH during the reaction and therefore hamper the possibility of a diminished activity caused by co-factor shortage. Further, a fraction of the defined total cell amount used for bioconversion will be present in broken form caused by mechanical stress during resuspending and through the lyophilization process. This results in a breakdown of the cells and as a consequence to the breakdown of the cells' metabolism. Enzymes can be released to the cells' environment. To make it more likely that the enzymes remain active in their free form, it could also be conducive to keep the entire co-factor recycling system.

4.4 IMPACT OF $NADP^+$

As mentioned above (Figure 5), NADPH supply is obligatory for the hydroxylation reaction conducted by P450s. When working with whole cell systems, the addition of external co-factor should be obsolete, however, Hanlon *et al.* suggested that addition

of the required cofactor has a positive effect on product formation [69]. Therefore, the biooxidation of chlorzoxazone after a period of 16 h was examined. Reactions took place under standard conditions as well as standard conditions where the $NADP^+$ solution was replaced with deionized water. Whole cells (lyophilized and frozen/thawed) as well as cell free extract (lyophilized) of the *E. coli* mutant 18.1 was used for biooxidation reactions. Figure 14 shows the impact of extra $NADP^+$ on product formation.

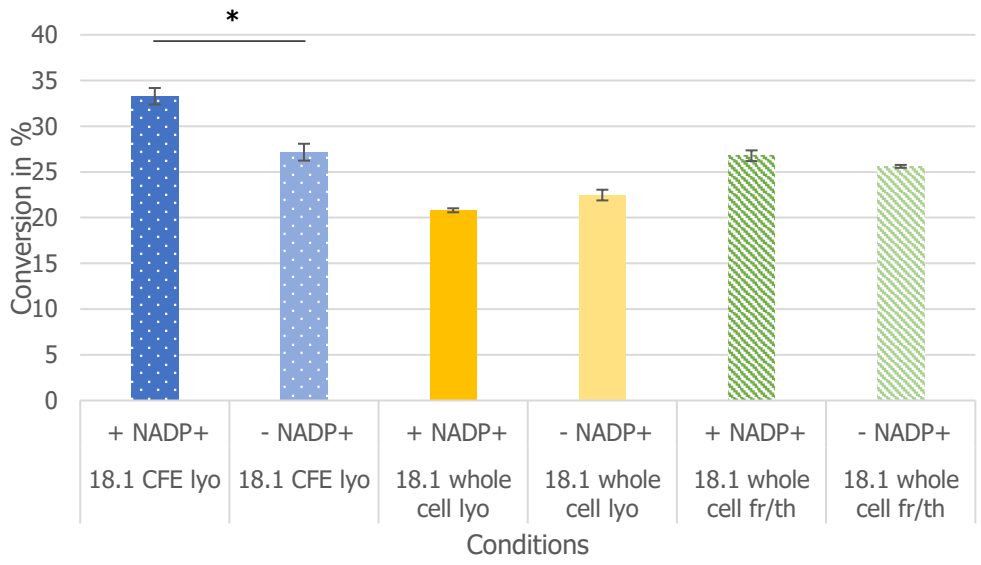

Figure 14: Impact of $NADP^+$ addition-biooxidation of chlorzoxazone by *E. coli* mutant 18.1: CFE (lyophilized), whole cells (lyophilized) and whole cells (frozen/thawed) over a period of 16 h with and without the addition of $NADP^+$; monitored in triplicates; * significantly more product formation when adding $NADP^+$

As expected, the greatest impact could be seen when cell free extract was used. When $NADP^+$ was added, about 34% conversion could be reached whereas without the co-factor about 27% product were formed. Even if there is a significantly higher product conversion when adding the co-factor, the difference of about 7% seems low. One explanation could be, that there is enough NADPH present in the cell free extract, provided through the cells metabolism before disruption. Additionally, GDH and glucose are added in the standard reaction. GDH can convert endogenous $NADP^+$ to NADPH. Further, cell free extract comprises not only the recombinant enzyme, but various host enzymes. One or more of these enzymes, could be capable of reducing the $NADP^+$ formed during the main reaction to NADPH. Another thought was, that the difference would be higher, when the reaction time, which was 16 h in this case, would have been prolonged. Since more reactions have been conducted with CFE of 18.1 over longer periods of time and chlorzoxazone, this assumption was overruled. One

reason was, that a conversion of 34% after 16 h comprises almost the maximum of conversion that we observed until now (Figure 22a: about 40% after 79 h). This fact implies that a maximum of about 12% of difference would be expected even if the reaction would run for 79 h. Again, this difference seems almost negligible, when considering the financial impact of co-factor addition (NADP-Na_2 – Roth: 1g á €109).

In accordance to our expectations, omitting or adding of the co-factor $NADP^+$ did neither increase nor decrease the amount of formed product (Figure 14) when working with whole cells. This outcome is in conformity with state of the art publications and constitutes one of the main advantages of whole cell biocatalysis [62, 64].

4.5 DETERMINATION OF APPARENT INITIAL RATE ACTIVITY OF CYP505X IN *P. PASTORIS*

Frozen/thawed *P. pastoris* cells expressing CYP505X wild-type (A15) and the CYP505X 5x mutant (A21) were used for ibuprofen biooxidation. The reaction time was 49 h at standard conditions according to the SOP (cf. 7.1). Seven end point measurements were conducted in triplicates and analyzed.

Figure 15 shows the results of the ibuprofen bioconversion for CYP505X mutant (A21). Three possible products were detected in both, the CYP505X wild-type (data not shown) and the CYP505X mutant biooxidation series. Interestingly, product formation for CYP505X wild-type starts somewhere between 3 and 16 h. After 16 h, conversion reached its maximum with about 15% of product. The 3 products were not formed in equal amounts but occurred always in approximately the same ratio. For CYP505X wild-type (A15) the product, that eluted last (P3) and the product that eluted first (P1) seem to be present in similar amounts. The product that eluted second (P2), represented approximately 1/3 of the other products. Due to the overall low conversion and the resulting three products, interpretation of the results was challenging especially regarding the 16 h value with high standard deviations. For all monitoring points after 16 h standard deviations were below 1.2 %. However, with a maximum total product formation of 15% CYP505X WT expressed in *P. pastoris* could not be considered as a catalyst for ibuprofen conversion on a preparative scale.

In contrast, the CYP505X quintuple mutant (A21) bioconversion gave traces of product already after 1 h and increased product titers steadily until 49 h, representing

approximately 50 % substrate conversion. Interestingly, the product that eluted last (P3) seems to be the most favorized for this mutant. For the other two products, ratios were the same as for the wild-type. For the CYP505X 5xmut expressed in *P. pastoris* (A21), the apparent initial rate activity[7] was calculated.

To determine the reaction rate of CYP505A30 5xmut (A21) expressed in *P. pastoris*, a trendline was drawn as a tangent to the fitted dynamical curve, which was defined by our end-point measuring points (Figure 16). The resulting tangent showed a coefficient of determination of 0.986. The calculated reaction rate *a* was 0.147 mM/h and the specific reaction rate *s* was 0.12 U/mg$_{(\text{used catalyst})}$. Generally, these values are difficult to compare to values from literature, since the reaction rates are not referred to values received from the pure CYP505X, but from the CYP used in whole cells. Further, no values are available for this specific CYP. However, compared to the reaction rates of CYP505X variants in *E. coli*, which range from 0.034 to 0.123 mM/h (determined by Lukas Kargl [70]), a reaction rate of 0.147 mM/h and a specific reaction rate of 0.12 U/mg $_{(\text{used catalyst})}$ was higher as expected.

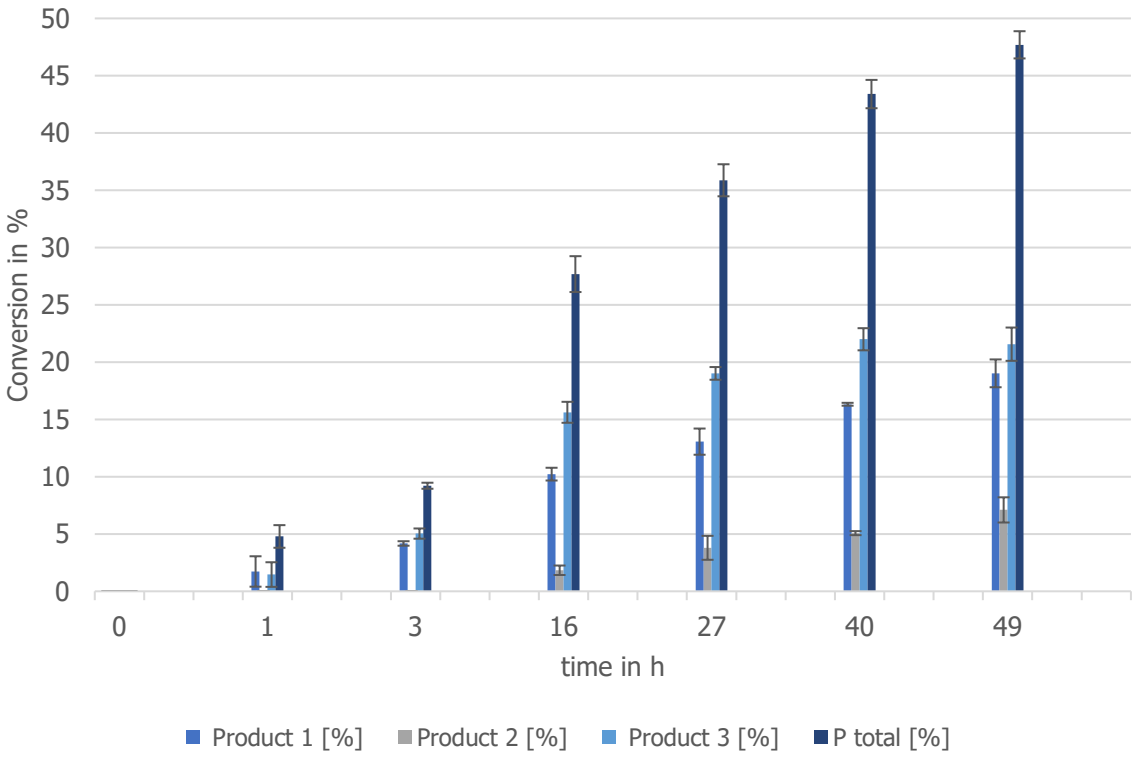

Figure 15: Whole cell ibuprofen biooxidation over 49 h by CYP505X 5xmutant (A21) expressed in *Pichia pastoris*

[7] Note that the whole cell system including cofactor recycling was studied here. Therefore, values must not be confused with enzyme kinetics of isolated CYP

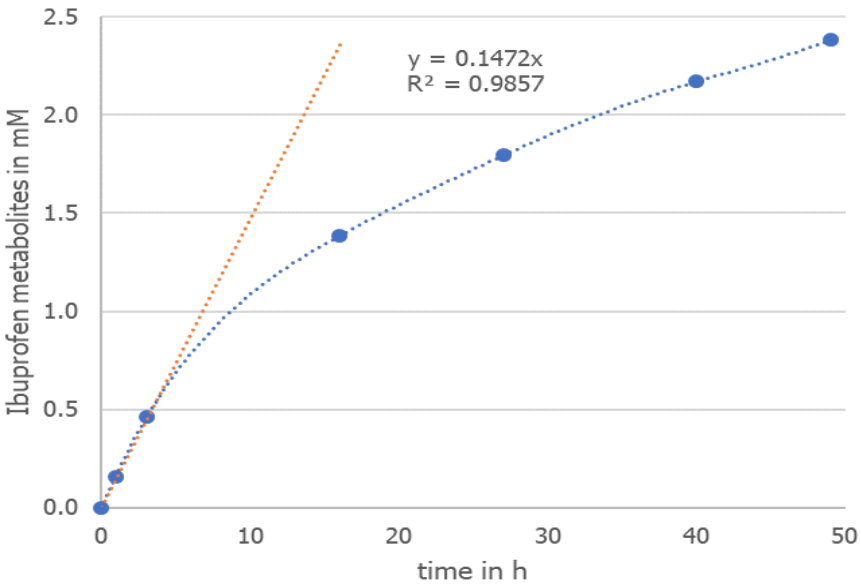

Figure 16: Determination of reaction rate *a* and specific reaction rate *s* of CYP505X 5xmut in *P. pastoris* (A21); monitoring points that followed a linear trend were used to generate a linear regression line. The slope represents the reaction rate *a*. The specific reaction rate *s* was determined by referring the reaction rate *a* to the used amount of catalyst (CDW [mg]).

4.6 INFLUENCE OF REACTION BUFFER AND GDH FEEDING – *P. PASTORIS*

Since frozen/thawed *P. pastoris* expressing CYP505X 5xmut (A21) showed good conversion of ibuprofen (Figure 15), this reaction has been chosen as a candidate for an up-scaling experiment. However, before upscaling was implemented, PS and PT buffer were evaluated as reaction buffers. Product formation under standard conditions as well as daily addition of GDH were investigated for both buffers. Reactions were monitored for 52 h. Per day, two end point measurements were conducted in duplicates.

Figure 17 shows the product formation over time for all tested conditions. No increased product formation could be reached through daily addition of GDH, indicating that GDH was not limiting. Further, no significant difference between the reaction buffers could be noticed.

Compared to the first experiment, where only PT buffer was used as reaction buffer (Figure 15), overall conversion of Ibuprofen was about 50% lower. This may be a result of repeated freezing and thawing of the cells between the experiments. Since

the results are consistent within the actual experiment, we are confident about the validity of the relative values.

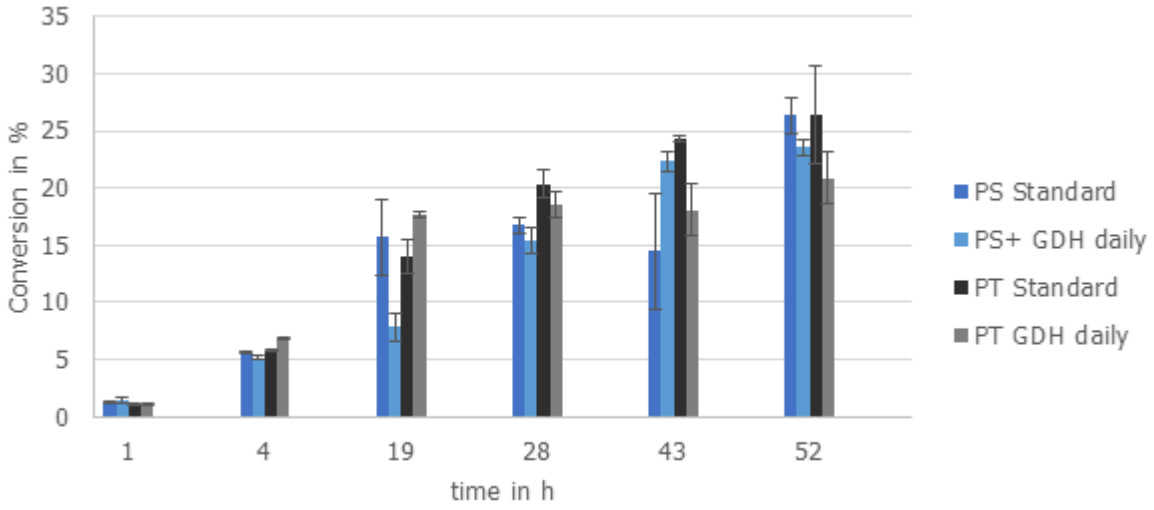

Figure 17: Ibuprofen biooxidation with frozen/thawed *P. pastoris* A21 cells expressing CYP505X 5xmut by using different buffer systems: biotransformation was conducted using 8.5% PS buffer and 1% PT buffer under standard conditions and standard conditions plus daily addition of GDH; bars represent product formation in % (blue: PS buffer, black: PT buffer) over a period of 52 h

Based on this outcome, it was decided to use 8.5% PS reaction buffer for further experiments. One reason was, that PS buffer was the preferred reaction buffer for biooxidations conducted with *E. coli* and previous experiments conducted with *P. pastoris* cells (unpublished data Winkler group). Further, regarding upscaling of CYP505 mediated bioconversions, sucrose is a more economical lyophilization additive. (D(+) Saccharose - Roth 1 kg 17.90 € vs. D(+) Trehalose-Dihydrate – Roth 10 g 25.90 €)

4.7 OPTIMAL OD_{600} FOR BIOOXIDATION WITH *P. PASTORIS* CELLS

After changing the reaction buffer in the standard operation procedure to PS 8.5%, the next aim was to determine the optimal amount of CYP505X expressing *P. pastoris* cells for biooxidation. Here, lyophilized cells were used. OD values of 25, 50, 100, 200 and 250 were assayed for biotransformation in triplicates each. For direct comparison, two substrates were investigated. Chlorzoxazone, because it represents the standard substrate and ibuprofen was chosen since it was a promising candidate for a reaction

on the preparative scale. All reactions were conducted under standard conditions in duplicates for a period of 16 h in glass vials.

In theory, one would expect, that doubling the amount of cells for conversion would lead directly to double the amount of product. This would be the result of a direct proportional behavior and thus a linear coherence.

Figure 18 shows that the highest conversion of chlorzoxazone could be reached at an optical density of 100 – 200. Further increase of cell density did not increase product formation – perhaps because of oxygen limitation or incomplete mixing due to high viscosity. Figure 19 shows the conversion of ibuprofen. For this API the optimal OD was around 100. An increase to a higher OD value also did not show enhanced product formation.

For the conversion of chlorzoxazone no obvious linear behavior can be seen for the tested OD values (Figure 18). Here should be mentioned that testing of additional values between OD 5 and OD 25 would probably reveal linear behavior in the span between OD 5 and OD 50. Regarding the catalyst efficiency an OD of 25 seems to be the best with a conversion of ≈12%. OD 50, OD 100 and OD 200 led to a conversion of ≈20%, ≈25% and ≈38%, respectively. Using an optical density of 250 did also give a conversion of ≈38%. Neglecting the "cell to product" ratio and regarding maximal product formation an OD near 200, but not higher, seems to be the best.

For the conversion of ibuprofen, OD 25 and OD 50, a linear behavior in terms of total product formation (Ptot) can be observed (Figure 19). Interestingly, this is not true for the single products P1, P2 and P3. At OD 25, P2 is completely missing. At OD 50, all three products were detected. This imbalance leads to the loss of the linear correlation of the single products. For the other OD values no linear correlation between "used cells" and "formed product" can be seen.

Regarding the ratio "used cells" and "formed product", an OD of 50 seem the best with a conversion of ≈18%. OD 100, OD 200 and OD 250 led to a conversion of ≈26%, ≈28% and ≈24%, respectively. Here should be mentioned that these values lie within the standard deviation and therefore the higher conversion cannot be seen as significant. Neglecting the "cell to product" ratio and regarding maximal product formation and OD of 100, but not higher, seems to be the best.

Possible reasons for limitation in product formation at a certain OD could be, that the substrate cannot reach all the cells. This might be due to their dense arrangement and the preset mixing rate of 120 rpm (set in SOP). If this is the case, it may be possible that at a higher mixing rate, conversion would increase. However, this suggestion would need further testing. Another suggestion was, that product inhibition could be the limiting factor. For ibuprofen and for chlorzoxazone this hypothesis will be discredited in chapter 4.12.1 and 0, because conversions of ≈82% and ≈70% were reached, respectively.

Concluding from these results we recommend using an OD of 50 to 100 in the standard operation procedure protocol since it seems to be a good compromise regarding maximal yield and used cells. Further, to work within the range of OD 50 to 100 constitutes a good chance to get a detectable amount of formed product also for poor substrates. For consistency, in this work all other experiments were conducted using OD 100. The general working protocol (cf. SOP 7.2) however, recommends using an OD of 50 for CYP505X reactions in *P. pastoris* as the host.

However, if maximal conversion of a substrate is the main objective, the optimal working OD should be evaluated for every substrate separately.

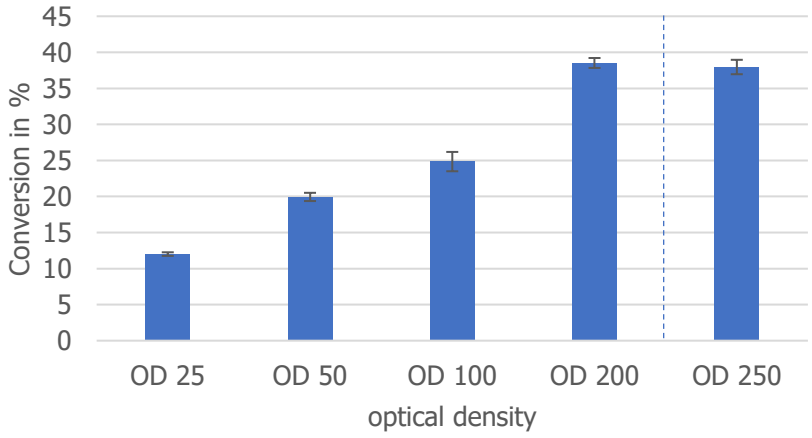

Figure 18: Chlorzoxazone biooxidation by different amounts of lyophilized *P. pastoris* cells: amount of cells that corresponds to OD_{600} values of 25, 50, 100, 200 and 250 in the final reaction volume were used; the dashed line indicates that after OD 200 the cell amount was not doubled any more

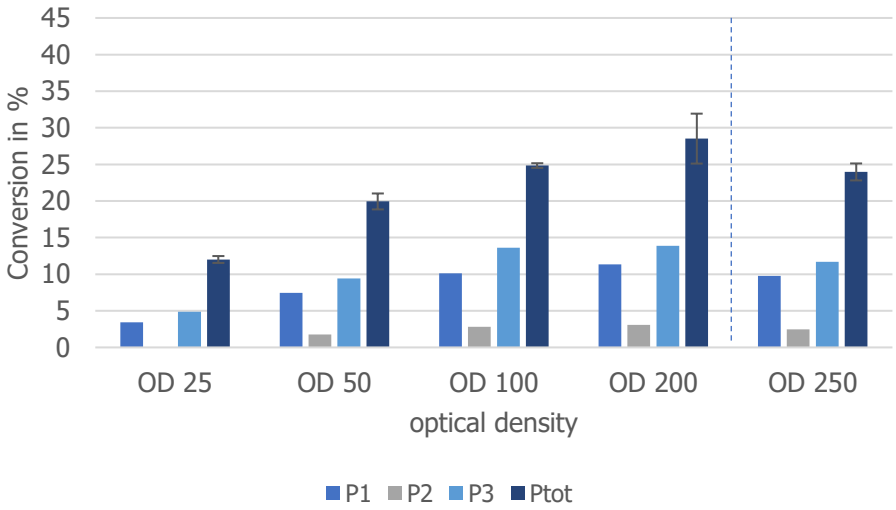

Figure 19: Ibuprofen biooxidation by using different amount of lyophilized *P. pastoris* cells: amount of cells that corresponds to OD_{600} values of 25, 50, 100, 200 and 250 in the final reaction volume were used; conversion of ibuprofen gives three monooxygenation products (P1-P3) according to HPLC/MS, Ptot is the sum of P1 to P3 and represents the overall total conversion; the dashed line indicates that after OD 200 the cell amount was not doubled any more

4.8 OPTIMAL CHLORZOXAZONE CONCENTRATION FOR CYP505X

To determinate the optimal substrate concentration for CYP505X mediated biooxidation of CX, 0.5 mM, 1 mM, 2 mM, 5 mM and 10 mM of chlorzoxazone were used (Figure 20). For each substrate concentration 11 points in time between 0 and 45 h were determined. Reactions were carried out with forzen/thawed CYP505X producing *E. coli* cells (variant 18.1) according to the protocol as described in the SOP (appendix 7.1). Reaction buffer pH 4.5 instead of 7.4 was used. First, a calibration curve was determined for CX, since product standards were not available (data not shown). Analysis and calculation was executed as described in the SOP (appendix 7.1). SigmaPlot was used to determine K_M and V_{max} (Figure 21).

Figure 20 shows the activity in µmol/min for each of the tested chlozoxazone concentrations and indicates the issue of starting substrate inhibition at concentrations of 5 mM. Values gained for 0.5 to 5 mM were transferred to SigmaPlot, while values gained for 10 mM of CX were excluded for determination of K_M and theoretical V_{max} (Figure 21). A V_{max} of 0.1449 µmol/min and a K_M of 2.8 mM were obtained. Since no further chlorzoxazone concentrations were tested in the range of 2 to 6 mM, it could not be safely stated, at which exact substrate concentration inhibition starts. Therefore, the determined V_{max} of 0.1449 µmol/min was most probably too low. Since the pH of the reaction buffer was pH 4.5 instead of an intended pH of 7.4, the

conversion was generally low. Still, the results indicate that the optimal substrate chlorzoxazone concentration is in the range between 2 to 5 mM. To get a more accurate result, more chlorzoxazone concentrations should be tested in the range between 2 and 6 mM of chlorzoxazone. For evaluation of our SOP (appendix 7.1) the results were considered as adequate, since the aim was to clarify whether 5 mM CX was a suitable substrate concentration near the optimum to get reliable results.

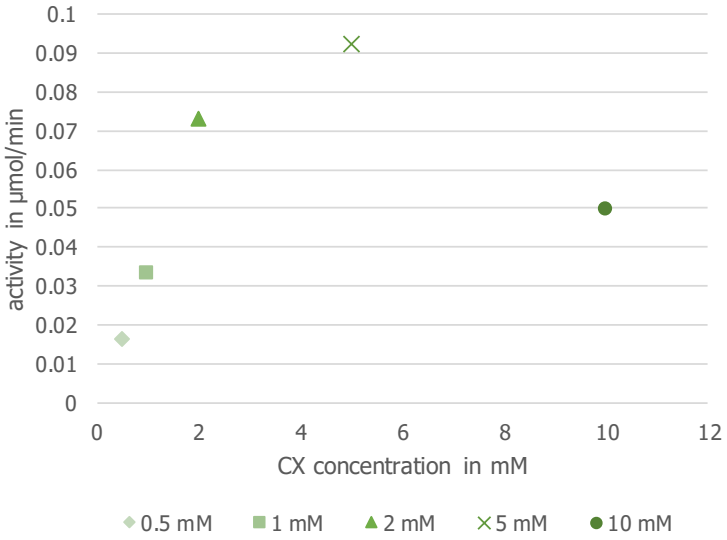

Figure 20: Determination of optimal chlorzoxazone concentration for CYP505X (variant 18.1) for whole cell biooxidations: Substrate concentrations of 0.5 mM, 1 mM, 2mM, 5 mM and 10 mM were investigated; 11 points in time in a period of 45 h were taken for each substrate concentration in duplicates

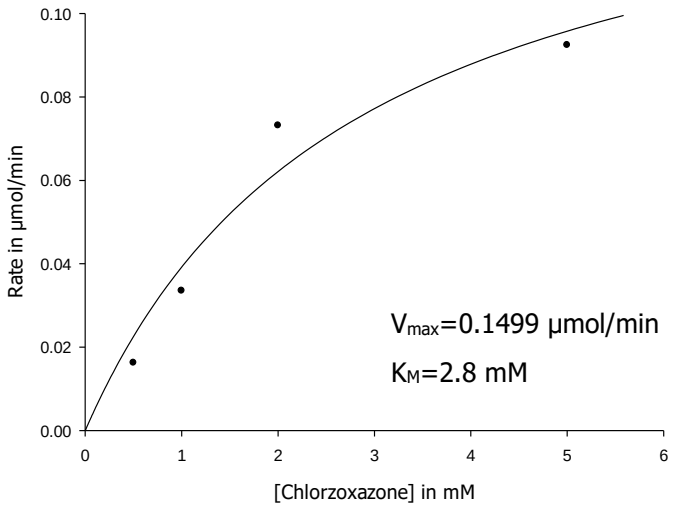

Figure 21: Determination of K_M and V_{max} for CYP505X (variant 18.1) in whole cell biocatalysis towards chlorzoxazone; validity of K_M and V_{max} is restrained by a beginning substrate inhibition in the range of 5 mM of CX: Substrate concentrations of 0.5 mM, 1 mM, 2 mM and 5 mM were investigated; 11 points in time in a period of 45 h were taken for each substrate concentration in duplicates

Further, the experiment showed, that CYP505X (variant 18.1) is exceptionally stable in whole cell biooxidations.

In preliminary experiments concerning calibration curve and dilutions for this experiment (data not shown), areas of the resulting chromatograms were often inconsistent and unexpectedly low. Most probably this was a result of substrate and/or product precipitation in the reaction vessel, where debris could be detected after the reaction, leading to a sampling error. Instead of removing 500 µl of the reaction mixture, tranferring it to a new vessel and adding 500 µl of ACN/MeOH to stop the reaction, sampling errors can be avoided by adding 1 ml of ACN/MeOH directly to the reaction vessel. Since Nunclon ∆ Surface 24-well plates are composed of PS (polystyrene) and therefore are not resistant against all solvents, it was tested, if this procedure has any impact on the results. Since adding of 1 ml of ACN/MeOH to the initial reaction volume of 1 ml, showed no visible effect on the Nunclon ∆ Surface 24-well plates (not directly after adding and also not after 24h), biooxidations were carried out according to the SOP (with the new stopping procedure) and chromatograms were compared to previous measurements (data not shown). No negative influence could be detected, instead, peak areas reached expected values and results became significantly more reliable.

4.9 CELL FREE EXCTRACT (CFE) FOR API OXIDATIONS

4.9.1 BUFFER OPTIMIZATION AND GDH FEEDING

Since CFE was more efficient than cells for Chlorzoxazone oxidation (see 4.3), we investigated whether lyophilization of CFE influenced the biooxidation activity. Therefore *E. coli* harboring CYP505X wild-type (variant 2.1) and the mutant with the highest activity towards chlorzoxazone (variant 18.1) were cultivated. The cells were resuspended to OD 100 in water, PS buffer pH 7.4 (1 or 8.5% sucrose, respectively) or PT buffer pH 7.4 (1% trehalose), sonicated and the CFE obtained after centrifugation. The supernatants were aliquoted in 24-well plates and lyophilized. The oxidation of chlorzoxazone was monitored under standard conditions. GDH stability in solution had been investigated by J. Wielińska (lab notebook 1075\JOW, 11/09/2017-21/09/2017). Upon incubation of GDH in solution at 28°C for about 72h, GDH lost 64% of activity. Therefore, we hypothesized that GDH feeding may increase the biooxidation

efficiency. The oxidation of CX was monitored using standard conditions and fresh portions of GHD were added daily.

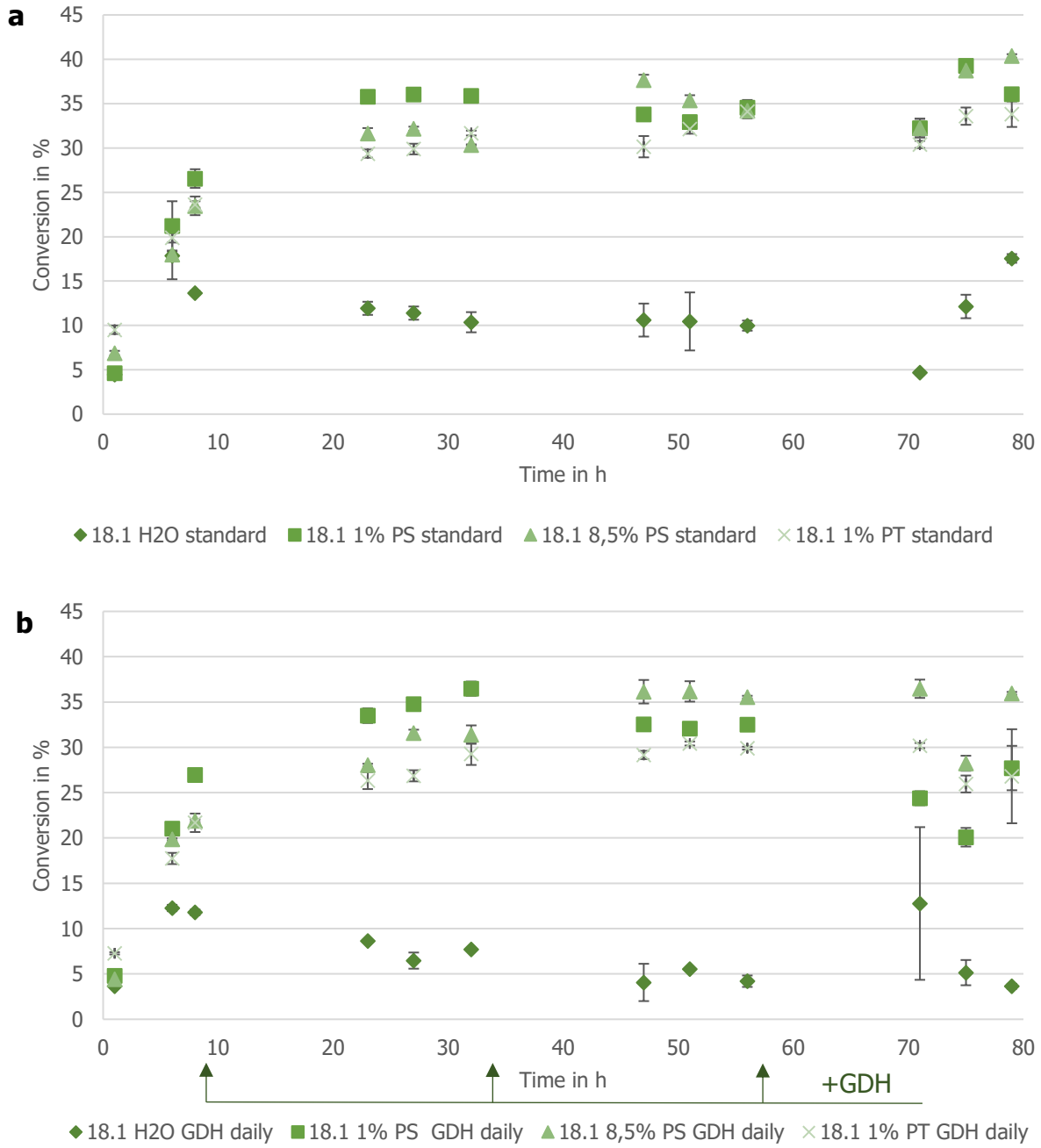

Figure 22: Formation of 6-hydroxy-chlorzoxazone catalyzed by lyophilized cell-free extract: CFE of best variant (18.1) in different buffers (H_2O, 1% and 8.5% PS, 1% PT) under standard conditions (a) and standard conditions + daily addition of GDH (b). Every point in time was measured in duplicates

Figure 22a shows the biooxidation of chlorzoxazone catalyzed by variant 18.1 over a time period of 79 h. Highest activity of CYP505X could be observed when phosphate buffer containing sugars was used. For a prolonged reaction, 8.5% PS buffer appeared to be the best choice, because a maximum conversion of about 40% could be reached.

1% PS buffer and 1% PT buffer showed a maximum product formation of about 35%. Stability of CYP505X in H_2O seems to decrease already after 6-8 hours and maximum product formation was about 18%. Figure 22b shows the same experiment with daily GDH addition. No improvements could be observed, suggesting that GDH stability was not a bottleneck.

For the wild-type (2.1) a similar result regarding conversion ratios was obtained, although the overall conversion was lower, as expected, with a maximum of about 9% (data not shown).

Using lyophilized CFE for biooxidation could represent a promising alternative to lyophilized whole cells, especially when poor substrate uptake may cause low or no reaction. For the CYP505X variant 18.1, probably an improvement of about 12% in product formation (6-hydroxychlorzoxazone) could be observed (cf. Figure 12 and Figure 22a) after 16 h. For the wild-type variant 2.1 no enhanced product formation could be observed compared to whole cells. Since product formation of 32% is already reached after a reaction time of 23 hours which only increased slowly to about 40% after 79 hours, longer reaction times than 23 hours are not considered as reasonable. Whether CYP505X stability or other factors are responsible for a stagnant product formation is not entirely clear. Yet, it seems that CYP505X stability could be the main reason. An indication therefore is, that the enzyme seems to be only active for the first 8 hours when water was used. Addition of lyophilization stabilizers like sucrose and trehalose led to a longer activity resulting in higher conversion rates. Other parameters like co-factor depletion or product inhibition should also be considered. However, a possible co-factor depletion due to instability of glucose dehydrogenase can be ruled out, since daily addition of freshly prepared GDH stock solution did not have any impact in product formation (cf. Figure 22a and Figure 22b). Product inhibition cannot be completely ruled out on basis of the performed experiments but seems unlikely since product conversion of about 70% could be reached with the same enzyme variant in *P. pastoris* in a preparative scale reaction (0).

However, comparison of activity of CYP505X variant 18.1 in a lyophilized whole cell system, and as lyophilized CFE regarding 6-hydroxychlorzoxazone formation, did not show sizeable differences. Maximum conversion (about 28%) was reached after 22 -

28 hours in lyophilized whole cell systems (data Lukas Kargl). With CFE a conversion of about 32% could be reached after 23 - 27 hours (Figure 22a). Interestingly, but not surprisingly, product formation proceeded faster when CFE was used. About 22% vs. 9% 6 -OH-chlorzoxazone was formed after 8 hours (Figure 22a vs. data Lukas Kargl). Most likely the substrate can more easily be accessed by the free catalyst. In whole cells, the substrate must be transported into the cell to reach CYP505X. Another possible reason could be, that oxygen, which is required for the reaction, solely could be used for enzyme catalyzed reactions (CYP505X catalyzed reactions as well as possible side reactions) when cell free extract is used. In whole cell systems, the cells themselves also need oxygen.

4.9.2 ACTIVITY OF CYP505X TOWARDS APIS: A COMPARISON OF CFE AND WHOLE CELL BIOCATALYST

A panel of substrates was tested with the specified conversion parameters, given in the SOP (appendix 7.1). Especially APIs, were no conversion could be seen when whole cells were used, were selected. CYP505X variants 11.1, 13.1, 15.1, 18.1 and 19.1 were engineered based on published knowledge about CYP102A1 (BM3), which was reported to convert testosterone. In our hands, CYP505X variants, however, did not show any activity towards the said substrate under biotransformation conditions with lyophilized whole cells (unpublished data Winkler group). For that reason, they were cultivated again and tested in different forms (frozen/thawed whole cells and cell free extract (CFE)) for different substrates. The results suggest, that using CFE instead of whole cell systems is significantly more efficient for some substrates (Bisy report 12/2017 and chapter 4.9.1). Therefore, 22 APIs were screened with four CYP505X variants (2.1, 7.1, 18.1 and 19.1) and CFE instead of whole cells. For direct comparison Table 11 gives an overview of the biooxidation results of the tested substrates by CYP505X variants when CFE was used (left) and previously gained data (retrieved from Table 1), when lyophilized whole cells were used (right).

Table 11: Analytical biooxidation yield of CYP505X variants 2.1, 7.1, 18.1 and 19.1 in CFE expressed in *E. coli* towards 22 selected substrates compared to whole cells; reactions with CFE were carried out in triplicates, data for whole cell bioconversion were taken from Table 1; N=negative ☐, T=trace ☐, values [%]: <1-10 ☐, 11-50 ☐, >50 ☐ multiple values represent multiple products: order from top (product that eluted last) to bottom (product that eluted first)

Substrates	Biocatalyst formulation: Lyophilized CFE				Biocatalyst formulation: Lyophilized whole cells (Data taken from Table 1 for direct comparison)			
	cyp505 2.1 M1	cyp505 7.1 M4	cyp505 18.1 M9	cyp505 19.1 M10	cyp505 2.1 M1	cyp505 7.1 M4	cyp505 18.1 M9	cyp505 19.1 M10
Benzydamin	N	N	N	N	N	N	N	N
Caffein	N	N	N	N	N	N	N	N
Capsaicin	3.6 19.8 46 1.9	2.3 0 2.9 13.1	7.5 1.4 13.7 8	11.9 13.7 22.1 24.6	59 26	9 11	12 28 10 3	15 33 14 2
Chlorzoxazone	9	1	41	34	7	N	25	16
Clopidogrel	N	N	N	N	N	N	5	2
Dextrometorphan	N	N	N	N	N	T	N	T
Diclofenac	T	T	T	T	N	N	N	N
Estriol	N	N	N	N	N	N	2	N
Famciclovir	N	N	N	N	N	N	<1	<1
Harmine	N	N	N	N	N	N	N	N
Hydrocortisol	T	T	T	T	N	N	N	N
Ibuprofen	0 1.6 0	0 0 4	10,5 <1 9	11 0 17	N	<1	8 7	13 6
Lidocain	N	N	N	N	N	N	N	N
Moclobemide	N	N	N	N	N	N	N	N
2-Naphthol	3 5 2	4 29 1	4 18 2	3 17 <1	N	12	6	2
Phenacetin	N	N	N	N	N	N	N	N
Piperine	T	T	T	T	N	N	<1	N
Progesterone	N	T	2	3	N	N	6 6	4 7
Propranolol	T	T	T	T	N	N	N	N
Salbutamol	N	N	N	N	N	N	N	N
Testosterone	N	N	4.2 2	13 2,3	N	N	N	N
Tolbutamide	<1	1	1	2	N	N	1	2

Table 11 summarizes the results.For seven of the 22 tested substrates, no effect on activity by using cell free extract compared to lyophilized whole cells could be detected. Still, no activity could be detected towards benzydamine, caffeine, harmine, lidocaine, moclobemide, phenacetin and salbutamol.

For four of the tested substrates, no activity could be detected by using CFE, where at least low activity could be seen, when lyophilized whole cells were used. In case of clopidogrel, CYP505X variants 18.1 and 19.1 reached 5% and 2% conversion when freeze-dried whole cells where used, while no activity could be seen, when lyophilized

CFE was used. In case of dextromethorphan CYP505X variant 7.1 and 19.1 showed traces of product formation when whole cells were used, while they did not, when CFE was used. For estriol, where variant 18.1 showed 2% product formation and for famciclovir, where variant 18.1 and 19.1 showed product formation <1%, also no conversion could be detected when CFE was used.

For six of the substrates, CYP505X activity could be detected by using cell free extract, where no activity was detected by using whole cells or only for some of the tested CYP505X variants. In case of diclofenac, hydrocortisone and propranolol for all of the tested variants traces of product could be seen by using CFE, while none of the CYP505X variants showed activity by using whole cells. In case of piperine, traces of product could be detected for the 4 CYP505X variants when CFE was used, while only for variant 18.1 product <1% could be detected when whole cells were used. In case of progesterone, the overall conversion seemed to be lower by using CFE: CYP505X variant 18.1 and 19.1 with a conversion of 2% and 3% (single product) versus multiple products for these variants in whole cells with an overall conversion of 12% (6% + 6%) and 11% (4% and 7%). Only for variant 7.1 the use of CFE seemed to be an improvement, where traces of product could be detected while no product could be seen by using whole cells. In case of tolbutamide, CYP505X variant 18.1 and 19.1 seemed to perform equally with 1% and 2% formed product no matter if CFE or whole cells were used. Only the wild-type and variant 7.1 seemed to be more active towards tolbutamide when CFE was used (<1% and 1% conversion) compared to whole cells (no conversion).

In case of capsaicin, where multiple products are formed, no improvement regarding overall conversion could be seen for CYP505X using of CFE. All variants and the wild-type showed lower or equal total conversion: wild-type (2.1) 71% vs. 85% conversion; variant 7.1 18% vs 20% conversion; variant 18.1 31% vs. 53% and variant 19.1 62% vs. 64%. Interestingly, the number of formed products (one to four formed products) as well as the distribution of these products differed. Differences could be observed among the variants themselves and regarding biocatalyst formulation depending on whether CFE or whole cells were used. For the wild-type (2.1) four products could be detected and for the variant 7.1 three products could be detected when CFE was used,

while using of whole cells resulted in only two products. For variants 18.1 and 19.1 four products were formed no matter, if CFE or whole cells were used.

In case of testosterone, CYP505X variant 18.1 and 19.1 in CFE performed better than the same variants in whole cell bioconversions where no conversion was detected. Two metabolites were formed. About 4.2% P1 and 2.0% P2 (18.1) as well as 13% P1 and 2.3% P2 (19.1) of product could be detected. Event though, these variants were designed upon CYP102A1 which is known to convert testosterone, we did not expect this outcome, since no conversion could be detected with these variants when using other biocatalyst formulations (lyophilized whole cells or frozen/thawed cells). This fact makes this observation even more remarkable. Wild -type CYP505X (variant 2.1) and CYP505X variant 7.1 were not able to hydroxylate testosterone, neither by using CFE nor by using whole cells.

For chlorzoxazone, significant improvements for all 4 CYP505X variants could be detected. When CFE was used, the wild-type CYP505X, variant 7.1, 18.1 and 19.1 reached 9%, 1%, 41% and 34% conversion, respectively. In contrast, the same variants reached 7%, 0%, 27% and 16% of conversion, when lyophilized whole cells were used. In case of CYP505X variant 18.1, these data and the data gained in chapter 4.9.1. further confirm the assumption that using lyophilized CFE is more effective in chlorzoxazone biooxidation than use of lyophilized whole cells.

In case of 2-naphthol, the four tested CYP505X variants showed higher activities towards the substrate when CFE was used (wild-type 2.1: 10% overall conversion, variant 7.1: 34% overall conversion, variant 18.1: 20% overall conversion and variant 19.1: 20% overall conversion) compared to lyophilized whole cells (wild-type 2.1: no conversion, variant 7.1: 12% conversion, variant 18.1: 6% conversion and variant 19.1: 2% conversion). Interestingly, three metabolites were formed according to HPLC/MS analysis when CFE was used where only one product was detected when whole cells were used. For all the variants the distribution of the three formed metabolites was consistent while P1 (eluted last) and P3 (eluted first) were less favored and P2 (eluted second) was always the most favored metabolite.

In case of ibuprofen, the four tested CYP505X variants showed higher activities towards the substrate when CFE was used (wild-type 2.1: 1.6% overall conversion,

variant 7.1: 4% overall conversion, variant 18.1: 20% overall conversion and variant 19.1: 28% overall conversion) compared to lyophilized whole cells (wild-type 2.1: no conversion, variant 7.1: <1% conversion, variant 18.1: 15% conversion and variant 19.1: 19% conversion). Interestingly, the number of metabolites (0-3 metabolites: P1 eluted last, P2 eluted second, P3 eluted first) differed not only due to used CYP505X variant but also due to biocatalyst formulation (lyophilized CFE or lyophilized whole cells). CYP505X wild type converted ibuprofen to one metabolite (1.6% conversion) when CFE was used, while no conversion could be detected when whole cells were used. When CFE was used CYP505X variant 7.1 also produced one metabolite (4% conversion) while they only converted 1% of ibuprofen when whole cells were used. Noteworthy, according to HPLC/MS analysis, the metabolite formed by the wild-type CYP505X and the variant 7.1 are not the same and elute at different points in time. The wild-type CYP505X preferred P2, while variant 7.1 preferred P3. Variant 18.1 (used in CFE) formed three metabolites, where P1 and P3 were preferred with amounts of 10.5% and 9%. P2 was only formed to an extent of <1%. When whole cells were used, 2 metabolites were formed. Most likely, these 2 metabolites are the same as P1 and P3 (when CFE were used). CYP505X variant 19.1 (CFE) produced two metabolites P1 and P3 with an extent of 11% and 17%. When whole cells were used, also 2 metabolites were formed with an extent of 13% and 6%.

Summarizing these results, using CYP505X in cell free extract instead of whole cells can be advantageous in regards of substrate acceptance. Even if for many tested substrates (7 out of 22) no improvement could be reached and for a few no conversion could be detected, where at least minor activity could be seen, when whole cells were used (4 out of 22), for some substrates improvement could be reached (11 out of 22). Most likely, the improved efficiency of CYP505X in cell free extract is a result of facilitated enzyme – substrate interaction. Whereas the cell wall and membranes in whole cell systems could be a major constraint, the substrate can be easily accessed when using cell free extract. Further, possible substrate and/or product toxicities could be a reason for reduced performance of CYP505X in whole cells. In this case, it could be beneficial, to change the reaction environment to a liquid two phase system, where in case of product toxicity, the product is continuously extracted into the organic phase. Interestingly, our results are contradictory to results in literature. Bracco *et al.* stated,

that CYP154C5 from *Nocardia farcinica* shows much higher conversion rates when whole cells were used compared to CYP154C5 in cell free extract [71]. Also, Bronwyn E. White *et al.* observed lower activities when working with CYP153A6 in CFE compared to other biocatalyst formulations [72]. In both cases, the better performance in whole cell systems compared to CFE was attributed to the protecting environment provided by the cells. However, since none of them did work with the same CYP as we did, direct comparison may be problematic.

Still, it should be mentioned that according to our results, CYP505X in form of cell free extract can outperform whole cell systems and therefore represents an applicable biocatalyst formulation.

4.10 ACTIVITY OF CYP505X TOWARDS FATTY ACIDS AND ALIPHATIC COMPOUNDS

We investigated if CYP505X variants lost their ability to accept fatty acids since they are natural substrates of CYPs. Therefore, we investigated the activity of CYP505X wild-type and variants of CYP505X towards lauric acid (Figure 24) and undecanoic acid (Figure 25). Furthermore, we investigated the activity towards undecatriene (Figure 26).

Therefore, biooxidation was performed under standard conditions using lyophilized whole cells expressing CYP505X variants and an empty vector control. Duplicates were used for each of the variants. After 16 h, reaction was stopped and product formation was investigated using GC/MS (fatty acids) and GC/FID (undecatriene). To get more reliable results, data were normalized by using tetradecane as internal standard.

As expected, CYP505X wild-type (2.1) showed high activity towards lauric acid (Figure 27) with a conversion of about 96% and towards undecenoic acid (Figure 28) with a conversion of about 86%. Variant 7.1 showed also high activity towards lauric acid. Here should be mentioned, that giving a concrete value is not possible since the standard deviation was high (± 30%). Still, the relatively high activity towards lauric acid in this case was interesting since variant 7.1 was engineered to convert geranylacetone. Geranylacetone belongs to the super class of lipids and lipid-like molecules and differs structurally from lauric acid (cf. Figure 23 and Figure 24).

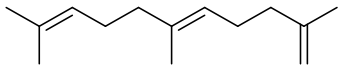

Figure 23: Structure of geranylacetone

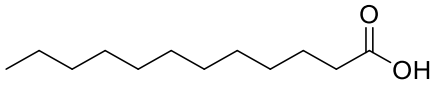

Figure 24: Structure of lauric acid

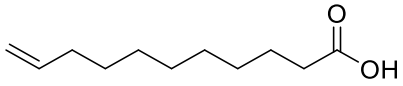

Figure 25: Strucutre of undecenoic acid

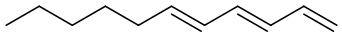

Figure 26: Structure of undecatriene

Aside from CYP505X variant 7.1, variants 9.1, 15.1, 18.1 and 19.1 accepted lauric acid as substrate with an overall conversion between 8 and 22%. Further, variant 11.1 and 13.1 converted lauric acid to an extent of 2.5% and 0.5%. Even if all of these variants were designed in regard to convert different defined substrates and therefore harbor different amino acid substitutions, they have one feature in common: they all have substitution F90A. Only variant 5.1 and 21.1 did not show any affinity to lauric acid. Interestingly, they do not have substitution F90A, which could mean, that phenylalanine at position 90 contributes to the acceptance of lauric acid in the modified CYP505X variants.

Figure 28 shows that for undecenoic acid, the overall picture is the same as for lauric acid (Figure 27), even if the overall conversions are lower (for all modified CYP505X variants < 4%). In contrast to lauric acid, CYP505X variant 7.1 shows low activity towards undecenoic acid. That was surprising, since lauric acid ($C_{12}H_{24}O_2$) (Figure 24) and undecanoic acid ($C_{11}H_{20}O_{2)}$ (Figure 25) are structurally closely related.

Another difference was, that CYP505X variant 11.1 did not show any conversion in case of undecenoic acid, while it accepted lauric acid as substrate.

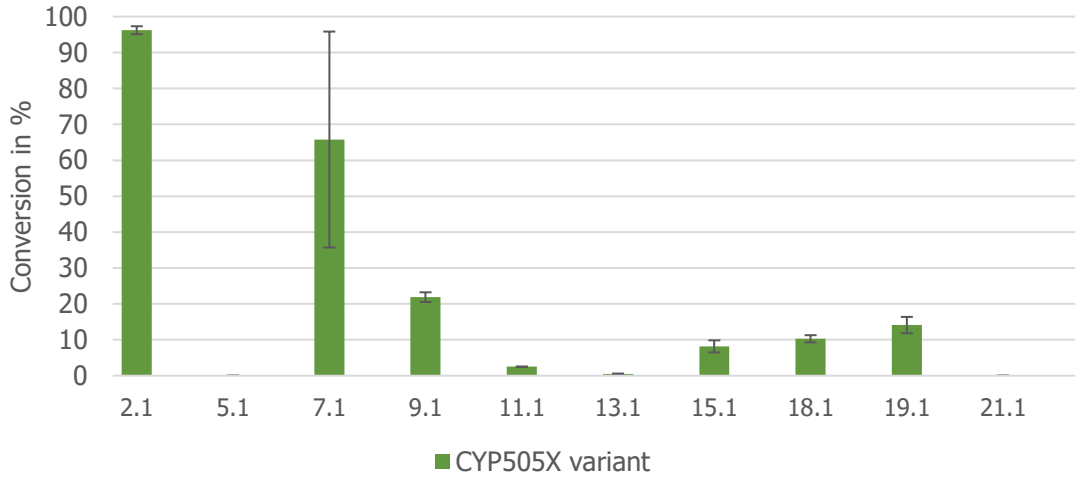

Figure 27: Biooxidation of lauric acid using wild-type and CYP505X variants expressed in *E. coli*; biocatalyst formulation: lyophilized whole cells; reaction time: 16h; reaction conditions: (see 3.4.9.1)

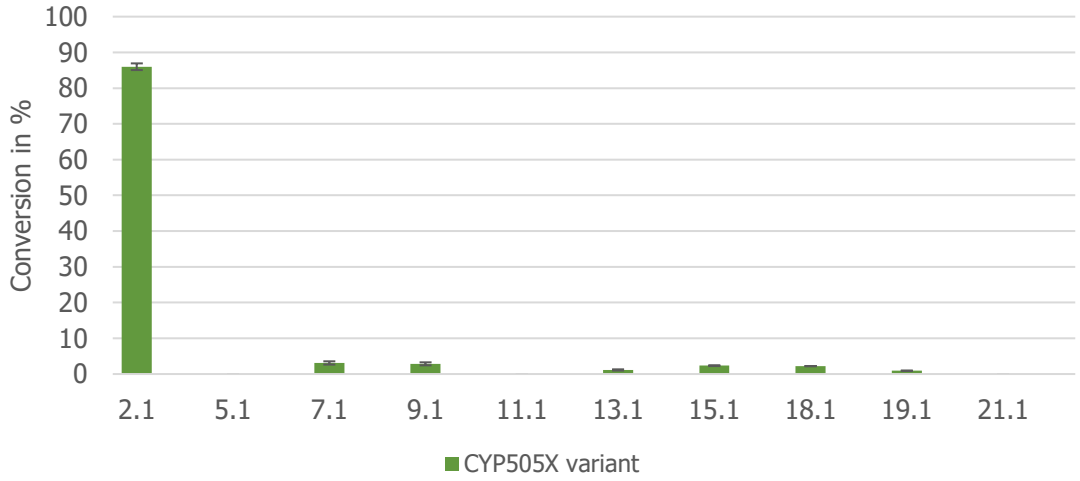

Figure 28: Biooxidation of undecenoic acid using wild-type and CYP505X variants expressed in *E. coli*; biocatalyst formulation: lyophilized whole cells; reaction time: 16h; reaction conditions: (see 3.4.9.1)

Finally, we saw that the wild-type CYP505X in lyophilized whole cells can convert fatty acids, which are their natural substrates. This happened, as expected to high extent and proves functionality of CYP505X in lyophilized whole cell systems. Further, modified variants lost their ability to convert their natural substrates partly or even totally.

Regarding undecatriene, no activity could be detected at all. Neither for any of the tested CYP505X variants nor for the CYP505X wild-type (data not shown).

4.11 API OXIDATION BY CYP505A30

Wild-type CYP505A30 and variants in purified form (Table 5) and the respective strains (Table 4) were investigated[8]. CO spectra and NADPH depletion tests were made at RUG and our aim was to test the enzymes with respect to their substrate scope.

4.11.1 PRELIMINARY EVALUATION OF CYP505A30: ACTIVITY OF PURIFIED CYP AND CYP IN WHOLE CELLS TOWARDS LAURIC ACID, CHLORZOXAZONE AND IBUPROFEN

Firstly, a GC/MS method for the determination of oxidized lauric acid hydroxylation was established. Purified enzymes were assayed first. Under the tested conditions, $P450_{BM-3}$ wild-type and CYP505A30 wild-type showed full conversion of lauric acid (mainly to the ω-1 product but also ω-2 and ω-3) whereas the *M. thermophila* 3x and 5x mutant did not oxidize the substrate under the tested conditions. Next, the strains were cultivated under the conditions suggested by M.J.L.J. Fürst (RUG) (see 3.4.2). The pellets were either frozen at -20 °C or lyophilized and stored at -20 °C and then used to determine their activity for the lauric acid hydroxylation as described in 3.4.9.1.

Table 12: CYP505A30 and CYP102A1 mediated whole cell biooxidation of lauric acid, chlorzoxazone and ibuprofen; biocatalyst formulations: frozen/thawed and lyophilized; reaction time: 16 h, each reaction was carried out in triplicates; < 20% -, 21-40% +, 41-60% ++, 61-80% +++, 81-100% ++++

Strain	**CYP**	**Lauric acid**	**Lauric acid**	**Chlorzoxazone**	**Ibuprofen**
		frozen/thawed	lyophilized	frozen/thawed	frozen/thawed
E. coli BL21 (DE3)	none	-	-	-	-
E. coli BL21 (DE3)	CYP505A30 wt	+++	++	+	+
E. coli BL21 (DE3)	CYP505A30 3x	+++	++	-	-
E. coli BL21 (DE3)	CYP505A30 5x	++++	+++	-	-
E. coli NEB10-beta	CYP102A1 ($P450_{BM-3}$)	-	-	-	-
E. coli NEB10-beta	none	-	-	-	-

Consistent with the expression data (Figure 9a), *M. thermophila* CYP505A30 variants showed activity under biotransformation conditions as described in our SOP (appendix 7.1). Surprisingly, $P450_{BM-3}$ did not. According to Figure 9a, it was not expressed at all, or to an extent that was too little to be visualized by Coomassie staining. Sequencing results (data not shown) from isolated plasmids retrieved from cultivated strains

[8] Provided by Fürst, M. & Fraaije, M., University of Groningen

according to the protocol (see 3.4.2) revealed, that $P450_{BM-3}$ was present in the plasmid.

Preliminary screening showed weak activity of the wild-type *M. thermophila* CYP505A30 for the oxidation of chlorzoxazone and ibuprofen (Table 12).

4.11.2 ACTIVITY OF CYP505A30 TOWARDS APIS: A COMPARISON OF WHOLE CELL BIOCATALYST AND PURIFIED ENZYME

Based on the results in Table 12, general activity of CYP505A30 in whole cells could be confirmed by applying the standard operation procedure protocol (cf. 7.1, chapter 5 and 6). Therefore, we decided to screen for activity towards a panel of APIs. The same substrates as for the screening CYP505X in form of cell free extract were used (see Table 11). Depending on the performance of the whole cell biooxidations, additional experiments with the purified CYP505A30 variants and the respective substrates were conducted (Table 13).

Results described in 4.11.1 revealed that frozen/thawed cells showed significantly higher activities towards lauric acid. Therefore, we used frozen/thawed cells instead of lyophilized cells (as stated in the SOP) for these experiments, to increase the probability of a positive hit since a lower activity, where only traces of product are produced, would have led to a false-negatives. To eliminate false-positive results, *E. coli* BL21 and NEB10beta strains which lacked their respective CYP (cf. Table 4) were used as negative controls. In case of purified enzymes, reactions were conducted as described in chapter 3.4.9.2.

Both, reactions with whole cells and reactions with purified enzymes were stopped after 16 to 17 h and product formation was analyzed by HPLC/MS. Concerning whole cell biooxidations, each reaction was carried out in triplicates. Since only limited amount of purified enzyme was available, unicates were used in case of bioconversions with purified enzyme.

Table 13: Analytical biooxidation yield of frozen/thawed CYP505A30 and CYP102A1 expressing *E. coli* towards 22 selected substrates: reactions with whole cells were carried out in triplicates, reactions with purified enzymes were carried out as unicates; N/T = not tested □, N=negative □, T=trace □, values [%]: <1-10 □, 11-50 □, >50 □, multiple values represent multiple products: order from top (product that (eluted last) to bottom (product that eluted first)

Substrates	Biocatalyst formulation: frozen/thawed whole cells				Biocatalyst formulation: purified enzyme			
	cyp505A30 WT	cyp505A30 3xmut	cyp505A30 5xmut	Cyp102A1 WT	cyp505A30 WT	cyp505A30 3xmut	cyp505A30 5xmut	Cyp102A1 WT
Benzydamin	N	N	N	N	N/T	N/T	N/T	N/T
Caffein	N	N	N	N	N/T	N/T	N/T	N/T
Capsaicin	1.2 10.2 76.7 6.6	12.4 3.4 57.8 0	6.1 3.8 22.7 0	N	6.1 5.6 19.8 0	3.6 0 0 0	1.83 5.2 <1 0	10.9 6.7 18.1 2.4
Chlorzoxazone	28.7	N	N	N	1.5	N	N	<1
Clopidogrel	N	N	N	N	N/T	N/T	N/T	N/T
Dextrometorphan	N	N	N	N	N/T	N/T	N/T	N/T
Diclofenac	N	10.2	2.4	N	N	N	N	N
Estriol	N	N	N	N	N/T	N/T	N/T	N/T
Famciclovir	N	N	N	N	N/T	N/T	N/T	N/T
Harmine	N	N	N	N	N/T	N/T	N/T	N/T
Hydrocortisol	N	N	N	N	N/T	N/T	N/T	N/T
Ibuprofen	14.9 11.5 16.7	3.6 <1 5.8	4.5 4 29	N	11.8 7.5 10.2	N	N	N
Lidocain	T	T	T	N	N/T	N/T	N/T	N/T
Moclobemide	N	N	N	N	N/T	N/T	N/T	N/T
2-Naphthol	5.6 <1 5.9	5.8 1 5.3	6.4 <1 3.7	<1 <1 1.6	N	N	N	N
Phenacetin	23.5	T	T	N	1.5	N	N	N
Piperine	T	T	T	N	T	T	T	T
Progesterone	N	N	N	N	N	N	N	N
Propranolol	N	N	N	N	N/T	N/T	N/T	N/T
Salbutamol	N	N	N	N	N/T	N/T	N/T	N/T
Testosterone	N/T	N/T	N/T	N/T	N	N	N	N
Tolbutamide	1.5	<1	3.5	N	N	N	N	N

Table 13 shows that for 13 of the 22 tested substrates, no activity could be detected when whole cells were used for biooxidation, neither for CYP505A30, nor for CYP102A1. In case of CYP102A1, again the low expression in the cells could be a reason (cf. 4.11.1). Since none of the CYP variants used in whole cells showed conversion of benzydamine, caffeine, clopidogrel, dextromethorphan, estriol, famciclovir, harmine, hydrocortisone, moclobemide, progesterone, propranolol, and salbutamol, no further experiments were made with purified enzymes. Only testosterone was investigated with purified enzymes since no data was available for

the whole cell screening. However, no hydroxylated product could be detected under these conditions.

For nine of the 22 substrates, products was detected using whole cells. Therefore, biooxidation reactions were repeated with purified enzymes.

In case of diclofenac, CYP505A30 wt and CYP102A1 wt did not show any activity. Interestingly, the engineered variants CYP505A30 3xmut and 5xmut showed conversions of 10.2% and 2.4%, respectively. No product formation could be detected when the respective purified enzymes were used for bioconversion. Compared to CYP505X, where at least all tested variants showed traces of products when CFE was used (Table 11), only CYP505A30 3xmut and 5xmut showed product formation - but, with a much higher extent. CYP505X mediated biooxidation with whole cells did not show any product formation. Even if direct comparison is not possible since frozen/thawed cells were used for CYP505A30 mediated biooxidation and lyophilized cells or CFE was used for CYP505X mediated bioconversion, CYP505A30 seems to be more active towards diclofenac.

In case of tolbutamide, whole cell biooxidation gave conversions of 1.5%, <1%, 3.5% and no reaction for CYP505A30 wt, 3xmut, 5xmut and CYP102A1, respectively. In contrast, no conversion could be detected for the respective purified CYPs.

In case of 2-naphthol, all variants of CYP505A30 as well as CYP102A1 showed formation of multiple products when whole cells were used. With total conversions of about 12.4%, 12.1% and 11.1%, all tested CYP505A30 variants seemed to convert 2-naphthol equally. Regarding the individual products, CYP505A30 wt and CYP505A30 3xmut seemed to favor P1 (eluted last) and P3 (eluted first) with balanced conversion with 5.6% and 5.9% (CYP505A30 wt) and 5.8% and 5.3% (CYP505A30 3xmut). P2 was only converted to an extent of about 1% in both cases. In contrast, distribution of the products formed by CYP505A30 5xmut, showed a slightly different trend. Here, P1 seemed to be the favored product with conversion of about 6.4%, while P3 was only produced in about 3.7%. Again, P2 was less favored and emerged in about 1%. CYP102A1 showed, compared to CYP505A30, lower total product formation with about 2.2%. P1 and P2 were found to an extent less than 1%. P3 was formed to an extent of about 1.6%. Here should be mentioned, that bioconversion of 2-naphthol gave the

only positive hit regarding CYP102A1 in whole cells in course of this screening. Further, none of the purified CYPs showed conversion of this substrate.

In case of lidocaine and piperine, whole cell bioconversions revealed at least traces of products for all CYP505A30 variants. No product could be detected, when CYP102A1 was used. Since piperine seemed to be a more promising candidate, bioconversion with the purified CYPs was also conducted. Here, traces of product could be detected, for all of the tested CYPs (CYP505A30 and CYP102A1). As far as CYP102A1 is concerned, the lacking activity in whole cell biotransformation, could be a result of low concentration in the cells (see 4.11.1).

In case of chlorzoxazone, CYP505A30 wild-type in whole cells showed product formation of 28.7% while the related 3x mutated and 5x mutated variant as well as the CYP102A1 wild-type did not show any activity. Biooxidation with the related purified enzymes revealed significantly lower conversion for CYP505A30 wt (1.5%), while also no conversion could be detected for the 3x and the 5x mutant. Only CYP102A1 showed minor conversion of <1%. CYP505A30 wt outperforms CYP505X wt in regards of chlozoxazone biooxidation (28.7 % conversion (frozen/thawed cells) versus 9% conversion (CFE) and 7% conversion (lyophilized whole cells, respectively). However, engineered variants of CYP505X clearly outperformed the engineered variants of CYP505A30, for which no product formation could be detected (cf. Table 11 and Table 13).

In case of phenacetin, wild-type CYP505A30 and its related variants showed activity towards the substrate in whole cell bioconversion. Product formation of about 23.5% were reached by CYP505A30 wt, where only traces could be detected for CYP505A30 3xmut and 5xmut. No products were formed by CYP102A1. The respective purified CYPs managed to convert 1.5% of phenacetin in case of CYP505A30 wt. No conversion could be detected for the purified CYP505A30 3xmut and 5xmut or CYP102A1 wt. Interestingly, the detected products for the CYP505A30 wt and its 3xmut and 5xmut variant seemed not to be the same according to their MS spectra. CYP505A30 produced a product that exhibited 152 g/mol while CYP505A30 3xmut and 5xmut produced a product that exhibited 196 g/mol. Most likely, the 196 g/mol product represents the hydroxy-phenacetin, which was expected to be formed. The 152 g/mol product is most

likely acetaminophen (paracetamol) which is formed due to a deethylation. Phenacetin is a common prodrug of acetaminophen, which is also is also formed by human CYPs like for example CYP1A2 [73].

Compared to CYP505X mediated biooxidation (whole cells and CFE, Table 11), which did not show any activity towards phenacetin, CYP505A30 wt did with an extent of 23.5%. Also, the CYP505A30 3xmut and the 5xmut variant showed traces of product formation (Table 13). Again, direct comparison was difficult, since different biocatalyst formulations were used.

In case of capsaicin, all variants of CYP505A30 (CYP505A30 wt, 3xmut and 5xmut) showed multiple product formation when whole cells were used, while *E. coli* expressing CYP102A1 did not show any product formation. With total conversions of about 94.7%, 73.6% and 32.6%, respectively, the wild type showed a remarkably high conversion rate. The related purified CYPs (CYP505A30 wt, 3xmut and 5xmut as well as CYP102A1) showed significantly lower conversion with total conversion rates of about 31.5%, 3.6%, 7.7% and 38.2%, respectively. Interestingly, the number of formed products (one to four formed products) as well as the distribution of these products differed. Differences could be observed among the variants themselves and regarding biocatalyst formulation depending on whether whole cells or purified CYPs were used. Using whole cell biooxidation, CYP505A30 wild-type converted capsaicin to 4 products (Figure 29), while for variant 3xmut and 5xmut only three products were detected (lacking P4 (mass=338 g/mol)). Generally, CYP505A30 wt as well as variant 3xmut and 5xmut clearly showed preference for P3 (mass=304 g/mol) and converted a sizable part of their total conversion to that product. The second favored product for CYP505A30 wt seemed to be P2 (mass=322 g/mol), whereas variant 3xmut and 5xmut show higher formation of P1 (mass=304 g/mol), which initially was the expected product. Using purified CYPs for biooxidation, as expected, the CYP505A30 wt showed higher conversion compared to its related 3xmut and 5xmut variant. Interestingly, products lacked P4. In conformity with the whole cell bioconversion results, P3 was the favored product. But, the preference to P1 and P2 changed (almost equal conversion, instead of favorized P2). For purified CYP505A30 3xmut only one product (P1) could be detected. Interestingly, for CYP505A30 5xmut, three products (P1-P3) were detected again. But now, the preferred product changed from P3 to P2.

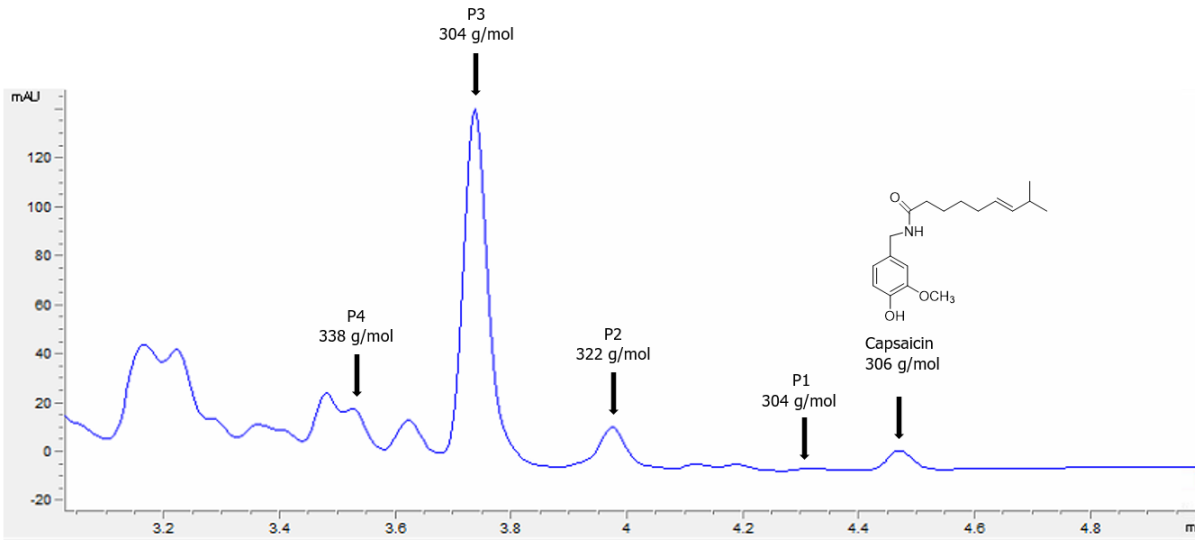

Figure 29: Excerpt of the HPLC/MS analysis of capsaicin biooxidation by CYP505A30 wild-type in frozen/thawed whole cells; shown is the chromatogram of the UV trace where masses of substrate and metabolites were added to the corresponding peaks; MS traces are not shown; Given masses correspond to M+1 due to positive ionization mode; capsaicin: RT 4.45 min, 306 g/mol; P1: RT 4.33 min, 304 g/mol; P2: RT 4.00 min, 322 g/mol; P3: RT 3.74 min, 304 g/mol; P4: RT 3.53 min, 338 g/mol

For CYP102A1, 4 products (representing the same masses as products of CYP505A30), were detected. Again, the favored product was P3, followed by P1 and P2 and finally P4. Migglautsch *et al.* (2018) managed to identify 2 of the 4 metabolites as 8-OH-capsaicin (P3 in this work) and *N*-(4-hydroxy-3-methoxybenzyl)-5-(3-isopropyloxiran-2-yl)pentanamide (P2 in this work) [74] .

In case of ibuprofen, all variants of CYP505A30 (wt, 3xmut and 5xmut) showed multiple product formation when whole cells were used, while *E. coli* expressing CYP102A1 did not show product formation. With total conversions of about 43.1%, 10.3% and 37.4%, respectively, the wild type and the 5xmut variant showed significantly higher conversions compared to the 3xmut variant. Biooxidations with the respective purified CYPs (CYP505A30 wt, 3xmut and 5xmut as well as CYP102A1) did only give product formation in case of CYP505A30wt with a total amount of 29.4%. Interestingly, the number of formed products (three products) stayed constant among the variants, but the distribution of these products differed. While the wild-type CYP505A30 as well as the 3xmut convert ibuprofen to relatively eve amounts to P1 (14.9% and 3.6%, respectively) and P3 (16.7% and 5.8%, respectively), the 5xmut variant showed significantly higher amounts of P3 (29%) compared to P1 (4.5%). Further, the wild-type CYP505A30 also formed P2 to a noteworthy amount (11.5%) compared to the 3xmut variant (P2=<1%) and the 5xmut variant (P2=4%). As

expected, the purified CYP505A30 wt showed the same distribution pattern of P1, P2 and P3 (11.8%, 7.5% and 10.2%, respectively) as CYP505A30 wild-type in whole cells.

Converting capsaicin, CYP505A30 wt seemed to outperform CYP505X wt mediated whole cell biooxidation in regards of formed product (94.7 % total conversion to 85% total conversion, respectively) and also CYP505X mediated biooxidation in CFE (71.3% total conversion) (Table 11). Further, the engineered variants also showed higher conversion rates for CYP505A30 compared to CYP505X. However, a direct comparison is not possible due to the fact that frozen/thawed cell were used for API screening with CYP505A30 and lyophilized cells and CFE were used for API screening with CYP505X.

Summarizing the results of the screening for CYP505A30 substrates revealed some promising results. Using CYP505A30 in whole cells under the conditions set in our SOP can lead to better performance of the biocatalyst compared to the related purified CYP. Even if for many tested substrates (13 out of 22) no activity could be detected, some compounds were converted to one or more products (9 out of 22). With a total conversion of 94.7% (CYP505A30 wild-type) and 73.6% (CYP505A30 3xmut), capsaicin was the most promising candidate for a following implementation of preparative scale experiment. Since experiments on preparative scale were already done with CYP505X and capsaicin [74], we decided to choose another substrate.

Further, CYP505A30 wild-type and CYP505A30 5xmut showed promising results for ibuprofen metabolite formation. Here, the wild-type produced roughly the same amount of P1 (14.9%) and P3 (16.7%) and a noteworthy amount of P2 (11.5%) comprising a total conversion of 43%. On the contrary, the 5xmut variant produced mainly the P3 metabolite (29%), where P1 and P2 were only produced to an extent of about 4.5% and 4% from a total conversion of about 37.4%. Even if the total conversion rates may not be excellent, the distribution pattern of the formed metabolites was pivotal here and led to the decision to implement an experiment on the preparative scale with both, the CYP505A30 wild-type and the CYP505A30 5xmut (cf. 4.12.3 and 4.12.4).

The activity towards APIs of the purified CYP505A30 compared the related CYPs in whole cell biooxidations, were significantly lower or sometimes, no activity could be found at all. Even if a definite proof is not available by now, this fact was mainly

attributed to a reduced stability of the CYP in purified form. A prominent hint for that assumption was, that the results were consistent. For none of the tested compounds, a higher activity could be found when the purified CYP was used. When conversion in whole cells was already low, no conversion could be seen when the purified form was used. Further, lower stability of the purified enzymes in biooxidation compared to whole cell biocatalysis is commonly known. After all, enzyme stabilization is one of the reasons why whole cell biocatalysis is so interesting.

4.12 PREPERATIVE SCALE API BIOOXIDATIONS

Promising enzyme/substrate combinations on the analytical scale were chosen in order to implement preparative scale reactions. For both, CYP505X as well as CYP505A30, an upscaling to a total reaction volume of 500 ml was realized. Reaction parameters were kept the same as for the analytical experiments. All components were multiplied by a factor of 500 (due to the increase of the total reaction volume from 1 ml to 500 ml, cf. methods 3.4.11.1). Since upscaling reactions aim to reach maximum possible conversion, frozen/thawed cells were used instead of lyophilized cells.

In case of CYP505X, the 5xmut variant (A21) expressed in *P. pastoris* was chosen as appropriate biocatalyst. Chlorzoxazone was chosen as a substrate since this API has not been used as a substrate for preparative scale reactions using *Pichia pastoris* before. Further, ibuprofen was chosen as a 2nd substrate, since three metabolites were formed to a total amount of about 47% (Figure 15)This offered the chance to obtain sufficient amounts of API metabolites for structural characterization by NMR.

In case of CYP505A30, ibuprofen was chosen as substrate. Here, the wild-type CYP505A30 was used, because it converted almost equal amounts of the three products (P1-P3) (cf. Table 12). Additionally, the 5xmut variant of CYP505A30 was chosen as biocatalyst because it significantly produced more amounts of P3 (eluted last of the three products) (cf. Table 12).

The progression of product formation was checked periodically for each of the reactions. Therefore 500 µl samples were removed from the reaction volume from time to time, stopped with the same amount of ACN/MeOH and then analyzed using HPLC/MS. When no significant increase of product formation could be detected, the reaction was stopped by freezing the broth at -20°C. There, the samples were stored

until further processing, which included extraction with ethyl acetate, separation of the fractions using HPLC and finally, identification of the metabolites by NMR spectroscopy.

4.12.1 IBUPROFEN BIOOXIDATION BY CYP505X 5XMUT (A21) IN *P. PASTORIS*

Figure 30 shows the progression of ibuprofen biooxidation by CYP505X 5xmut in *P. pastoris* (A21) over a time of 30.5 hours. Several samples were withdrawn and analyzed by HPLC/MS during this period to determine conversion. After 22 hours about 81% of substrate were converted and only increased to about 83% after 30.5 hours. Therefore, the reaction was stopped at that time. The data indicate that reaction could already have been stopped between 7 and 22 hours. As expected, three metabolites were formed to an extent of 30.1% (P1), 16.7% (P2) and 30.5% (P3).

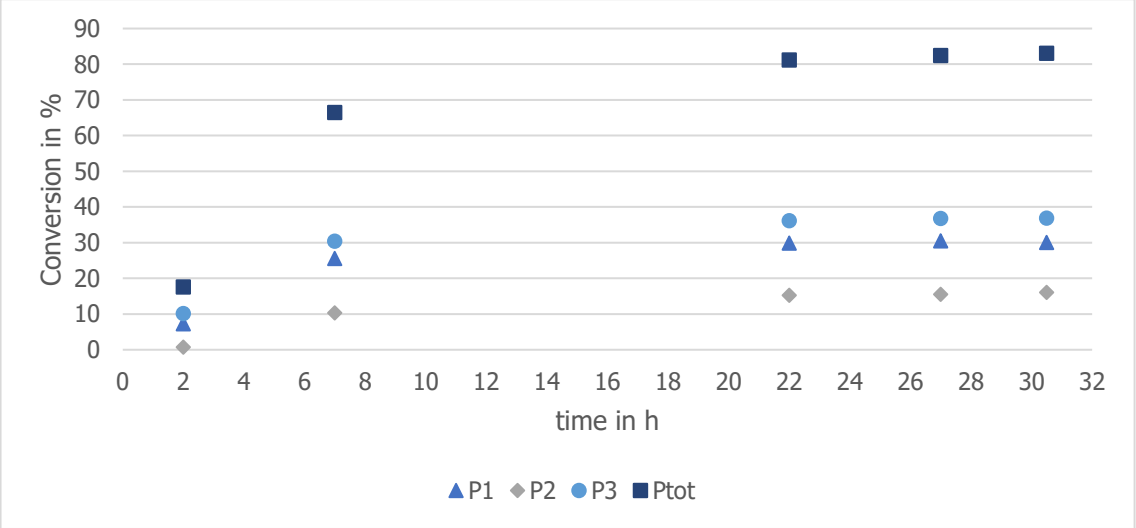

Figure 30: Ibuprofen biooxidation by CYP505X 5xmut expressing *P. pastoris* cells (A21 frozen/thawed): reaction volume: 500 ml; bioconversion conditions: according to SOP (upscaled from 1 ml to 500 ml); conversion of ibuprofen gives three monooxygenation products (P1-P3) according to HPLC/MS, Ptot is the sum of P1 to P3 and represents the overall total conversion

According to HPLC/MS, P1 to P3 had a mass of 221 g/mol and therefore are most likely 1-OH-ibuprofen, 2-OH-ibuprofen or 3-OH-ibuprofen. Purification of the fractions by HPLC turned out to be challenging and very time consuming. We tried to identify the products (gathered by pooling the fractions of 11 runs (cf. 3.4.11.4.2) by NMR analysis. Results showed that our developed extraction method as well as our fraction purification method were not optimal. Since no clear results could be gathered with this method, we tried to identify the formed metabolites by matching the gained fragmentation patterns against fragmentation patterns found in literature.

Neunzig *et al.* published MSD spectra of 2-OH- and 3-OH-ibuprofen [75]. Even if they measured in negative ion mode, we tried to compare our chromatograms and MSD spectra with their data, since previous measurement of ibuprofen conversion were performed in negative mode (unpublished data T. Bachler) and chromatograms look the same. Unfortunately, we were also not able clearly identify any of the products (P1 to P3) with this approach. Since we presumed, that one of these metabolites would be 2-OH-IBU, which is commercially available, we purchased a standard (LGC, item no.: DRE-C14278160). Comparison of the NMR spectra revealed, that P1 is indeed 2-hydroxyibuprofen (Figure 31).

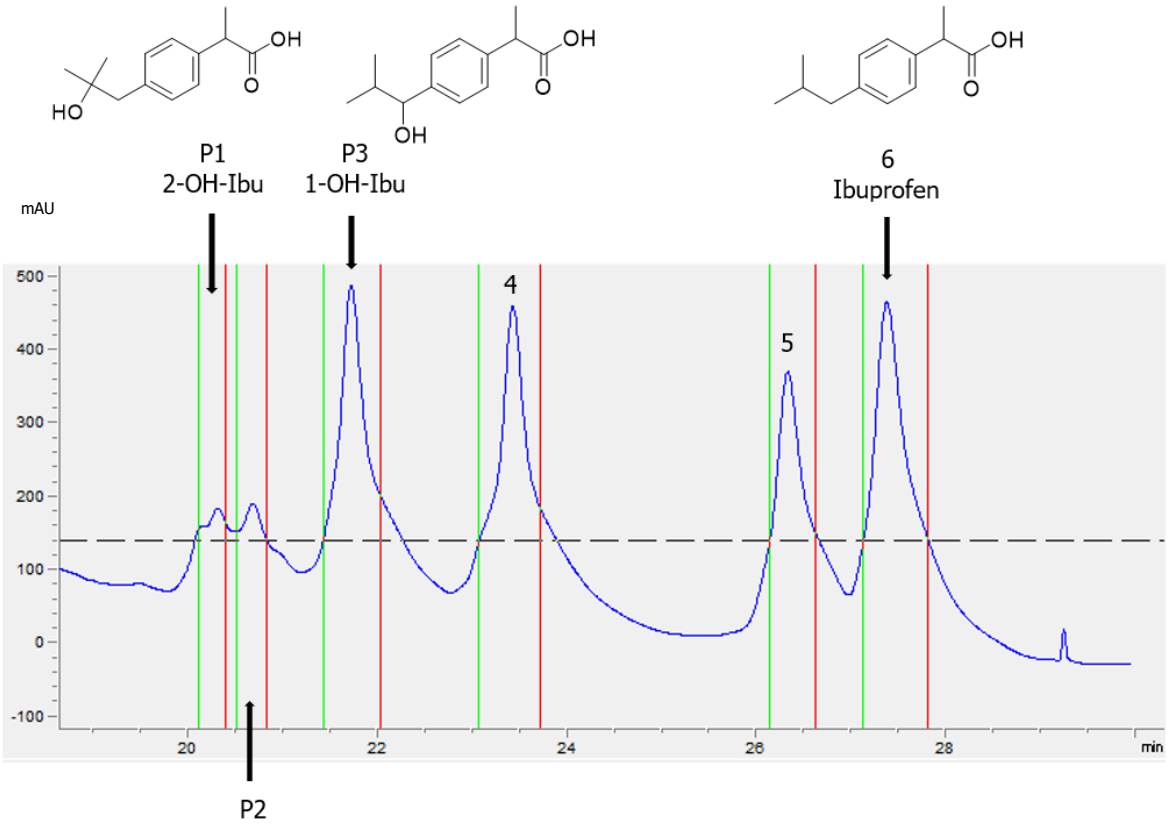

Figure 31: Chromatogram of CYP505X mediated ibuprofen bioconversion in *P. pastoris* on preparative scale and chemical structures of analyzed fractions; P1= 2-hydroxyibupofen (2-OH-Ibu), P2= unknown, P3= 1-hydroxyibuprofen (1-OH-Ibu), fraction 4 and fraction 5 = unknown (most probably extraction artefacts), fraction 6= Ibuprofen; fraction collection settings: threshold 137.918 mAU (indicated by dashed line), up slope 0.10 mAU/s, down slope 5 mAU/s, start of a single fraction collection: indicated by green line, stop of a single fraction collection: indicated by red line

Since the main restriction for a clear NMR signal was the little yield of the isolated metabolites, we decided to collect more material. Therefore, the respective fractions of 100 runs were collected, pooled and lyophilized (cf. 3.4.11.4.2). With this approach P3 could clearly be identified as 1-hydroxyibuprofen (Figure 31).

Even if we do not know by now, what exactly the remaining ibuprofen metabolite besides 1-OH-Ibu and 2-OH-Ibu formed by CYP505X is, a total conversion of about 83% seems promising and makes further investigation and optimization reasonable. However, this high conversion rate was surprising, since on analytical scale, the highest total conversion reached was about 47% (cf. Figure 15 Figure 17). Better oxygen supply and better mixing in bigger reaction vessels might be the reason for the observed increased conversion rates. Also, the fact that frozen cells were used for conversion instead of lyophilized ones might have contributed.

4.12.2 CHLORZOXAZONE BIOOXIDATION BY CYP505X 5XMUT (A21) IN *P. PASTORIS*

Figure 32 shows the progression of chlorzoxazone biooxidation by CYP505X 5xmut in *P. pastoris* (A21) over 24 hours. Several samples were withdrawn and analyzed by HPLC/MS during this period to estimate the conversion. After seven hours, about 69% of substrate were converted to one product: 6-OH-chlorzoxazone. After 24 hours, no increase of product formation could be detected and therefore, the reaction was stopped at that time. The data indicate that reaction could already have been stopped after seven hours.

Again, an enhanced 6-OH-chlorzoxazone formation could be detected on the preparative scale (69%) compared to analytical scale (about 40% by lyo CFE, cf. Figure 22). With a conversion of 63% after 2 hours the reaction seems to proceed much faster compared to the analytical scale.

Like for ibuprofen, the extraction and fraction purification method were not optimal. Instead of inefficient preparative HPLC, metabolite and substrate were purified by use of a silica gel column (cf. 3.4.11.4.1). The metabolite was identified as 6-OH-chlorzoxazone by NMR analysis. Initially 442.5 mg chlorzoxazone were used. 69% of conversion would lead to a theoretical product yield of 305 mg. However, 147 mg of 6-OH-CX could be recovered, which represents 48.2% of isolated yield. As expected,

the total recovery is not optimal, but can be easily explained due to inefficient extraction from the bulk liquid and also by loss of sample during method evaluation. With a price of 57 € per 25 g (Sigma Aldrich, item no.: C4397-25G), chlorzoxazone is cheap compared to 6-OH-CX (Sigma Aldrich, item no.: UC148-5MG, 760 € per 5 mg). Assuming further optimization in extraction and product workup, CYP505X driven production of 6-OH-CX could constitute a reasonable alternative to conventional methods.

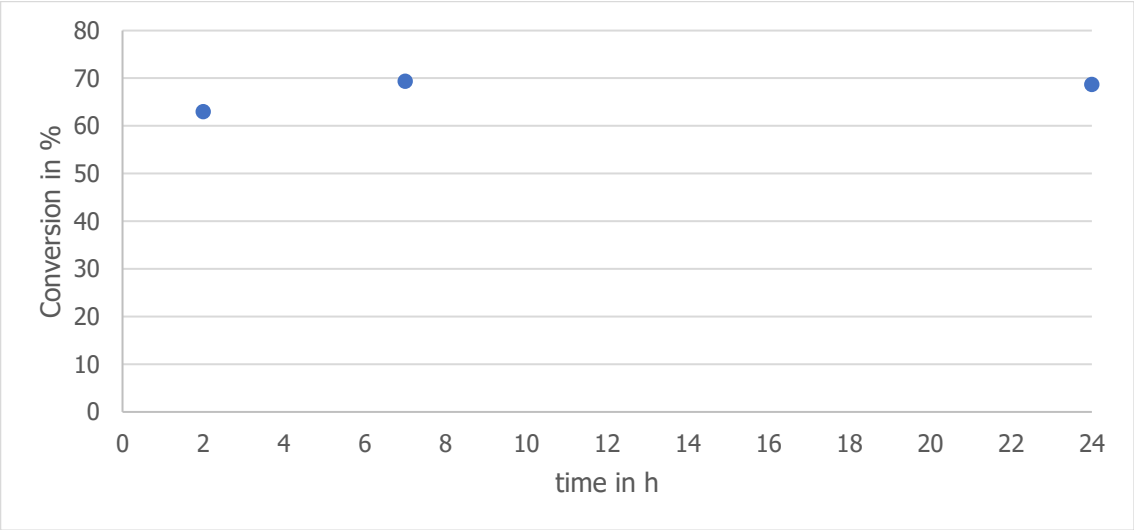

Figure 32: Chlorzoxazone biooxidation by CYP505X 5xmut expressing *P. pastoris* cells (A21 frozen/thawed): reaction volume: 500 ml; bioconversion conditions: according to SOP (upscaled from 1 ml to 500 ml); conversion of CX gives one monooxygenation product (6-OH-CX) according to HPLC/MS

4.12.3 IBUPROFEN BIOOXIDATION BY CYP505A30 WT IN *E. COLI*

Figure 33 shows the progression of ibuprofen biooxidation by CYP505A30 wild-type in *E. coli* over a time of 9 hours. Several samples were withdrawn and analyzed by HPLC/MS during this period to estimate the maximum conversion. After 8 and 9 hours about 58% and 59% of substrate were converted, respectively. Data showed no further increase of product formation and therefore, the reaction was stopped at that time.

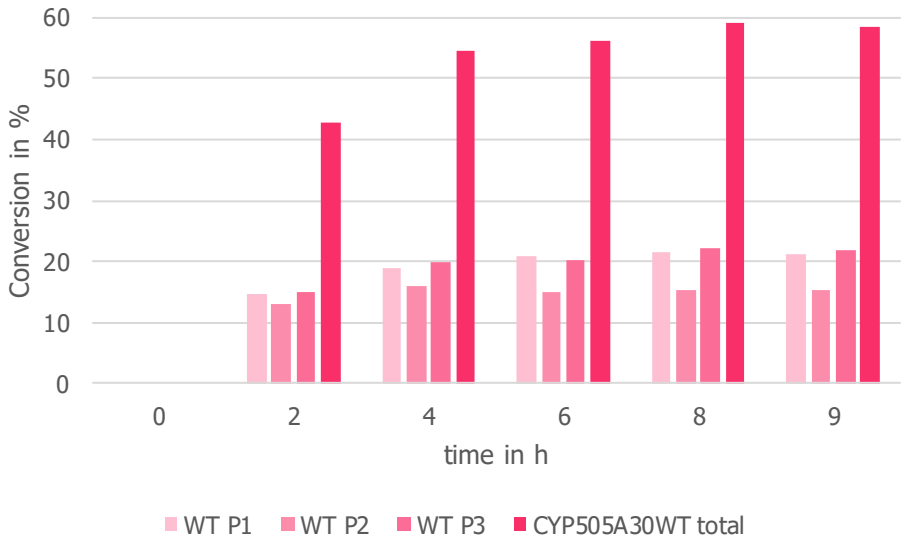

Figure 33: Ibuprofen biooxidation by CYP505A30 wt expressing *E. coli* cells (frozen/thawed): reaction volume: 500 ml; bioconversion conditions: according to SOP (upscaled from 1 ml to 500 ml); conversion of ibuprofen gives three monooxygenation products (P1-P3) according to HPLC/MS, Ptot is the sum of P1 to P3 and represents the overall total conversion

As expected, three metabolites have been formed showing a preference for P1 and P3 with a conversion of 21% and 22%, respectively and a third product with about 15% conversion (P2).

Again, the total conversion rates were higher for the preparative scale experiment compared to the analytical scale (about 59% total conversion vs. about 43% (cf. Table 13)). Here should be mentioned, that the total conversion rate could possibly be further increased, when 2L unbaffled flasks would be used as bioconversion vessel instead of baffled ones. Compared to *P. pastoris*, *E. coli* cells seemed to be highly stressed by the baffles which led to damaged cells and enormous foam building due to denatured proteins during biooxidation. Increased foam building could already be detected between two and four hours.

HPLC/MS data indicate, that the three metabolites formed are the same as formed by CYP505X in *P. pastoris* (cf. 4.12.1.). However, using the same extraction protocol seemed not be successful in this case, since no product peaks could be detected after extraction and evaporation. Interestingly, the substrate peak was still prominent. We speculated that the metabolites dehydrated to sterol derivatives which polymerized and formed insoluble gel.

4.12.4 IBUPROFEN BIOOXIDATION BY CYP505A30 5XMUT IN *E. COLI*

Figure 34 shows the progression of ibuprofen biooxidation by CYP505A30 5xmut in *E. coli* over a time of 9 hours. Several samples were withdrawn and analyzed by HPLC/MS during this period to estimate the maximum conversion. After 8 and 9 hours about 37% of substrate were converted. Data showed no further increase of product formation and therefore, the reaction was stopped at that time.

In this preparative scale experiment, the total conversion rate was not higher for the preparative scale experiment compared to the analytical scale, but about the same with 37% for both (cf. Table 13). Again, product formation may be increased by using an appropriate reaction vessel (see 4.12.3)

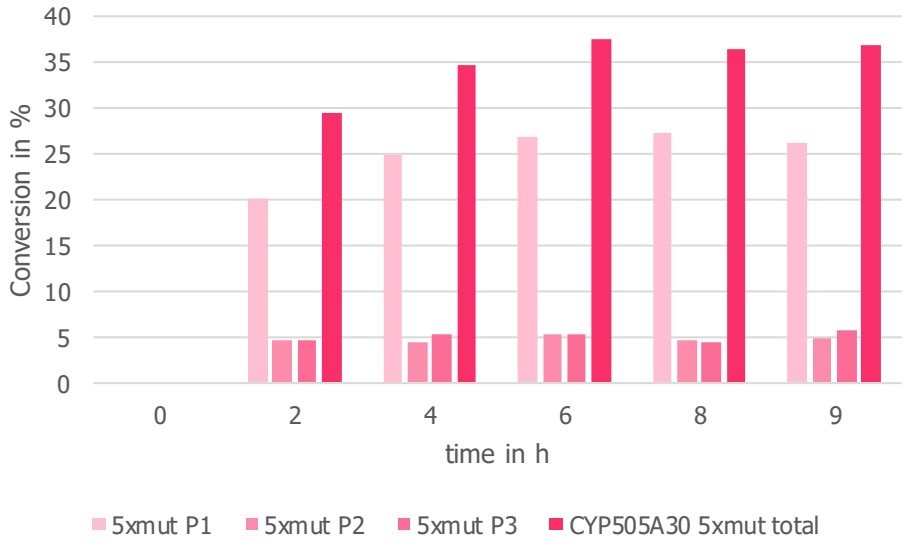

Figure 34: Ibuprofen biooxidation by CYP505A30 5xmut expressing *E. coli* cells (frozen/thawed): reaction volume: 500 ml; bioconversion conditions: according to SOP (upscaled from 1 ml to 500 ml); conversion of ibuprofen gives three monooxygenation products (P1-P3) according to HPLC/MS, Ptot is the sum of P1 to P3 and represents the overall total conversion

As expected, three metabolites have been formed showing a clear preference for P1 with a conversion of about 27% and two further products with about 5% conversion each (P2 and P3).

HPLC/MS data indicate, that the three metabolites formed are the same as formed by CYP505X in *P. pastoris* (cf. 4.12.1.). However, using the same extraction protocol seemed not be successful in this case, since no product peaks could be detected after extraction. Interestingly, the substrate peak was still prominent.

5 CONCLUSION AND FUTURE PERSPECTIVES

In this work, the SOP "Preparation and use of CYP505 expressed in *E. coli* for the oxidation of small molecules" could be further optimized and was successfully applied to another bifunctional CYP: CYP505A30. Optimization regarding biocatalyst formulation as well as reaction conditions and following stopping procedure were obtained. In regards of enzyme stability, we confirmed, that the buffer system, that we already used was the best option among the tested conditions.

Using lyophilized CFE instead of whole *E. coli* cells in biooxidative screening processes showed to be a promising alternative since not only higher conversion rates were observed for many of the tested substrates, but also facilitated handling. To state safely, whether the maximum of conversion is limited by enzyme stability, more investigations would be necessary. A promising approach could be feeding of the catalyst at predefined points in time over a certain reaction period, not only for reactions with CFE but also for whole cell bioconversions.

Further, it turned out that external addition of the co-factor $NADP^+$ was not crucial when working with whole cells and only led to a minor increase in conversion when working with CFE. Additionally, the reaction termination procedure originally described in the SOP was improved, which led to an easier handling and more accurate results.

Further on, a new SOP "Preparation and use of CYP505 expressed in *Pichia pastoris* (*Komagataella phaffii*) for the oxidation of small molecules" was drafted and successfully applied.

Upscaling to a reaction volume of 500 ml gave higher conversions compared to analytical scale experiments. Most probably, this was an effect of better mass transfer and therefore better oxygen supply. Since drug metabolites represent high value products, repeating the experiments under monitored conditions in a fermenter could be reasonable future perspective.

During this work, two metabolites were successfully identified. Chlorzoxazone was converted to 6-hydroxychlorzoxazone (48% isolated yield) and two out of three ibuprofen metabolites were identified as 1- and 2-hydroxyibuprofen. Yet, extraction and fractionation methods should still be improved to obtain higher yields in product isolation and allow for more easy identification by NMR.

6 REFERENCES

[**1**] Caswell, J. M., O'Neill, M., Taylor, S. J. C., Moody, T. S., Engineering and application of P450 monooxygenases in pharmaceutical and metabolite synthesis. *Current opinion in chemical biology* 2013 Apr;17(2):271-5, DOI: 10.1016/j.cbpa.2013.01.028.

[**2**] Kumar, S., Engineering cytochrome P450 biocatalysts for biotechnology, medicine and bioremediation. *Expert opinion on drug metabolism & toxicology* 2010 Feb;6(2):115-31, DOI: 10.1517/17425250903431040.

[**3**] Di Nardo, G., Gilardi, G., Optimization of the bacterial cytochrome P450 BM3 system for the production of human drug metabolites. *International journal of molecular sciences* 2012 Nov 28;13(12):15901-24, DOI: 10.3390/ijms131215901.

[**4**] O'Reilly, E., Köhler, V., Flitsch, S. L., Turner, N. J., Cytochromes P450 as useful biocatalysts: Addressing the limitations. *Chemical communications (Cambridge, England)* 2011 Mar 7;47(9):2490-501, DOI: 10.1039/c0cc03165h.

[**5**] Iyanagi, T., Molecular Mechanism of Phase I and Phase II Drug-Metabolizing Enzymes: Implications for Detoxification, in: Jeon, K. W. (Ed.). *International Review of Cytology* 2007;260:35-112, DOI:10.1016/S0074-7696(06)60002-8

[**6**] Poraj-Kobielska, M., Kinne, M., Ullrich, R., Scheibner, K. *et al.*, Preparation of human drug metabolites using fungal peroxygenases. *Biochemical pharmacology* 2011 Oct 1;82(7):789-96, DOI: 10.1016/j.bcp.2011.06.020.

[**7**] Girhard, M., Bakkes, P. J., Mahmoud, O., Urlacher, V. B., P450 Biotechnology, in: Ortiz de Montellano, P. R. (Ed.). *Cytochrome P450*, Springer International Publishing, Cham, 451–520.

[**8**] Bernhardt, R., Urlacher, V. B., Cytochromes P450 as promising catalysts for biotechnological application: Chances and limitations. *Applied microbiology and biotechnology* 2014;98(14):6185-203, DOI: 10.1007/s00253-014-5767-7.

[**9**] Urlacher, V. B., Eiben, S., Cytochrome P450 monooxygenases: Perspectives for synthetic application. *Trends in biotechnology* 2006 Jul;24(7):324-30, DOI: 10.1016/j.tibtech.2006.05.002.

[**10**] Fasan, R., Tuning P450 Enzymes as Oxidation Catalysts. *ACS Catal.* 2012, 2(4): 647–666, DOI: 10.1021/cs300001x

[**11**] Jung, S. T., Lauchli, R., Arnold, F. H., Cytochrome P450: Taming a wild type enzyme. *Current opinion in biotechnology* 2011 Dec;22(6):809-17, DOI: 10.1016/j.copbio.2011.02.008.

[**12**] Claude, A., The constitution of protoplasm. *Science (New York, N.Y.)* 1943 May 21;97(2525):451-6, DOI: 10.1126/science.97.2525.451.

[**13**] Mason H.S., Fowlks W.L., Peterson E., Oxygen transfer and electron transport by the phenolase complex. *J. Am. Chem. Soc.* 1955 May; 77(10):2914-2915, DOI: 10.1021/ja01615a088

[**14**] Klingenberg, M., Pigments of rat liver microsomes. *Archives of biochemistry and biophysics* 1958 Jun;75(2):376-86, DOI: 10.1016/0003-9861(58)90436-3

[**15**] Omura, T., Sato R., Fractional solubilization of haemoproteins and partial purification of carbon monoxide-binding cytochrome from liver microsomes. *Biochimica et biophysica acta* 1963; *71*, 224–226, DOI: 10.1016/0006-3002(63)91015-1

[**16**] Omura, T., Sato, R., The carbon monoxide-binding pigment of liver microsomes. I. Evidence for its hemoprotein nature. *The Journal of biological chemistry* 1964 Jul;239:2370-8

[**17**] Omura, T., Sato, R., A new cytochrome in liver microsomes. *The Journal of biological chemistry* 1962 Apr;237:1375-6

[**18**] Omura, T., Sato, R., The carbon monoxide-binding pigment of liver microsomes. II. Solubilization, purification, and properties. *The Journal of biological chemistry* 1964 Jul;239:2379-85

[**19**] Omura, T., Recollection of the early years of the research on cytochrome P450. *Proceedings of the Japan Academy. Ser. B: Physical and Biological Sciences* 2011 Dec;87:617–640, DOI: 10.2183/pjab.87.617.

[**20**] Yamazaki, H., *Fifty Years of Cytochrome P450 Research*, Springer Japan, Tokyo, 2014.

[**21**] Ullrich, R., Hofrichter, M., Enzymatic hydroxylation of aromatic compounds. *Cellular and molecular life sciences CMLS* 2007 Feb;64(3):271-93, DOI: 10.1007/s00018-007-6362-1

[**22**] Bak, S., Beisson, F., Bishop, G., Hamberger, B. *et al.*, Cytochromes p450. *The Arabidopsis book* 2011;9:e0144, DOI: 10.1199/tab.0144.

[**23**] Nelson, D. R., Cytochrome P450 nomenclature, 2004. *Methods in molecular biology (Clifton, N.J.)* 2006;320:1-10, DOI: 10.1385/1-59259-998-2:1

[**24**] Kurumbail G. Ravichandran, Sekhar S. Boddupalli, Charles A. Hasemann, Julian A. Peterson, Johann Deisenhofer, Crystal Structure of Hemoprotein Domain of P450BM-3, a Prototype for Microsomal P450's. *Science (New York, N.Y.)* 1993 Aug;261(5122):731–736

[**25**] RCSB Protein Data Bank, RCSB PDB - Search Results. https://www.rcsb.org/pdb/results/results.do?tabtoshow=Current&qrid=D16EFEC1. Accessed 20 October 2017

[**26**] Munro, A. W., Leys, D. G., McLean, K. J., Marshall, K. R. *et al.*, P450 BM3: The very model of a modern flavocytochrome. *Trends in Biochemical Sciences* 2002 May;27(5):250–257, DOI: 10.1016/S0968-0004(02)02086-8

[**27**] Ortiz de Montellano, P. R. (Ed.), *Cytochrome P450: Structure, Mechanism, and Biochemistry,* 4th edn., Springer International Publishing, 2015.

[**28**] Poulos, T. L., Johnson, E. F., Structures of Cytochrome P450 Enzymes, in: Ortiz de Montellano, P. R. (Ed.). *Cytochrome P450*, Springer International Publishing, Cham, 2015, 3–32

[**29**] Hrycay, E. G., Bandiera, S. M., *Monooxygenase, Peroxidase and Peroxygenase Properties and Mechanisms of Cytochrome P450*, Springer International Publishing, Cham, 2015, 851:1-61

[**30**] Nanda, A., Cytochrome P450 CYP11A1. https://collab.its.virginia.edu/access/content/group/f85bed6c-45d2-4b18-b868-6a2353586804/2/Ch24_Nanda_A_Cytochrome_P450_Cyp11A1-_-/Ch24_Nanda_A_Cytochrome_P450_Cyp11A1_CytochromeP450.html. Accessed Tuesday, 12 June 2018

[**31**] Eichmann, J. P.-R., Expression of cytochrome P450 variants: design, enzyme production and assessment of the catalytic activity. Master thesis, Graz, 2016

[**32**] Durairaj, P., Hur, J.-S., Yun, H., Versatile biocatalysis of fungal cytochrome P450 monooxygenases. *Microbial cell factories* 2016 Jul 18;15(1):125, DOI: 10.1186/s12934-016-0523-6

[**33**] Munro, A. W., Girvan, H. M., McLean, K. J., Variations on a (t)heme--novel mechanisms, redox partners and catalytic functions in the cytochrome P450 superfamily. *Natural product reports* 2007 Jun;24(3):585-609, DOI: 10.1039/b604190f

[**34**] Munro, A. W., Girvan, H. M., Mason, A. E., Dunford, A. J. *et al.*, What makes a P450 tick? *Trends in Biochemical Sciences* 2013 Mar;38(3):140-50, DOI: 10.1016/j.tibs.2012.11.006

[**35**] Denisov, I. G., Makris, T. M., Sligar, S. G., Schlichting, I., Structure and chemistry of cytochrome P450. *Chemical reviews* 2005 Jun;105(6):2253-77, DOI: 10.1021/cr0307143

[**36**] Urlacher, V. B., Girhard, M., Cytochrome P450 monooxygenases: An update on perspectives for synthetic application. *Trends in biotechnology* 2012 Jan;30(1):26-36, DOI: 10.1016/j.tibtech.2011.06.012

[**37**] Hannemann, F., Bichet, A., Ewen, K. M., Bernhardt, R., Cytochrome P450 systems--biological variations of electron transport chains. *Biochimica et biophysica acta* 2007 Mar;1770(3):330-44, DOI: 10.1016/j.bbagen.2006.07.017

[**38**] Cook, D. J., Finnigan, J. D., Cook, K., Black, G. W. *et al.*, Cytochromes P450: History, Classes, Catalytic Mechanism, and Industrial Application. *Advances in protein chemistry and structural biology* 2016;105:105-26, DOI: 10.1016/bs.apcsb.2016.07.003

[**39**] Baker, G. J., Girvan, H. M., Matthews, S., McLean, K. J. *et al.*, Expression, Purification, and Biochemical Characterization of the Flavocytochrome P450 CYP505A30 from *Myceliophthora thermophila*. *ACS Omega* 2017 Aug 31;2(8):4705-4724, DOI: 10.1021/acsomega.7b00450

[**40**] Wen, L. P., Fulco, A. J., Cloning of the gene encoding a catalytically self-sufficient cytochrome P-450 fatty acid monooxygenase induced by barbiturates in *Bacillus megaterium* and its functional expression and regulation in heterologous (*Escherichia coli*) and homologous (*Bacillus megaterium*) hosts. *The Journal of biological chemistry* 1987 May 15;262(14):6676-82

[**41**] Narhi, L. O., Fulco, A. J., Characterization of a catalytically self-sufficient 119,000-dalton cytochrome P-450 monooxygenase induced by barbiturates in *Bacillus megaterium*. *The Journal of biological chemistry* 1986 Jun 5;261(16):7160-9

[**42**] Kang, J.-Y., Kim, S.-Y., Kim, D., Kim, D.-H. *et al.*, Characterization of diverse natural variants of CYP102A1 found within a species of *Bacillus megaterium*. *AMB Express* 2011 Mar 28;1(1):1, DOI: 10.1186/2191-0855-1-1

[**43**] Cao, Y., Cheng, T., Zhao, G., Niu, W. *et al.*, Metabolic engineering of *Escherichia coli* for the production of hydroxy fatty acids from glucose. *BMC biotechnology* 2016 Mar 8;16:26, DOI: 10.1186/s12896-016-0257-x

[**44**] Fulco, A. J., P450BM-3 and other inducible bacterial P450 cytochromes: Biochemistry and Regulation. *Annu. Rev. Pharmacol. Toxicol.* 1991;31:177–203

[**45**] Whitehouse, C. J. C., Bell, S. G., Wong, L.-L., P450(BM3) (CYP102A1): Connecting the dots. *Chemical Society reviews* 2012 Feb 7;41(3):1218-60, DOI: 10.1039/C1CS15192D

[**46**] Ichinose, H., Molecular and functional diversity of fungal cytochrome P450s. *Biological & pharmaceutical bulletin* 2012;35(6):833-7

[**47**] Ichinose, H., Metabolic Diversity and Cytochromes P450 of Fungi, in: Yamazaki, H. (Ed.). *Fifty Years of Cytochrome P450 Research*, Springer Japan, Tokyo, 2014; 187–205

[**48**] Deng, J., Carbone, I., Dean, R. A., The evolutionary history of cytochrome P450 genes in four filamentous Ascomycetes. *BMC evolutionary biology* 2007 Feb 26;7:30, DOI: 10.1186/1471-2148-7-30

[**49**] Weis, R., Winkler, M., Schittmayer, M., Kambourakis, S. *et al.*, A Diversified Library of Bacterial and Fungal Bifunctional Cytochrome P450 Enzymes for Drug

Metabolite Synthesis. *Adv. Synth. Catal.* 2009 Sep 351(13):2140–2146, DOI: 10.1002/adsc.200900190

[**50**] Baker, G., The characterisation of the flavocytochrome P4 50 - CPR fusion enzymes CYP505A30 from *Myceliophthora thermophila* and CYP102A1 from *Bacillus megaterium.* PhD thesis, Manchester, 2015

[**51**] van Vugt-Lussenburg, B. M. A., Stjernschantz, E., Lastdrager, J., Oostenbrink, C. *et al.*, Identification of critical residues in novel drug metabolizing mutants of cytochrome P450 BM3 using random mutagenesis. *Journal of medicinal chemistry* 2007 Feb 8;50(3):455-61, DOI: 10.1021/jm0609061

[**52**] van Vugt-Lussenburg, B. M. A., Damsten, M. C., Maasdijk, D. M., Vermeulen, N. P. E. *et al.*, Heterotropic and homotropic cooperativity by a drug-metabolising mutant of cytochrome P450 BM3. *Biochemical and biophysical research communications* 2006 Aug 4;346(3):810-8, DOI: 10.1016/j.bbrc.2006.05.179

[**53**] Rosano, G. L., Ceccarelli, E. A., Recombinant protein expression in *Escherichia coli*: Advances and challenges. *Frontiers in microbiology* 2014 Apr 17;5:172, DOI: 10.3389/fmicb.2014.00172

[**54**] The University of Queensland, Australia, General Information - Bacteria Expression - UQ Protein Expression Facility - The University of Queensland, Australia. https://www.uq.edu.au/pef/content/general-information-bacteria-expression. Accessed 21.11.2017

[**55**] Yin, J., Li, G., Ren, X., Herrler, G., Select what you need: A comparative evaluation of the advantages and limitations of frequently used expression systems for foreign genes. *Journal of biotechnology* 2007 Jan 10;127(3):335-47, DOI: 10.1016/j.jbiotec.2006.07.012

[**56**] Sintupachee, S., Ngamrojanavanich, N., Sitthithaworn, W., De-Eknamkul, W., Molecular cloning, bacterial expression and functional characterisation of cytochrome P450 monooxygenase, CYP97C27, and NADPH-cytochrome P450 reductase, CPR I, from Croton stellatopilosus Ohba. *Plant science an international journal of experimental plant biology* 2014 Dec;229:131-141, DOI: 10.1016/j.plantsci.2014.09.001

[**57**] Labiotech.eu, Is Pichia Pastoris the Best Protein Expression System? https://labiotech.eu/pichia-pastoris-protein-expression/. Accessed 23 November 2017

[**58**] Ahmad, M., Hirz, M., Pichler, H., Schwab, H., Protein expression in Pichia pastoris: Recent achievements and perspectives for heterologous protein production. *Applied microbiology and biotechnology* 2014 Jun;98(12):5301-17, DOI: 10.1007/s00253-014-5732-5

[**59**] Krainer, F. W., Dietzsch, C., Hajek, T., Herwig, C. *et al.*, Recombinant protein expression in Pichia pastoris strains with an engineered methanol utilization pathway. *Microbial cell factories* 2012 Feb 13;11:22, DOI: 10.1186/1475-2859-11-22

[**60**] Lee, E. C., Ohk, S. O., Suh, B. Y., Park, N. *et al.*, Cloning and Expression in Pichia pastoris of a New Cytochrome P450 Gene from a Dandruff-causing Malassezia globosa. *Toxicological Research* 2010 Mar; 26(1): 47–52

[**61**] Alkofer, A., *Engineering of human P450s employing Pichia Pastoris*. Master thesis, Graz, 2017

[**62**] Lin, B., Tao, Y., Whole-cell biocatalysts by design. *Microbial cell factories* 2017 Jun 13;16(1):106, DOI: 10.1186/s12934-017-0724-7

[**63**] Carvalho, C. C. C. R. de, Whole cell biocatalysts: Essential workers from Nature to the industry. *Microbial biotechnology* 2017 Mar;10(2):250-263, DOI: 10.1111/1751-7915.12363

[**64**] Wachtmeister, J., Rother, D., Recent advances in whole cell biocatalysis techniques bridging from investigative to industrial scale. *Current opinion in biotechnology* 2016 Dec;42:169-177, DOI: 10.1016/j.copbio.2016.05.005

[**65**] Schwab, H., Strain improvement in industrial microorganisms by recombinant DNA techniques, in: *Bioprocesses Including Animal Cell Culture*, Springer-Verlag, Berlin/Heidelberg, 1988;37:129–168

[**66**] Schmitz, D., Janocha, S., Kiss, F. M., Bernhardt, R., CYP106A2-A versatile biocatalyst with high potential for biotechnological production of selectively hydroxylated steroid and terpenoid compounds. *Biochimica et biophysica acta* 2018 Jan;1866(1):11-22, DOI: 10.1016/j.bbapap.2017.07.011

[**67**] Linder, T., Mikrobiologisches Praktikum- Zellzahlbestimmung. http://www.genstrom.net/public/biology/microbiology/microbiology_module/protocols/protokoll_e.html#versuch_e2

[**68**] Agilent Technologies. https://www.genomics.agilent.com/biocalculators/calcODBacterial.jsp

[**69**] Hanlon, S. P., Friedberg, T., Wolf, C. R., Ghisalba, O. *et al.*, Recombinant Yeast and Bacteria that Express Human P450s: Bioreactors for Drug Discovery, Development, and Biotechnology, in: Schmid, R. D., Urlacher, V. B. (Ed.). *Modern Biooxidation*, Wiley-VCH Verlag GmbH & Co. KGaA, Weinheim, Germany, 2007; 233–252

[**70**] Kargl, L., Kinetic characterization of CYP505 expressing biocatalysts. Bachelor thesis, Graz, 2017

[**71**] Bracco, P., Janssen, D. B., Schallmey, A., Selective steroid oxyfunctionalisation by CYP154C5, a bacterial cytochrome P450. *Microbial cell factories* 2013 Oct 17;12:95, DOI: 10.1186/1475-2859-12-95

[**72**] White, B. E., Fenner, C. J., Smit, M. S., Harrison, S. T. L., Effect of cell permeability and dehydrogenase expression on octane activation by CYP153A6-based whole cell

Escherichia coli catalysts. *Microbial cell factories* 2017 Sep 20;16(1):156, DOI: 10.1186/s12934-017-0763-0

[**73**] Venkatakrishnan, K., Moltke, L. L.V., Greenblatt, D. J., Human cytochromes P450 mediating phenacetin O-deethylation in vitro: Validation of the high affinity component as an index of CYP1A2 activity. *Journal of Pharmaceutical Sciences* 1998 Jan, 87(12):1502-7, DOI: 10.1021/js980255z

[**74**] Migglautsch, A. K., Willim, M., Schweda, B., Glieder, A., Breinbauer, R., Winkler, M., Aliphatic hydroxylation and epoxidation of capsaicin by bifunctional Cytochrome P450 CYP505X, in progress

[**75**] Neunzig, I., Göhring, A., Drăgan, C.-A., Zapp, J. *et al.*, Production and NMR analysis of the human ibuprofen metabolite 3-hydroxyibuprofen. *Journal of biotechnology* 2012 Feb 10;157(3):417-20, DOI: 10.1016/j.jbiotec.2011.12.016

[**76**] Waraksa, E., Wójtowicz-Zawadka, M., Kwiatkowska, D., Jarek, A. *et al.*, Simultaneous determination of ibuprofen and its metabolites in complex equine urine matrices by GC-EI-MS in excretion study in view of doping control. *Journal of pharmaceutical and biomedical analysis* 2018 Apr 15;152:279-288., DOI: 10.1016/j.jpba.2018.02.004

LIST OF FIGURES

Figure 1: Overview of tasks performed. The SOP "Preparation and use of CYP505 expressed in *E. coli* for the oxidation of small molecules" created the basis for the following experiments. The green path includes experiments performed in order to optimize the current standard protocol for CYP505X expressed in *E. coli* and following substrate scope examinations (green path). Based on the protocol and results of the *E. coli* experiments, a SOP for CYP505X expressing *Komagataella phaffii (Pichia pastoris)* strains was created and further evaluated (blue path). The pink path shows experiments that aimed to test the applicability of the determined biooxidation conditions in the SOP on a different CYP variant: CYP505A30. After successful improvement the most promising conditions were identified and used for implementation of preparative scale reactions. Finally, the metabolites were isolated and characterized. 2

Figure 2: Illustration of CYP designation on the example of CYP101A1 from *Pseudomonas putida* 5

Figure 3: The structure of $P450_{cam}$ indicating the most important elements: Image of CYP structure taken and adjusted from [31] and named according to T.L. Poulos and E.F. Johnson – Structures of Cytochrome P450 Enzymes [28]. Additionally, the structure and arrangement of the heme iron is shown in the protein and separately (highlighted in blue). 7

Figure 4: Schematic representation of the catalytic cycle of P450 enzymes. Taken from Munro *et al.* [30]. 8

Figure 5: Schematic representation of P450 enzyme system - class VIII: (adapted from F. Hannemann *et al.* [29]) 9

Figure 6: Overview of the general workflow 23

Figure 7: HPLC system diagram showing used modules and their specifications 33

Figure 8: Fraction preview of CYP505X mediated ibuprofen bioconversion in *P. pastoris* on preparative scale; detector: diode array detector (DAD), fractions were labeled from 1 to 6; settings of fraction collector: start of collection after 20.10 min, trigger mode: peak based, maximum peak duration: 0.70 min, threshold 137.918 mAU (indicated by dashed line), up slope 0.10 mAU/s, down slope 5 mAU/s, start of a single fraction collection: indicated by green line, stop of a single fraction collection: indicated by red line 34

Figure 9: NUPAGE of CYP 505 variants: (a) cell disruption: sonication. (b) purified enzymes. 10 µg protein loaded; expected size: 120-123 kDa (as indicated by the red box); empty v. CO = empty vector control 38

Figure 10: NUPAGE of CYP505 variants: (a) and (b) cell disruption: BugBuster. (c) and (d) cell disruption: sonication. 10 µg protein loaded; expected size: 120-123 kDa (as indicated by the red box); empty v. CO = empty vector control 39

Figure 11: Schematic representation of the reaction setup for a CYP505 driven whole cell biooxidation in *E. coli* according to the SOP (cf. 7.1) 40

Figure 12: (left) CX Bioconversion *E. coli* - Effect of washing rehydrated, lyophilized cells and effect of glucose and citrate: w (washed), S (standard conditions), -C (without citrate), -g (without glucose) 41

Figure 13: (right) CX Bioconversion *P. pastoris* - Effect of washing rehydrated, lyophilized cells and effect of glucose and citrate: w (washed), S (standard conditions), -C (without citrate), -g (without glucose) 42

Figure 14: Impact of $NADP^+$ addition-biooxidation of chlorzoxazone by *E. coli* mutant 18.1: CFE (lyophilized), whole cells (lyophilized) and whole cells (frozen/thawed) over a period of 16 h with and without the addition of $NADP^+$; monitored in triplicates; * significantly more product formation when adding $NADP^+$43
Figure 15: Whole cell ibuprofen biooxidation over 49 h by CYP505X 5xmutant (A21) expressed in *Pichia pastoris* 45
Figure 16: Determination of reaction rate *a* and specific reaction rate *s* of CYP505X 5xmut in *P. pastoris* (A21); monitoring points that followed a linear trend were used to generate a linear regression line. The slope represents the reaction rate *a*. The specific reaction rate *s* was determined by referring the reaction rate *a* to the used amount of catalyst (CDW [mg]). 46
Figure 17: Ibuprofen biooxidation with frozen/thawed *P. pastoris* A21 cells expressing CYP505X 5xmut by using different buffer systems: biotransformation was conducted using 8.5% PS buffer and 1% PT buffer under standard conditions and standard conditions plus daily addition of GDH; bars represent product formation in % (blue: PS buffer, black: PT buffer) over a period of 52 h 47
Figure 18: Chlorzoxazone biooxidation by different amounts of lyophilized *P. pastoris* cells: amount of cells that corresponds to OD_{600} values of 25, 50, 100, 200 and 250 in the final reaction volume were used; the dashed line indicates that after OD 200 the cell amount was not doubled any more 49
Figure 19: Ibuprofen biooxidation by using different amount of lyophilized *P. pastoris* cells: amount of cells that corresponds to OD_{600} values of 25, 50, 100, 200 and 250 in the final reaction volume were used; conversion of ibuprofen gives three monooxygenation products (P1-P3) according to HPLC/MS, Ptot is the sum of P1 to P3 and represents the overall total conversion; the dashed line indicates that after OD 200 the cell amount was not doubled any more 50
Figure 20: Determination of optimal chlorzoxazone concentration for CYP505X (variant 18.1) for whole cell biooxidations: Substrate concentrations of 0.5 mM, 1 mM, 2mM, 5 mM and 10 mM were investigated; 11 points in time in a period of 45 h were taken for each substrate concentration in duplicates 51
Figure 21: Determination of K_M and V_{max} for CYP505X (variant 18.1) in whole cell biocatalysis towards chlorzoxazone; validity of K_M and V_{max} is restrained by a beginning substrate inhibition in the range of 5 mM of CX: Substrate concentrations of 0.5 mM, 1 mM, 2 mM and 5 mM were investigated; 11 points in time in a period of 45 h were taken for each substrate concentration in duplicates 51
Figure 22: Formation of 6-hydroxy-chlorzoxazone catalyzed by lyophilized cell-free extract: CFE of best variant (18.1) in different buffers (H_2O, 1% and 8.5% PS, 1% PT) under standard conditions (a) and standard conditions + daily addition of GDH (b). Every point in time was measured in duplicates 53
Figure 23: Structure of geranylacetone 61
Figure 24: Structure of lauric acid 61
Figure 25: Strucutre of undecenoic acid 61
Figure 26: Structure of undecatriene 61
Figure 27: Biooxidation of lauric acid using wild-type and CYP505X variants expressed in *E. coli*; biocatalyst formulation: lyophilized whole cells; reaction time: 16h; reaction conditions: (see 3.4.9.1) 62

Figure 28: Biooxidation of undecenoic acid using wild-type and CYP505X variants expressed in *E. coli*; biocatalyst formulation: lyophilized whole cells; reaction time: 16h; reaction conditions: (see 3.4.9.1) 62
Figure 29: Excerpt of the HPLC/MS analysis of capsaicin biooxidation by CYP505A30 wild-type in frozen/thawed whole cells; shown is the chromatogram of the UV trace where masses of substrate and metabolites were added to the corresponding peaks; MS traces are not shown; Given masses correspond to M+1 due to positive ionization mode; capsaicin: RT 4.45 min, 306 g/mol; P1: RT 4.33 min, 304 g/mol; P2: RT 4.00 min, 322 g/mol; P3: RT 3.74 min, 304 g/mol; P4: RT 3.53 min, 338 g/mol 69
Figure 30: Ibuprofen biooxidation by CYP505X 5xmut expressing *P. pastoris* cells (A21 frozen/thawed): reaction volume: 500 ml; bioconversion conditions: according to SOP (upscaled from 1 ml to 500 ml); conversion of ibuprofen gives three monooxygenation products (P1-P3) according to HPLC/MS, Ptot is the sum of P1 to P3 and represents the overall total conversion..... 72
Figure 31: Chromatogram of CYP505X mediated ibuprofen bioconversion in *P. pastoris* on preparative scale and chemical structures of analyzed fractions; P1= 2-hydroxyibupofen (2-OH-Ibu), P2= unknown, P3= 1-hydroxyibuprofen (1-OH-Ibu), fraction 4 and fraction 5 = unknown (most probably extraction artefacts), fraction 6= Ibuprofen; fraction collection settings: threshold 137.918 mAU (indicated by dashed line), up slope 0.10 mAU/s, down slope 5 mAU/s, start of a single fraction collection: indicated by green line, stop of a single fraction collection: indicated by red line..... 73
Figure 32: Chlorzoxazone biooxidation by CYP505X 5xmut expressing *P. pastoris* cells (A21 frozen/thawed): reaction volume: 500 ml; bioconversion conditions: according to SOP (upscaled from 1 ml to 500 ml); conversion of CX gives one monooxygenation product (6-OH-CX) according to HPLC/MS 75
Figure 33: Ibuprofen biooxidation by CYP505A30 wt expressing *E. coli* cells (frozen/thawed): reaction volume: 500 ml; bioconversion conditions: according to SOP (upscaled from 1 ml to 500 ml); conversion of ibuprofen gives three monooxygenation products (P1-P3) according to HPLC/MS, Ptot is the sum of P1 to P3 and represents the overall total conversion 76
Figure 34: Ibuprofen biooxidation by CYP505A30 5xmut expressing *E. coli* cells (frozen/thawed): reaction volume: 500 ml; bioconversion conditions: according to SOP (upscaled from 1 ml to 500 ml); conversion of ibuprofen gives three monooxygenation products (P1-P3) according to HPLC/MS, Ptot is the sum of P1 to P3 and represents the overall total conversion 77

LIST OF TABLES

TABLE 1: OVERVIEW OF CYP VARIANTS EXPRESSED IN *E. COLI* AND THEIR ACTIVITY TOWARDS 30 SELECTED SUBSTRATES: N=NEGATIVE ☐ T=TRACE ☐ VALUES [%]: <1% ☐ 1-10% ☐ 11-25% ☐ 26-40% ☐ 41-50% ☐ MULTIPLE VALUES REPRESENT MULTIPLE PRODUCTS ☐ 16

TABLE 2: OVERVIEW OF CYP VARIANTS EXPRESSED IN *K. PHAFFII* AND THEIR ACTIVITY TOWARDS 30 SELECTED SUBSTRATES: N=NEGATIVE ☐ T=TRACE ☐ VALUES [%]: <1% ☐ 1-10% ☐ 11-25% ☐ 26-40% ☐ 41-50% ☐ MULTIPLE VALUES REPRESENT MULTIPLE PRODUCTS ☐; * MULTIPLE PEAKS IN MS, NO PEAK IN UV, CYPS SHADED IN GRAY WERE NOT FURTHER EVALUATED IN THIS THESIS 17

TABLE 3: ALPHABETIC LISTING OF ALL TESTED SUBSTRATES WITH THEIR RESPECTIVE SUPPLIER AND RELEVANT SPECIFICATIONS 18

TABLE 4: LIST OF SELF-SUFFICIENT CYP VARIANTS WITH THEIR RESPECTIVE EXPRESSION HOST AND RELEVANT SPECIFICATIONS 22

TABLE 5: LIST OF PURIFIED CYP505A30 VARIANTS SHOWING ALL RELEVANT SPECIFICATIONS 22

TABLE 6: PREPARATIVE HPLC METHOD SPECIFICATIONS FOR IBUPROFEN 33

TABLE 7: SUMMARY OF WCW AND DCW DETERMINATION 35

TABLE 8: THEORETICAL CALCULATION OF NUMBER OF *P. PASTORIS* CELLS AND NUMBER OF *E. COLI* CELLS (OD_{600}=100/ML) AND THEORETICAL CONVERSION OF CHLORZOXAZONE TO 6-OH-CHLORZOXAZONE CONDUCTED BY ONE CELL 36

TABLE 9: (RIGHT) CX BIOCONVERSION *E. COLI* - EFFECT OF WASHING REHYDRATED, LYOPHILIZED CELLS AND EFFECT OF GLUCOSE AND CITRATE: W (WASHED), S (STANDARD CONDITIONS), -C (WITHOUT CITRATE), -G (WITHOUT GLUCOSE) 41

TABLE 10: (LEFT) CX BIOCONVERSION *P. PASTORIS* - EFFECT OF WASHING REHYDRATED, LYOPHILIZED CELLS AND EFFECT OF GLUCOSE AND CITRATE: W (WASHED), S (STANDARD CONDITIONS), -C (WITHOUT CITRATE), -G (WITHOUT GLUCOSE) 42

TABLE 11: ANALYTICAL BIOOXIDATION YIELD OF CYP505X VARIANTS 2.1, 7.1, 18.1 AND 19.1 IN CFE EXPRESSED IN *E. COLI* TOWARDS 22 SELECTED SUBSTRATES COMPARED TO WHOLE CELLS; REACTIONS WITH CFE WERE CARRIED OUT IN TRIPLICATES, DATA FOR WHOLE CELL BIOCONVERSION WERE TAKEN FROM TABLE 1; N=NEGATIVE ☐, T=TRACE ☐, VALUES [%]: <1-10 ☐, 11-50 ☐, >50 ☐ MULTIPLE VALUES REPRESENT MULTIPLE PRODUCTS: ORDER FROM TOP (PRODUCT THAT ELUTED LAST) TO BOTTOM (PRODUCT THAT ELUTED FIRST) 56

TABLE 12: CYP505A30 AND CYP102A1 MEDIATED WHOLE CELL BIOOXIDATION OF LAURIC ACID, CHLORZOXAZONE AND IBUPROFEN; BIOCATALYST FORMULATIONS: FROZEN/THAWED AND LYOPHILIZED; REACTION TIME: 16 H, EACH REACTION WAS CARRIED OUT IN TRIPLICATES; < 20% -, 21-40% +, 41-60% ++, 61-80% +++, 81-100% ++++ 63

TABLE 13: ANALYTICAL BIOOXIDATION YIELD OF FROZEN/THAWED CYP505A30 AND CYP102A1 EXPRESSING *E. COLI* TOWARDS 22 SELECTED SUBSTRATES: REACTIONS WITH WHOLE CELLS WERE CARRIED OUT IN TRIPLICATES, REACTIONS WITH PURIFIED ENZYMES WERE CARRIED OUT AS UNICATES; N/T = NOT TESTED ☐, N=NEGATIVE ☐, T=TRACE ☐, VALUES [%]: <1-10 ☐, 11-50 ☐, >50 ☐, MULTIPLE VALUES REPRESENT MULTIPLE PRODUCTS: ORDER FROM TOP (PRODUCT THAT (ELUTED LAST) TO BOTTOM (PRODUCT THAT ELUTED FIRST) 65

TABLE 14: HPLC METHOD SPECIFICATIONS FOR BENZYDAMINE XLVI

TABLE 15: HPLC METHOD SPECIFICATIONS FOR CAFFEINE XLVI

TABLE 16: HPLC METHOD SPECIFICATIONS FOR CAPSAICIN XLVII

TABLE 17: HPLC METHOD SPECIFICATIONS FOR CHLORZOXAZONE XLVII

TABLE 18: HPLC METHOD SPECIFICATIONS FOR CLOPIDOGREL XLVIII

TABLE 19: HPLC METHOD SPECIFICATIONS FOR DEXTROMETHORPHAN XLVIII

TABLE 20: HPLC METHOD SPECIFICATIONS FOR DICLOFENAC XLIX
TABLE 21: HPLC METHOD SPECIFICATIONS FOR ESTRIOL XLIX
TABLE 22: HPLC METHOD SPECIFICATIONS FOR FAMCICLOVIR L
TABLE 23: HPLC METHOD SPECIFICATIONS FOR HARMINE L
TABLE 24: HPLC METHOD SPECIFICATIONS FOR HYDROCORTISONE LI
TABLE 25: HPLC METHOD SPECIFICATIONS FOR IBUPROFEN LI
TABLE 26: HPLC METHOD SPECIFICATIONS FOR LIDOCAINE LII
TABLE 27: HPLC METHOD SPECIFICATIONS FOR MOCLOBEMIDE LII
TABLE 28: HPLC METHOD SPECIFICATIONS FOR NAPHTHOL LIII
TABLE 29: HPLC METHOD SPECIFICATIONS FOR PHENACETIN LIII
TABLE 30: HPLC METHOD SPECIFICATIONS FOR PIPERINE LIV
TABLE 31: HPLC METHOD SPECIFICATIONS FOR PROGESTERONE LIV
TABLE 32: HPLC METHOD SPECIFICATIONS FOR PROPRANOLOL LV
TABLE 33: HPLC METHOD SPECIFICATIONS FOR SALBUTAMOL LV
TABLE 34: HPLC METHOD SPECIFICATIONS FOR TESTOSTERONE LVI
TABLE 35: HPLC METHOD SPECIFICATIONS FOR TOLBUTAMIDE LVI

7 APPENDIX

7.1 *E. COLI* SOP

ACIB Protocol

Preparation and use of CYP505 expressed in *E. coli* for the oxidation of small molecules

Authors: Thorsten Bachler, Margit Winkler
thorsten.bachler@acib.at, margit.winkler@acib.at

Creation date: January.2018 Restrictions: yes Validity: until updated, revoked or cancelled This ACIB protocol replaces the version from: June.2017 Developed in project/working group: 21.061 / 33		
Notice of modification:		
Written by: Margit Winkler and Thorsten Bachler		
Date/signature:		
Checked:	by:	Date/Signature
Approved by:		
Released by		

1. Purpose and Field of Application

This method is used to

- cultivate *E. coli* strains with the ability to express CYP505 variants,
- lyophilize said strains
- use them for the oxidation (e.g. hydroxylation, demethylation) of small molecule compounds such as active pharmaceutical ingredients (APIs)
- analyse results of the oxidation of the model API chlorzoxazone

2. Principle

The method comprises of four steps: in the first step, *E. coli* cells are cultivated under optimized conditions and the expression of CYP505 (variants) is induced. In the second step, the cells are harvested, washed and lyophilized. In the third step, the oxidative activity of the cells is assessed using an optimized biotransformation protocol. In the last step, the results are analysed for the model API chlorzoxazone.

Chlorzoxazone 2

Figure 1. Reaction scheme of the model reaction.

3. Key Words, Definitions & Abbreviations

Cytochrome P450 – Active Pharmaceutical Ingredient – Drug Metabolite – Biooxidation

CYP:	Cytochrome P450
CYP505:	*Aspergillus fumigatus* CYP (wild type: Accession No EAL92660)
CX:	Chlorzoxazone
Amp:	Ampicillin
IPTG:	isopropyl-β-D-1-galactopyranoside
TB:	Terrific broth
ACN:	Acetonitrile
Δ-ALA	δ-aminolevulinic acid
rt	room temperature
GDH	glucose dehydrogenase
EDTA	Ethylenediaminetetraacetic acid
DMSO	Dimethylsulfoxide

4. Methodology

4.1.Reagents

General

Deionized Water is used from Satorius stedim Biotech arium® basic water purification system.

Cultivation and expression

Name	Formula	MW	Purity	Supplier	CAS No.	Comments
Tryptone			≥99%	Sigma Aldrich	91079-40-2	Pancreatic digest of casein
Yeast extract			≥99%	Carl Roth	8010-01-2	
Glycerol	$C_3H_8O_3$	92.09	≥99.5%	Carl Roth	56-81-5	
Dipotassium hydrogenphosphate	K_2HPO_4	174.19	≥99%	Carl Roth	7758-11-4	
Potassium dihydrogen phosphate	KH_2PO_4	136.09	≥99%	Carl Roth	7778-77-0	
Sodium Chloride	NaCl	58.44	≥99.5%	Carl Roth	7647-14-5	
Magnesium chloride hexahydrate	$MgCl_2 * 6 H_2O$	203.3	≥99%	Carl Roth	7791-18-6	
Ampicillin sodium salt	$C_{16}H_{18}N_3NaO_4S$	371.39	≥97%	Carl Roth	69-52-3	
Δ-ALA hydrochloride	$C_5H_{10}ClNO_3$	167.59	≥96%	Carl Roth	5451-09-2	optional
IPTG	$C_9H_{18}O_5S$	238.30	≥99%	Carl Roth	367-93-1	
HCl	HCl	26.46	37%	Carl Roth	7647-01-0	Toxic; corrosive
Copper chloride dihydrate	$CuCl_2*2H_2O$	170.48	≥99.99%	Sigma Aldrich	10125-13-0	Xn; N
Cobalt chloride	$CoCl_2$	129.84	≥ 98.0 %	Sigma Aldrich	7646-79-9	N; T
Sodium molybdate	Na_2MoO_4	205.92	≥98%	Sigma Aldrich	7631-95-0	
Boric acid	H_3BO_3	61.83	≥99.5%	Sigma Aldrich	10043-35-3	Xi
Zinc chloride	$ZnCl_2$	136.29	99.99	Sigma Aldrich	7646-85-7	
Ferric Citrate	$C_6H_5FeO_7$	244.94		Sigma Aldrich	3522-50-7	

XX

Harvest and lyophilization

Name	Formula	MW	Purity	Supplier	CAS No.	Comments
Dipotassium hydrogenphosphate	K_2HPO_4	174.19	≥99%	Carl Roth	7758-11-4	
Sucrose	$C_{12}H_{22}O_{11}$	342.3	≥99.5%	Carl Roth	57-50-1	
EDTA	$C_{10}H_{14}N_2Na_2O_8$* 2 H_2O	372.24	≥99%	Carl Roth	6381-92-6	
liquid nitrogen	N_2	28		Linde	7727-37-9	

Biotransformation

Name	Formula	MW	Purity	Supplier	CAS No.	Comments
Dipotassium hydrogenphosphate	K_2HPO_4	174.19	≥99%	Carl Roth	7758-11-4	
Sucrose	$C_{12}H_{22}O_{11}$	342.3	≥99.5%	Carl Roth	57-50-1	
Chlorzoxazone	$C_7H_4ClNO_2$	169.57		Sigma Aldrich	95-25-0	
DMSO	C_2H_6SO	78.13	≥99.8%	Carl Roth	67-68-5	
Trisodium citrate dihydrate	$C_6H_5O_7$ 2H_2O 3Na	294.1	≥99%	Carl Roth	6132-04-3	
Magnesium chloride hexahydrate	$MgCl_2$ * 6 H_2O	203.3	≥99%	Carl Roth	7791-18-6	
NADP+*2 Na	$C_{21}H_{28}N_7Na_2O_{17}P_3$	787.4		Roche	24292-60-2	
Glucose	$C_6H_{12}O_6$*H_2O	198.17	≥99.5%	Carl Roth	14431-43-7	
GDH.002				DSM Innovative Synthesis BV		NADP 2.7 U/mg; NAD 3.4 U/mg
Methanol	CH_3OH	32.04	≥99%	Roth	67-56-1	
ACN	CH_3CN	41.05	HPLC Grade	J.T.Baker/ VWR	75-05-8	
Formic acid	CH_2O_2	46.03	≥99%	Fluka	64-18-6	

Analysis

Name	Formula	MW	Purity	Supplier	CAS No.	Com-ments
ACN	CH_3CN	41.05	HPLC Grade	J.T.Baker/ VWR	75-05-8	
Methanol	CH_3OH	32.04	≥99%	Roth	67-56-1	
Formic acid	CH_2O_2	46.03	HPLC Grade	Fluka	64-18-6	

4.2.Solutions

Cultivation and expression

Media

- TB

Tryptone	12 g
Yeast Extract	24 g
Glycerol	4 mL
Deionized Water	900 mL

Sterilize by autoclaving. Cool to rt.

- TB Medium
  900 mL TB
  100 mL of sterile 'Buffer for TB medium'.

Use within 2 days

Stock solutions

- Buffer for TB medium pH 7.6

KH_2PO_4	23.1 g
K_2HPO_4	125.4 g
Deionized Water	fill up to 1000 mL

Check pH value and correct with KOH. Sterilize by autoclaving. Store at room temperature.

- Amp, 100 mg/mL

Ampicillin	1 g
Deionized Water	10 mL

Filter sterilize. Store at -20°C in 1 mL aliquots.

- Trace salt solution
  2.45 g Fe(III)Citrate in 50 mL H_2O → heat and stir until it is solved
  0.121g $ZnCl_2$
  0.2 g $CoCl_2$*6 H_2O
  0.1 g $NaMoO_4$*2 H_2O
  0.127 $CuCl_2$*2 H_2O
  0.05 g H_3BO_3

Fill up to 100 mL with H_2O, filter sterilize; store at rt.

- $MgCl_2$ 1M

Magnesium chloride	20.3 g
Deionized Water	100 mL

Store at 4°C.

- IPTG 1M

IPTG	2.383g
Deionized Water	10 mL

Filter sterilize. Store at -20°C in 1 mL aliquots.

- Optional: Δ-ALA 1M

Δ-ALA	1.676 g
Deionized Water	10 mL

Filter sterilize. Store at -20°C.

Harvest and Lyophilization

Buffers

- PSE Buffer (1X) 50 mM, pH 7.4, 8.5% sucrose

KH_2PO_4	6.75 g
EDTA	0.92 g
Sucrose	85.5 g
Deionized Water	1000 mL

Add EDTA freshly before use and adjust pH with KOH.

Biotransformation

- Reaction buffer: PS Buffer 100 mM pH 7.4

KH_2PO_4	13.5 g
Sucrose	85.5 g
Deionized Water	1000 mL

Adjust pH with KOH and store at rt.

- Stop solution: MeOH/ACN 1:1

MeOH	50 mL
ACN	50 mL

Mix and store at room temperature.

Stock solutions

- Substrate, 100 mM

Chlorzoxazone	16.9 mg
DMSO	1 mL

Store at 4°C.

- Trisodium citrate, 1 M

Trisodium citrate dihydrate	14.7g
Deionized Water	50 mL

Filter sterilize and store at 4°C.

- Magnesium chloride, 1 M

Magnesium chloride hexahydrate	20.3 g
Deionized Water	100 mL

Filter sterilize and store at rt

- NADP+, 1 mM

NADP+	7.4 mg
Deionized Water	10 mL

Prepare freshly every time.

- Glucose, 1 M

Glucose	19.8 g
Deionized Water	100 mL

Autoclave and store at rt.

- Glucose dehydrogenase

GDH	100 mg
Deionized Water	10 mL

The solution remains turbid. Prepare freshly every time.

Analysis

- Aqueous mobile phase: formic acid 0.1%

Formic acid	1 mL
Deionized Water	1000 mL

4.3.Materials

Name	Supplier	Order No.	Comments
Flask VK	Geiner Bio One	227261	
Non-baffeled 2L flasks	Simax		
Disposible Cuvettes	Geiner Bio One	613101	
Syringes	Braun		
Syringe filters (0.22µm), CME sterile	Rotilabo		
Sterile loop	Simport	L200-2A	
Pipettes and pipette tips	Geiner Bio One	740290/ 739290	200 µl and 1000 µl volume tips
50 mL Falcon tubes	Geiner Bio One		
250/500 mL round bottom flasks	Schott		For lyophilisation
1.5 mL glass vials	Bruckner Analysentechnik	610002/ 610003	Alternative for lyophilisation
Nunclon Δ Surface 24-well plates	Nunc	144530	
Gas permeable Adhesive Seals	Thermo Scientific	# AB-0718	
1.5 mL Reaction tubes	Sarstedt	72.690.001	For protein removal
Polypropylene Microtiter plates V-shaped bottom	Geiner Bio One	651201	
Adhesive seals	Geiner Bio One	676070	

4.4.Apparatus

Name	Supplier	Comments
Analytic scale	Sartorius Practum 124-15	
Orbital shaker	Infors AG	
Biophotometer to measure absorption at 600 nm	Eppendorf	
Beckmann Coulter Avanti J-20 XP		Rotor JA-10
alpha 1-4 lsc freeze dryer	Martin Christ Gefriertrock-nungsanlagen GmbH	For lyophilisation with round bottom flasks only
Advantage Pro freeze-dryer	SP Scientific	See (Figure 2)
Orbital shaker HT orbitron	Infors AG	for 24 well plates
Eppendorf 5810 R	Eppendorf	
Eppendorf Thermomixer	Eppendorf	
1200 HPLC Series equipped with G1379B degasser, G1312B binary pump, SL G1367C HiP-ALS SL au-tosampler, G1314C VWD SL UV detec-tor, G1316B TCC SL column oven and G1956B mass selective detector (MSD)	Agilent	Or alternative HPLC sys-tem, at least with UV de-tector
Kinetex 50x4.6 mm; 2.6u; C18; 100 Å HPLC column	phenomenex	P No.: 00B-4462-E0

4.6.Procedure

1. **Preculture**
    a. 20 mL of TB or LB in 50 mL Greiner flask
    b. Add 20 µL Amp to give a final concentration of 100 µg/mL
    c. To start the culture, use 20 µL of a glycerol stock of *E. coli* [BL21(DE3) or DH5α] strain harbouring plasmids pMS470_CYP505 (plasmids of the BSYEJE series). Don't forget appropriate control strains (e.g. pMS470d8 in the respective *E. coli* strain as the negative control)
    d. Incubate at 37°C in a rotary shaker at approximately 120 rpm over night
2. **Main culture**
    a. 400 mL of TB medium in 2 L non-baffled Erlenmeyer flask
    b. Add 400 µL Amp to give a final concentration of 100 µg/mL
    c. Add 100 µL Trace salt solution
    d. Add 50 µL $MgCl_2$ stock solution (1 M)
    e. Measure OD_{600} of the pre-culture
    f. To start the culture, use the amount of pre-culture necessary to obtain OD_{600} = 0.05
    g. Cultivate at 37°C and 120 rpm
    h. Determine OD_{600} regularly
    i. At OD_{600}= 0.6 transfer the flaks to 4°C for 1h
    j. Induce CYP505 expression by the addition of 40µL of IPTG 1M (0.1 mM final concentration)
    k. *Optional: the addition of Δ-ALA (final concentration of 0.5 mM) may increase the activity up to 20%*
    l. Incubate at 28°C in a rotary shaker at approximately 120 rpm for 20-24h
3. **Cell harvest**
    a. Centrifuge the culture at 4000 rpm at 4°C for 15 min
    b. Discard supernatant and resuspend the pellet in 15 mL of ice cold PSE buffer, pH7.4
    c. Centrifuge at 4000 rpm at 4°C for 15 min
    d. Repeat step b and c one time
    e. Discard supernatant and resuspend the pellet in 20 mL of PS buffer pH7.4 (per g wet cell weight approximately 10 mL buffer)
    f. *Optional: to determine the activity of non-lyophilized cells skip 'Lyophilisation and storage'. Instead resuspend cells in PS buffer and freeze them for at least 1h at -20°C to permeabilize them. Continue with 'Determination of oxidative activity (Biotransformation)*

4. **Lyophilisation and storage**
    a. Pipette portions of the cell suspensions e.g. into GC vials, 24-well plates or similar. Freeze with liquid nitrogen. Short storage at -80°C is possible, if needed, preferably continue with b. immediately.
    b. Lyophilize 24 well plates on the Advantage Pro freeze-dryer (Figure 2) under the following conditions: Use program 'CYP 505'; Approximately 30 min before the samples are ready, pre freeze off shelf temperature -40°C

Program drying steps 1 - 6:

Temp	Ramp	Hold (min)
-40°C	5	180
-20°C	5	480
+10°C	5	120
-20°C	5	180
-40°C	5	360

c. For GC vials the detailed program is not necessary. Lyophilize ON with shelf temperature -40°C.
   i. ***Alternative***: *Transfer the cells to 250 or 500mL round bottom flask*
   ii. *Freeze the suspension in liquid nitrogen. Make sure that the surface of frozen cell suspension is maximal by turning the flask*
   iii. *Lyophilize on the Advantage Pro freeze-dryer (Figure 2) outer valves or any other freeze dryer for round bottom flasks*

d. Store lyophilized cells at -20°C. The cells will retain activity for at least 1 year
e. ***Alternative***: *store lyophilized cells at +4°C. The cells will retain activity for approximately 6 months. Activity decreases upon longer storage (approximately 40% within 6 months).*
f. ***Alternative***: *store lyophilized cells at rt. The cells will retain activity for approximately 1 week if stored at 37°C. Activity decreases upon longer storage but the cells show residual activity for at least 1 year.*

Figure 2. Advantage Pro freeze-dryer. Use the chamber for plates or vials, and use the tabs for up to 4 round bottom flasks

5. Determination of oxidative activity (Biotransformation)

a. Resuspend lyophilized cells in Reaction buffer to OD_{602}=100
b. Transfer 825 µL of cell suspension to each well in 24-well plates (final volume 1 mL)
c. ***Alternative***: *instead of 24 well plates use GC vials and use one fifth of all given volumes (final volume is 200 µL)*
d. Add 50 µL of sodium citrate stock
e. Add 50 µL of $NADP^+$ stock
f. Add 10 µL of magnesium chloride stock
g. Add 10 µL of glucose stock

h. Add 5 µL of GDH stock
i. Start the reaction by addition of 50 µL of chlorzoxazone stock
j. Seal the plate with Gas permeable Adhesive Seal
k. Incubate at 30°C and 120 rpm in an orbital shaker for 16 h.
l. Transfer 500 µL of the reaction mixture into a 1.5 mL Eppendorf vessel
m. Add 500µL of a MeOH/ACN mix
n. Mix for 10 min in Eppendorf Thermomixer at rt and 700 rpm
o. Centrifuge for 5 min at maximum speed in a tabletop centrifuge
p. Transfer 200µL of the supernatant into wells of Polypropylene Microtiter plates
q. Seal with adhesive seal. Store at +4°C if the samples are analyzed within 24h, otherwise freeze at -20°C. Preferably analysis should be carried out on the same day.

6. Analysis

a. Prepare for HPLC analysis [insert correct column (Kinetex 50x4.6 mm; 2.6u; C18; 100 Å HPLC column for chlorzoxazone and many other APIs), purge Channel A1 with 0.1% aqueous formic acid, refill ACN on channel B2 when needed, clean spray unit, remove splitter if it is mounted]
b. Load method BAC_CHLORXOXAZONE_ROBOX_25°.M or the respective substrate specific program and equilibrate the column until pressure and UV signal are constant. The details of the method are given here:
   i. Injection volume: 10µL
   ii. Flow: 1.000 mL/min
   iii. Solvent Gradient:

Time	% acetonitrile
0.00 min	0
1.00 min	0
4.00 min	100
5.00 min	100
5.01 min	0
6.00 min	0

   iv. Column temperature: 25°C
   v. MSD settings: API/ES, Fast Scan mode, peak width 0.100 min, Cycle time 0.70 sec/cycle
      1. MSD1 Scan, Negative, Mass range 100-500, fragmentor 70, Gain 1, Threshold 150
      2. MSD2 SIM, Negative, SIM Ion 168.00, fragmentor 70, Gain 1, Dwell 140 ms
      3. MSD3 SIM, Negative, SIM Ion 184.00, fragmentor 70, Gain 1, Dwell 140 ms
c. Create Sequence Table and start measurement
d. Evaluate data using the UV trace (VWD1, wavelength 290 nm), see **Error! Reference source not found.**.
   i. Go to 'Data analysis' mode in the Chemstation software
   ii. Choose datafile, choose VWD1A according to Figure 3

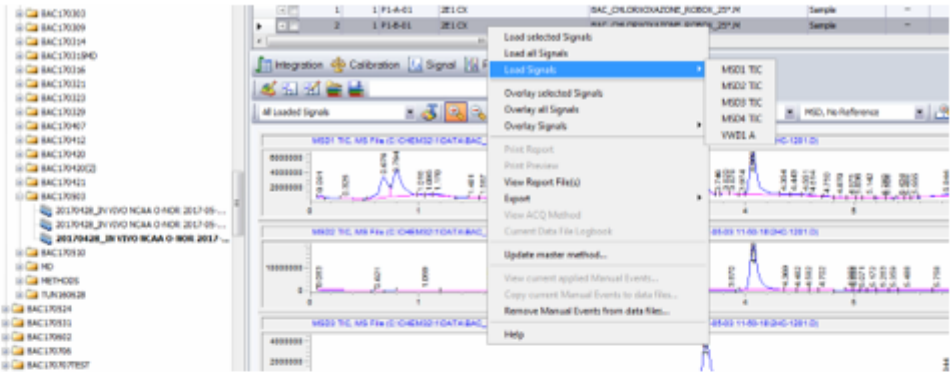

Figure 3: Screenshot of how to load the chromatogram in Data Analysis mode

iii. Choose 'Integration' mode and click on the peak with the arrow to mark the result in the table (Figure 4).

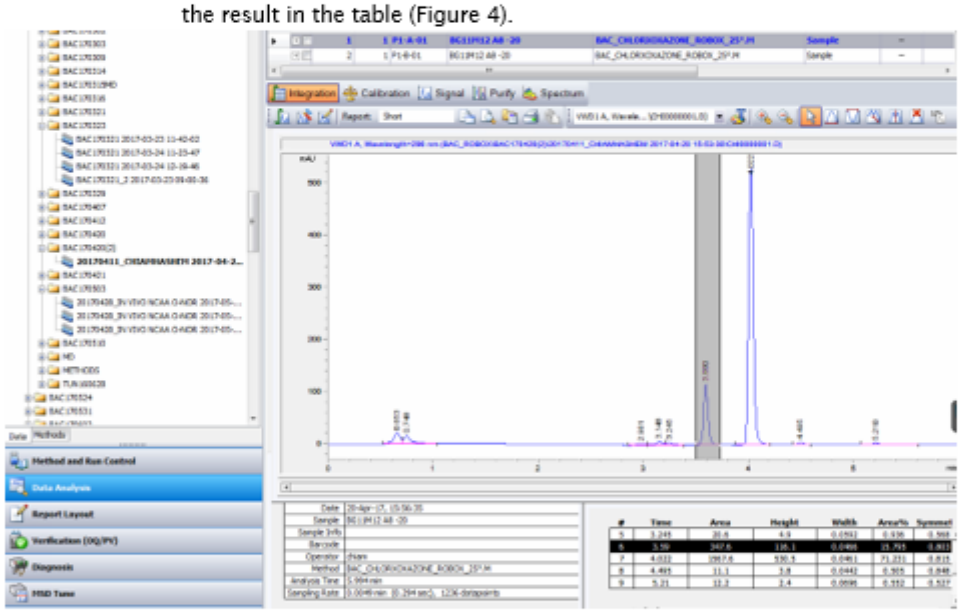

Figure 4: Screenshot of how to retrieve the peak area

iv. Correct integration manually, if necessary
v. Note that substrate and product must have similar absorption maxima, otherwise this 'area-normalization' method is misleading

e. ***Alternative***: *if compounds are not baseline separated, use MS traces for data evaluation. MSD1 is typically SCAN, MSD2 is typically monitoring substrate (in positive mode: M+1, in negative mode: M-1). Note that quantification via MS signals may cause errors due to differences in ionizability of substrate and product. Moreover, signals are less reproducible, but you will get a trend. Do not understand such numbers as trustful quantitative values.*

7. Result examples

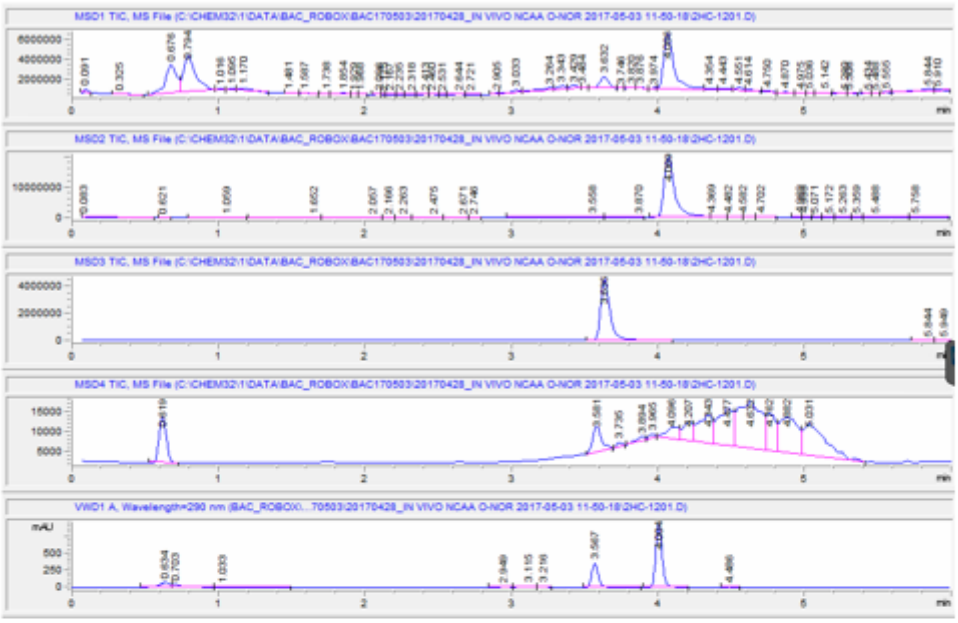

Figure 5: Example of CX biotransformation reaction. MSD1 corresponds to the SCAN mode. Clicking into the peaks will reveal their MS spectra in negative mode. MSD2 corresponds to the SIM (single ion monitoring) of the substrate in negative mode (the mass of CX is 169.57 g/mol, in negative mode, the ion with m/z of 168 is monitored). MSD3 corresponds to the SIM of the product in negative mode. MSD4 is useless in this case but offers the possibility to look for another ion for compound with multiple reaction possibilities. VWD1 corresponds to the UV signal at a wavelength of 290 nm (the optimum for CX). All chromatograms were integrated automatically.

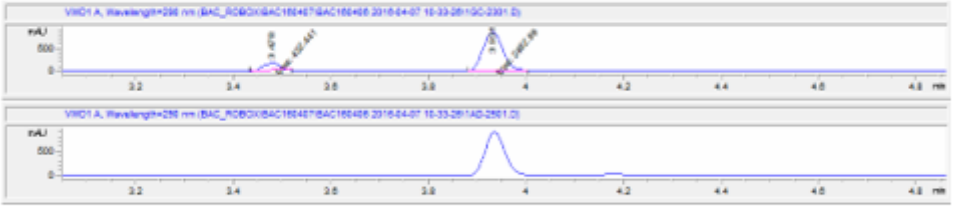

Figure 6 Two exemplary UV chromatograms of CX biotransformation reactions. Top: reaction with active mutant, bottom: reaction with inactive mutant. Hydroxychlorzoxazone elutes at approximately 3.5 min and CX at approximately 3.9 min.

4.7.Calculations

The result is shown in Figure 5. For the calculation, use the UV trace as shown in Figure 6 and Figure 4.
Use the following formula:
Conversion % = Area OH-CX * 100/(Area OH-CX + Area CX)
Using the numbers from Figure 6 (top chromatogram): Conversion % = 432.44 * 100/(432.44 + 2482.99) = 14.8%

XXX

5. Safety Precautions

Please follow instructions described in "acib-Mitarbeiterleitfaden Gefahrstoff- und Laborordnung"

6. Documentation

All observations, protocol deviations and calculations must be recorded in the lab book

7. References

R. Weis, *et al. Adv. Syn. Catal.*, **2009**, *351(13)*, 2140ff

8. Acknowledgements

This work received funding from the EU project ROBOX (grant agreement n° 635734) under EU's H2020 Programme Research and Innovation actions H2020-LEIT BIO-2014-1 and from the Austrian BMWFJ, BMVIT, SFG, Standortagentur Tirol and ZIT through the Austrian FFG-COMET- Funding Program. Disclaimer: This publication reflects the author's view and the *Agency* is not responsible for any use that may be made of the information it contains.

This project is funded by the European Union

7.2 *P. PASTORIS SOP*

ACIB Protocol

Preparation and use of CYP505 expressed in *Pichia pastoris* (*Komagataella phaffii*) for the oxidation of small molecules

Authors: Bianca Kerschbaumer, Margit Winkler
bianca.kerschbaumer@acib.at, margit.winkler@acib.at

Creation date: Restrictions: yes Validity: until updated, revoked or cancelled This ACIB protocol replaces the version from: Developed in project/working group: 21.061 / 33		
Notice of modification:		
Written by: Bianca Kerschbaumer and Margit Winkler		
Date/signature:		
Checked:	by: Melissa Willim	Date/Signature
Approved by:		
Released by		

1. Purpose and Field of Application

This method is used to

- cultivate *Pichia pastoris* (***Komagataella phaffii)*** strains with the ability to express CYP505 variants,
- lyophilize said strains
- use them for the oxidation (e.g. hydroxylation, demethylation) of small molecule compounds such as active pharmaceutical ingredients (APIs)
- analyse results of the oxidation of the model API chlorzoxazone

2. Principle

The method comprises of four steps: in the first step, *P. pastoris* cells are cultivated under optimized conditions and the expression of CYP505 (variants) is induced. In the second step, the cells are harvested, washed and lyophilized. In the third step, the oxidative activity of the cells is assessed using an optimized biotransformation protocol. In the last step, the results are analysed for the model API chlorzoxazone.

Chlorzoxazone **2**

Figure 1. Reaction scheme of the model reaction.

3. Key Words, Definitions & Abbreviations

Cytochrome P450 – Active Pharmaceutical Ingredient – Drug Metabolite – Biooxidation

CYP	Cytochrome P450
CYP505	*Aspergillus fumigatus* CYP (wild type: Accession No EAL92660)
CX	Chlorzoxazone
ACN	Acetonitrile
rt	room temperature
DMSO	Dimethylsulfoxide

4. Methodology

4.1.Reagents

General
Deionized Water is used from Sartorius stedim Biotech arium® basic water purification system.

Cultivation and expression

Name	Formula	MW	Purity	Supplier	CAS No.	Comments
Yeast nitrogen base (YNB)	N/A	N/A	N/A	Becton Dickinson	7783-20-2	
Dextrose	$C_6H_{12}O_6*H_2O$	198.17	≥99 %	Carl Roth	14431-43-7	
D(+)Biotin	$C_{10}H_{16}N_2O_3S$	244.31	≥98.5 %	Carl Roth	58-85-5	
Dipotassium hydrogenphosphate	K_2HPO_4	174.19	≥99 %	Carl Roth	7758-11-4	
Potassium dihydrogen phosphate	KH_2PO_4	136.09	≥99 %	Carl Roth	7778-77-0	
Methanol	CH_3OH	32.04		Carl Roth	67-56-1	
KOH	KOH	56,11	≥85 %	Carl Roth	1310-58-3	

Harvest and lyophilization

Name	Formula	MW	Purity	Supplier	CAS No.	Comments
Dipotassium hydrogenphosphate	K_2HPO_4	174.19	≥99 %	Carl Roth	7758-11-4	
Sucrose	$C_{12}H_{22}O_{11}$	342.3	≥99.5%	Carl Roth	57-50-1	
liquid nitrogen	N_2	28		Linde	7727-37-9	

Biotransformation

Name	Formula	MW	Purity	Supplier	CAS No.	Comments
Dipotassium hydrogenphosphate	K_2HPO_4	174.19	≥99%	Carl Roth	7758-11-4	
Sucrose	$C_{12}H_{22}O_{11}$	342.3	≥99.5%	Carl Roth	57-50-1	
Chlorzoxazone	$C_7H_4ClNO_2$	169.57		Sigma Aldrich	95-25-0	
DMSO	C_2H_6SO	78.13	≥99.8%	Carl Roth	67-68-5	
Trisodium citrate dihydrate	$C_6H_5O_7$, $2H_2O$ 3Na	294.1	≥99%	Carl Roth	6132-04-3	
Magnesium chloride hexahydrate	$MgCl_2 * 6\ H_2O$	203.3	≥99%	Carl Roth	7791-18-6	
NADP+*2 Na	$C_{21}H_{26}N_7Na_2O_{17}P_3$	787.4		Roche	24292-60-2	
Glucose	$C_6H_{12}O_6*H_2O$	198.17	≥99.5%	Carl Roth	14431-43-7	

GDH.002				DSM Innovative Synthesis BV		NADP 2.7 U/mg; NAD 3.4 U/mg
Methanol	CH_3OH	32.04	≥99%	Roth	67-56-1	
ACN	CH_3CN	41.05	HPLC Grade	J.T.Baker/ VWR	75-05-8	

Analysis

Name	Formula	MW	Purity	Supplier	CAS No.	Comments
ACN	CH_3CN	41.05	HPLC Grade	J.T.Baker/ VWR	75-05-8	
Methanol	CH_3OH	32.04	≥99%	Roth	67-56-1	
Formic acid	CH_2O_2	46.03	HPLC Grade	Fluka	64-18-6	

4.2.Solutions

Cultivation and expression

Media

- **1M PPB (Potassium Phosphate buffer) pH 6.0**
  KH_2PO_4 136.09 g
  Dissolve KH_2PO_4 in approx. 900 mL of ddH_2O. Adjust pH with KOH conc. Fill up to 1L with ddH_2O. Autoclave and store at rt.

- **10x YNB**
  YNB 67 g
  Dissolve in a final volume of 1L ddH_2O and autoclave. Store at +4 °C.

- **10X Dextrose (20 % Dextrose)**
  Dextrose 200 g
  Dissolve in a final volume of 1L deionized H_2O filter sterilize. Store at rt.

- **500x Biotin (0.02% Biotin)**
  Biotin 20 mg

  Dissolve in 100 ml of deionized water and filter sterilize. Store at +4°C. The shelf life of this solution is approximately one year.

- **BMD 1%**

1M PPB (Potassium Phosphate buffer) pH 6.0	200 mL
10x YNB (Yeast Nitrogen Base) solution	100 mL
10x Dextrose	50 mL
500x Biotin	2 mL
ddH_2O	650 mL

- **BMM10**

1M PPB (Potassium Phosphate buffer) pH 6.0	200 mL
10x YNB (Yeast Nitrogen Base)	100 mL
Methanol	50 mL

500x Biotin	2 mL
ddH_2O	650 mL

Harvest and Lyophilization

Stock solutions

- **1M KH_2PO_4**

KH_2PO_4	68.045 g
Deionized Water	fill up to 500 mL

- **1M K_2HPO_4**

K_2HPO_4	87.09 g
Deionized Water	fill up to 500 mL

Buffers

- **PPi (KPi) Buffer 100 mM, pH 7.4**

  Mix 80.2 mL of 1M K_2HPO_4 stock and 19.8 mL of 1M KH_2PO_4 stock and dilute combined stock solution to a final volume of 1000 mL of distilled water. Check pH and adjust if necessary.

  Autoclave and store at rt.

- **PS Buffer 100 mM pH 7.4**

KH_2PO_4	13.5 g
Sucrose	85.5 g
Deionized Water	fill up to 1000 mL

Adjust pH with KOH, autoclave and store at rt

Biotransformation

- **Reaction buffer: PS Buffer 100 mM pH 7.4**

KH_2PO_4	13.5 g
Sucrose	85.5 g
Deionized Water	fill up to 1000 mL

Adjust pH with KOH, autoclave and store at rt
Optional: in case of color change caused by autoclaving (strong yellow) prepare fresh buffer and sterile filter.

- **Stop solution: MeOH/ACN 1:1**

MeOH	50 mL
ACN	50 mL

Mix and store at room temperature.

Stock solutions

- **Substrate, 100 mM**

Chlorzoxazone	16.9 mg
DMSO	1 mL

Store at 4 °C

- **Trisodium citrate, 1 M**

Trisodium citrate dihydrate	14.7g
Deionized Water	50 mL

Filter sterilize and store at 4 °C

- **Magnesium chloride, 1 M**

Magnesium chloride hexahydrate	20.3 g
Deionized Water	100 mL

Filter sterilize and store at rt

- **$NADP^+$, 1 mM**

$NADP^+$	7.4 mg
Deionized Water	10 mL

Prepare freshly every time.

- **Glucose, 1 M**

Glucose	19.8 g
Deionized Water	100 mL

Autoclave and store at rt

- **Glucose dehydrogenase**

GDH	100 mg
Deionized Water	10 mL

The solution remains turbid. Prepare freshly every time.

Analysis

- **Aqueous mobile phase: formic acid 0.1%**

Formic acid	1 mL
Deionized Water	1000 mL

4.3. Materials

Name	Supplier	Order No.	Comments
Flask VK	Greiner Bio One	227261	
Baffled 2L flasks	Simax		
Disposable Cuvettes	Greiner Bio One	613101	
Syringes	Braun		
Syringe filters (0.22µm), CME sterile	Rotilabo		
Sterile loop	Simport	L200-2A	

Pipettes and pipette tips	Geiner Bio One	740290/ 739290	200 µl and 1000 µl volume tips
50 mL Falcon tubes	Geiner Bio One		
250/500 mL round bottom flasks	Schott		For lyophilisation
1.5 mL glass vials	Bruckner Analysentechnik	610002/ 610003	Alternative for lyophilisation
Gas permeable Adhesive Seals	Thermo Scientific	# AB-0718	
1.5 mL Reaction tubes	Sarstedt	72.690.001	For protein removal
Polypropylene Microtiter plates V-shaped bottom	Greiner Bio One	651201	
Adhesive seals	Greiner Bio One	676070	

4.4.Apparatus

Name	Supplier	Comments
Analytic scale	Sartorius Practum 124-15	
Orbital shaker	Infors AG	
Biophotometer to measure absorption at 600 nm	Eppendorf	
Beckmann Coulter Avanti J-20 XP		Rotor JA-10
alpha 1-4 lsc freeze dryer	Martin Christ Gefriertrocknungsanlagen GmbH	For lyophilisation with round bottom flasks only
Advantage Pro freeze-dryer	SP Scientific	See (Figure 2)
Orbital shaker HT orbitron	Infors AG	for 24 well plates
Eppendorf 5810 R	Eppendorf	
Eppendorf Thermomixer	Eppendorf	
1200 HPLC Series equipped with G1379B degasser, G1312B binary pump, SL G1367C HiP-ALS SL autosampler, G1314C VWD SL UV detector, G1316B TCC SL column oven and G1956B mass selective detector (MSD)	Agilent	Or alternative HPLC system, at least with UV detector
Kinetex 50x4.6 mm; 2.6u; C18; 100 Å HPLC column	phenomenex	P No.: 00B-4462-E0

4.6. Procedure

1. **Preculture**
    a. 20 mL of BMD 1 % in 50 mL Greiner flask
    b. To start the culture, use 20 µL of a glycerol stock of *K. phaffii*. Don't forget appropriate control strains.
    c. Incubate at 28 °C in a rotary shaker at approximately 100 rpm over night
2. **Main culture**
    a. 270 mL of BMD 1 % in 2 L baffled Erlenmeyer flask
    b. Add 2 mL of *K. phaffii* preculture
    c. Cultivate at 28 °C and approx. 120 rpm for 60 h
    d. After approximately 60 h cultivation induce CYP505 expression by the addition of 30 mL BMM10
    e. Incubate at 28 °C in a rotary shaker at approximately 120 rpm until cell harvest and induce according to the following time schedule:
        i. After approx. 70 h: induction with 3 mL MeOH
        ii. After approx. 93 h: induction with 1.5 mL MeOH
        iii. After approx. 117 h: induction with 1.5 mL MeOH
3. **Cell harvest**
   After 20 – 24 h after the last induction, the cells are harvested:
    a. Centrifuge the culture at 4,000 rpm at 4 °C for 15 min
    b. Discard supernatant and resuspend the pellet in 20 - 25 mL of ice cold KPi buffer, pH 7.4
    c. Centrifuge at 4,000 rpm at 4 °C for 15 min (use table top centrifuge)
    d. Repeat step b and c one time
    e. Discard supernatant and resuspend the pellet in 20 mL of PS buffer pH 7.4 (per g wet cell weight approximately 10 mL buffer)
    f. *Optional: to determine the activity of non-lyophilized cells skip 'Lyophilisation and storage'. Instead resuspend cells in PS buffer and freeze them for at least 1h at -20 °C to permeabilize them. Continue with 'Determination of oxidative activity (Biotransformation)*

4. **Lyophilisation and storage**
    a. Pipette portions of the cell suspensions e.g. into GC vials, deep-well plates or similar. Freeze with liquid nitrogen. Short storage at -80 °C is possible, if needed, preferably continue with b. immediately.
        i. ***Alternative:*** *If liquid nitrogen is not available it is possible to freeze the cells at -80°C for at least 1 hour. It is important to check whether the samples are frozen.*
    b. Lyophilize 24 well or deep well plates on the Advantage Pro freeze-dryer (Figure 2) under the following conditions: Use program 'CYP 505'; Approximately 30 min before the samples are ready, pre-freeze off shelf temperature -40 °C

XL

Program drying steps 1 - 6:

Temp	Ramp	Hold (min)
-40 °C	5	180
-20 °C	5	480
+10 °C	5	120
-20 °C	5	180
-40 °C	5	360

c. For lyophilization in GC vials, the detailed program is not necessary. Lyophilize ON with shelf temperature -40°C.
   i. ***Alternative***: *Transfer the cells to 250 or 500mL round bottom flask*
   ii. *Freeze the suspension in liquid nitrogen. Make sure that the surface of frozen cell suspension is maximal by turning the flask*
   iii. *Lyophilize on the Advantage Pro freeze-dryer (Figure 2) outer valves (Manifold) or any other freeze dryer for round bottom flasks*

d. Store lyophilized cells at -20 °C or -80 °C. The cells will retain activity for at least 40 days (prolonged storage currently under investigation).

Figure 2. Advantage Pro freeze-dryer. Use the chamber for plates or vials, and use the tabs for up to 4 round bottom flasks

5. Determination of oxidative activity (Biotransformation)

a. Resuspend lyophilized cells in Reaction buffer to OD_{600}=50 in 165 µL of reaction buffer in each well or vial
   i. *Optional*: increase cell density e.g. to OD_{600}=200
b. Add 10 µL of sodium citrate stock
c. Add 10 µL of $NADP^+$ stock
d. Add 2 µL of magnesium chloride stock
e. Add 2 µL of glucose stock
f. Add 1 µL of GDH stock
g. Start the reaction by addition of 10 µL of chlorzoxazone stock
h. Seal with Gas Permeable Adhesive Seal
i. Incubate at 28 °C and 120 rpm in an orbital shaker for 16 h.
j. Add 150 µL of a MeOH/ACN mix
k. Transfer mixture into a 1.5 mL Eppendorf vessel
l. Mix for 10 min in Eppendorf Thermomixer at rt and 700 rpm

m. Centrifuge for 5 min at maximum speed in a tabletop centrifuge
n. Transfer 200µL of the supernatant into wells of Polypropylene Microtiter plates
o. Seal with adhesive seal. Store at +4 °C if the samples are analyzed within 24h, otherwise freeze at -20 °C. Preferably analysis should be carried out on the same day.

6. Analysis

a. Prepare for HPLC analysis [insert correct column (Kinetex 50x4.6 mm; 2.6u; C18; 100 Å HPLC column for chlorzoxazone and many other APIs), purge Channel A1 with 0.1% aqueous formic acid, refill ACN on channel B2 when needed, clean spray unit, remove splitter if it is mounted]
b. Load method BAC_CHLORXOXAZONE_ROBOX_25".M or the respective substrate specific program and equilibrate the column until pressure and UV signal are constant. The details of the method are given here:
   i. Injection volume: 10µL
   ii. Flow: 1.000 mL/min
   iii. Solvent Gradient:

Time	% acetonitrile
0.00 min	0
1.00 min	0
4.00 min	100
5.00 min	100
5.01 min	0
6.00 min	0

   iv. Column temperature: 25 °C
   v. MSD settings: API/ES, Fast Scan mode, peak width 0.100 min, Cycle time 0.70 sec/cycle
      1. MSD1 Scan, Negative, Mass range 100-500, fragmentor 70, Gain 1, Threshold 150
      2. MSD2 SIM, Negative, SIM Ion 168.00, fragmentor 70, Gain 1, Dwell 140 ms
      3. MSD3 SIM, Negative, SIM Ion 184.00, fragmentor 70, Gain 1, Dwell 140 ms
c. Create Sequence Table and measure
d. Evaluate data using the UV trace (VWD1, wavelength 290 nm), see Figure 3.
   i. Go to 'Data analysis' mode in the Chemstation software
   ii. Choose datafile, choose VWD1A according to Figure 3

Figure 3: Screenshot of how to load the chromatogram in Data Analysis mode

iii. Choose 'Integration' mode and click on the peak with the arrow to mark the result in the table (Figure 4).

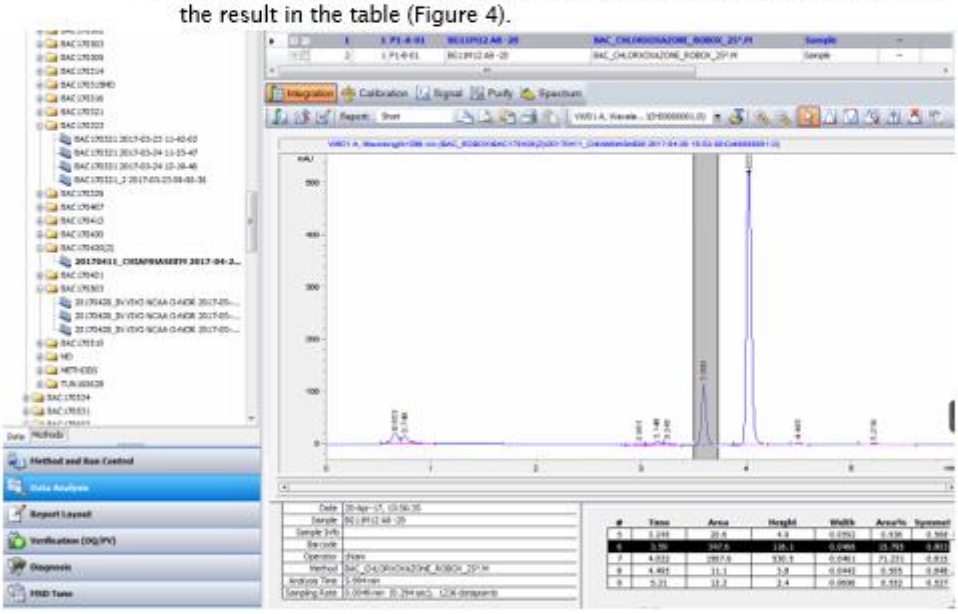

Figure 4: Screenshot of how to retrieve the peak area

iv. Correct integration manually, if necessary
v. Note that substrate and product must have similar absorption maxima, otherwise this 'area-normalization' method is misleading

e. ***Alternative**: if compounds are not baseline separated, use MS traces for data evaluation. MSD1 is typically SCAN, MSD2 is typically monitoring substrate (in positive mode: M+1, in negative mode: M-1). Note that quantification via MS signals may cause errors due to differences in ionizability of substrate and product. Moreover, signals are less reproducible, but you will get a trend. Do not understand such numbers as trustful quantitative values.*

7. Result examples

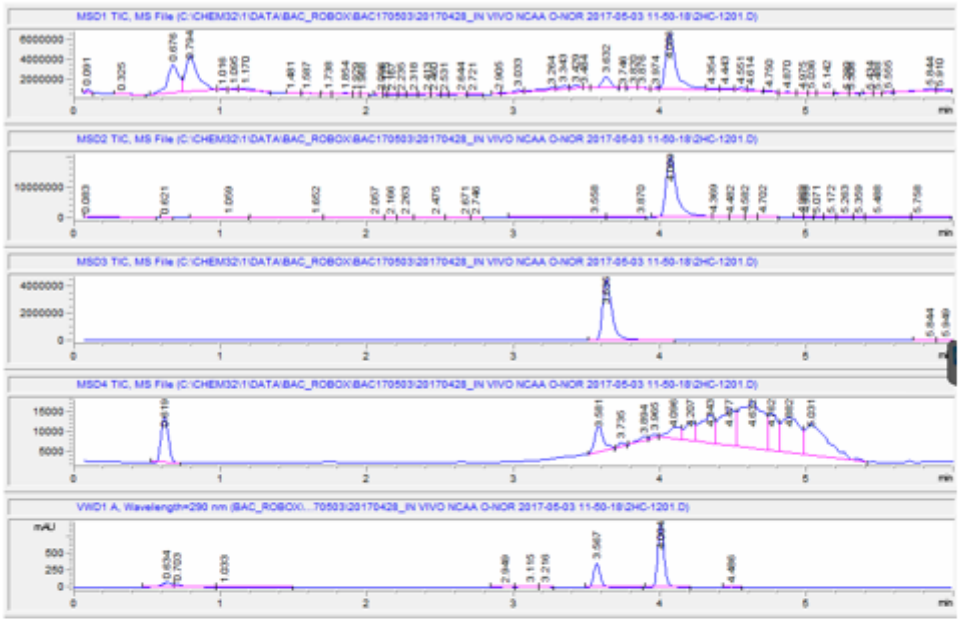

Figure 5: Example of CX biotransformation reaction. MSD1 corresponds to the SCAN mode. Clicking into the peaks will reveal their MS spectra in negative mode. MSD2 corresponds to the SIM (single ion monitoring) of the substrate in negative mode (the mass of CX is 169.57 g/mol, in negative mode, the ion with m/z of 168 is monitored). MSD3 corresponds to the SIM of the product in negative mode. MSD4 is useless in this case but offers the possibility to look for another ion for compound with multiple reaction possibilities. VWD1 corresponds to the UV signal at a wavelength of 290 nm (the optimum for CX). All chromatograms were integrated automatically.

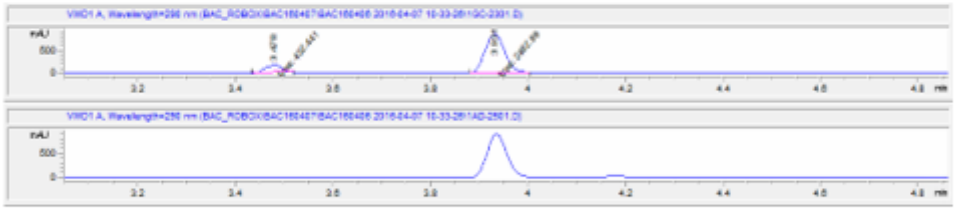

Figure 6 Two exemplary UV chromatograms of CX biotransformation reactions. Top: reaction with active mutant, bottom: reaction with inactive mutant. Hydroxychlorzoxazone elutes at approximately 3.5 min and CX at approximately 3.9 min.

4.7.Calculations

Use the following formula:
Conversion % = Area OH-CX * 100/(Area OH-CX + Area CX)
Using the numbers Figure 6: Conversion % = 432.44 * 100/(432.44 + 2482.99) = 14.8%

5. Safety Precautions

Please follow instructions described in "acib-Mitarbeiterleitfaden Gefahrstoff- und Laborordnung"

6. Documentation

All observations, protocol deviations and calculations must be recorded in the lab book

7. References

R. Weis, *et al. Adv. Syn. Catal.*, **2009**, *351(13)*, 2140ff

8. Acknowledgements

This work received funding from the EU project ROBOX (grant agreement n° 635734) under EU's H2020 Programme Research and Innovation actions H2020-LEIT BIO-2014-1 and from the Austrian BMWFJ, BMVIT, SFG, Standortagentur Tirol and ZIT through the Austrian FFG-COMET- Funding Program. Disclaimer: This publication reflects the author's view and the *Agency* is not responsible for any use that may be made of the information it contains.

This project is funded by the European Union

7.3 HPLC-METHODS

Table 14: HPLC method specifications for benzydamine

Benzydamine		BAC_BENZYDAMIN_ROBOX_25°C1.M				
Injection volume		10 µl				
Flow		1.1 ml/min				
Solvents		**A**			**B**	
		H_2O - 0.1 % formic acid			acetonitrile (ACN)	
Solvent gradient		**Time [min]**			**ACN %**	
		0.00			20	
		6.00			100	
		8.00			20	
Column		Kinetex 50x4.6 mm; 2.6µ C18; 100 Å (Phenomenex)				
Precolumn		SecurityGuard™ Ulltra Cartridges (AJ0-8775)				
Column temperature		25°C				
Substrate		Benzydamine (309.405 g/mol)				
Product(s)		no products detected by now				
Detection	**Trace**	**MSD1**	**MSD2**	**MSD3**	**MSD4**	**VWD1**
	Mode	SCAN	SIM	SIM	SIM	UV
	Signal polarity	pos	pos	pos	pos	pos
	Signal	100 - 450 Da	310 Da (M+1)	326 Da (M+16)	296 Da (M-14)	260 nm
Trace used for evaluation		UV				
Method for evaluation		Area normalization				
Retention time substrate		2.1 min				
Retention time product(s)		N/A				

Table 15: HPLC method specifications for caffeine

Caffeine		BAC_CAFFEINE_ROBOX_25°C.M				
Injection volume		10 µl				
Flow		1 ml/min				
Solvents		**A**			**B**	
		H_2O - 0.1 % formic acid			acetonitrile (ACN)	
Solvent gradient		**Time [min]**			**ACN %**	
		0.00			0	
		1.00			0	
		4.00			100	
		5.00			100	
		5.01			0	
		6.00			0	
Column		Kinetex 50x4.6 mm; 2.6µ C18; 100 Å (Phenomenex)				
Precolumn		SecurityGuard™ Ulltra Cartridges (AJ0-8775)				
Column temperature		25°C				
Substrate		Caffeine (194.19 g/mol)				
Product(s)		no products detected by now				
Detection	**Trace**	**MSD1**	**MSD2**	**MSD3**	**MSD4**	**VWD1**
	Mode	SCAN	SIM	SIM	SIM	UV
	Signal polarity	pos	pos	pos	pos	pos
	Signal	100 - 500 Da	195 Da (M+1)	181 Da (M-14)	211 Da (M+16)	275 nm
Trace used for evaluation		UV				
Method for evaluation		Area normalization				
Retention time substrate		3.28 min				
Retention time product(s)		N/A				

Table 16: HPLC method specifications for capsaicin

Capsaicin		BAC_CP_ROBOX_25°.M				
Injection volume		10 µl				
Flow		1 ml/min				
Solvents		**A**			**B**	
		H_2O - 0.1 % formic acid			acetonitrile (ACN)	
Solvent gradient		**Time [min]**			**ACN %**	
		0.00			0	
		1.00			0	
		4.00			100	
		5.00			100	
		5.01			0	
		6.00			0	
Column		Kinetex 50x4.6 mm; 2.6µ C18; 100 Å (Phenomenex)				
Precolumn		SecurityGuard™ Ulltra Cartridges (AJ0-8775)				
Column temperature		25°C				
Substrate		Capsaicin (305.41 g/mol)				
Product(s)		304 g/mol; 322 g/mol; 338 g/mol;				
Detection	**Trace**	**MSD1**	**MSD2**	**MSD3**	**MSD4**	**VWD1**
	Mode	SCAN	SIM	SIM	SIM	UV
	Signal polarity	pos	pos	pos	pos	pos
	Signal	100 - 500 Da	306 Da (M+1)	322 Da (M+16)	308 Da (M+3)	254 nm
Trace used for evaluation		UV				
Method for evaluation		Area normalization				
Retention time substrate		4.45 min				
Retention time product(s)		3.5 min	3.7 min	3.9 min	4.3 min	

Table 17: HPLC method specifications for chlorzoxazone

Chlorzoxazone		BAC_CHLORXOXAZONE_ROBOX_25°_POS.M				
Injection volume		10 µl				
Flow		1 ml/min				
Solvents		**A**			**B**	
		H_2O - 0.1 % formic acid			acetonitrile (ACN)	
Solvent gradient		**Time [min]**			**ACN %**	
		0.00			0	
		1.00			0	
		4.00			100	
		5.00			100	
		5.01			0	
		6.00			0	
Column		Kinetex 50x4.6 mm; 2.6µ C18; 100 Å (Phenomenex)				
Precolumn		SecurityGuard™ Ulltra Cartridges (AJ0-8775)				
Column temperature		25°C				
Substrate		Chlorzoxazone (169.57 g/mol)				
Product(s)		6-Hydroxychlorzoxazone (185.57 g/mol)				
Detection	**Trace**	**MSD1**	**MSD2**	**MSD3**	**MSD4**	**VWD1**
	Mode	SCAN	SIM	SIM	SIM	UV
	Signal polarity	pos	pos	pos	pos	pos
	Signal	100 - 500 Da	170 Da (M+1)	186 Da (M+16)	inactive	290 nm
Trace used for evaluation		UV				
Method for evaluation		Area normalization				
Retention time substrate		4 min				
Retention time product(s)		3.5 min				

Table 18: HPLC method specifications for clopidogrel

Clopidogrel		BAC_CLOPIDOGREL_ROBOX_25°C.M				
Injection volume		10 µl				
Flow		1 ml/min				
Solvents		**A**			**B**	
		H_2O - 0.1 % formic acid			acetonitrile (ACN)	
Solvent gradient		**Time [min]**			**ACN %**	
		0.00			30	
		1.00			30	
		4.00			100	
		5.50			100	
		5.51			30	
		6.50			30	
Column		Kinetex 50x4.6 mm; 2.6µ C18; 100 Å (Phenomenex)				
Precolumn		SecurityGuard™ Ulltra Cartridges (AJ0-8775)				
Column temperature		25°C				
Substrate		Clopidogrel (321.82 g/mol)				
Product(s)		OH-CLO (338 g/mol)				
Detection	**Trace**	**MSD1**	**MSD2**	**MSD3**	**MSD4**	**VWD1**
	Mode	SCAN	SIM	SIM	SIM	UV
	Signal polarity	pos	pos	pos	pos	pos
	Signal	100 - 500 Da	322 Da (M+1)	338 Da (M+16)	inactive	254 nm
Trace used for evaluation		UV				
Method for evaluation		Area normalization				
Retention time substrate		3.69 min				
Retention time product(s)		3.59 min				

Table 19: HPLC method specifications for dextromethorphan

Dextromethorphan		BAC_DEXTROMETHORPHAN_ROBOX_25°C.M				
Injection volume		10 µl				
Flow		1 ml/min				
Solvents		**A**			**B**	
		H_2O - 0.1 % formic acid			acetonitrile (ACN)	
Solvent gradient		**Time [min]**			**ACN %**	
		0.00			0	
		1.00			0	
		5.00			100	
		6.00			100	
		6.01			0	
		7.00			0	
Column		Kinetex 50x4.6 mm; 2.6µ C18; 100 Å (Phenomenex)				
Precolumn		SecurityGuard™ Ulltra Cartridges (AJ0-8775)				
Column temperature		25°C				
Substrate		Dextromethorphan (271.4 g/mol)				
Product(s)		OH-DEX (288 g/mol)				
Detection	**Trace**	**MSD1**	**MSD2**	**MSD3**	**MSD4**	**VWD1**
	Mode	SCAN	SIM	SIM	SIM	UV
	Signal polarity	pos	pos	pos	pos	pos
	Signal	100 - 600 Da	272 Da (M+1)	258 Da (M-14)	288 Da (M+16)	210 nm
Trace used for evaluation		MSD2, MSD4				
Method for evaluation		Area normalization				
Retention time substrate		3.9 min				
Retention time product(s)		3.8 min				

Table 20: HPLC method specifications for diclofenac

Diclofenac		BAC_DICLOFENAC_ROBOX_25°C.M				
Injection volume		10 µl				
Flow		1.3 ml/min				
Solvents		**A**			**B**	
		H_2O - 0.1 % formic acid			acetonitrile (ACN)	
Solvent gradient		**Time [min]**			**ACN %**	
		0.00			10	
		1.00			10	
		1.01			100	
		3.50			100	
		4.00			10	
Column		Kinetex 50x4.6 mm; 2.6µ C18; 100 Å (Phenomenex)				
Precolumn		SecurityGuard™ Ulltra Cartridges (AJ0-8775)				
Column temperature		25°C				
Substrate		Diclofenac (296.148 g/mol)				
Product(s)		OH-DIC (312 g/mol)				
Detection	**Trace**	**MSD1**	**MSD2**	**MSD3**	**MSD4**	**VWD1**
	Mode	SCAN	SIM	SIM	SIM	UV
	Signal polarity	pos	pos	pos	pos	pos
	Signal	100 - 400 Da	296 Da (M+1)	312 Da (M+16)	inactive	230 nm
Trace used for evaluation		UV				
Method for evaluation		Area normalization				
Retention time substrate		2.34 min				
Retention time product(s)		2.20 min				

Table 21: HPLC method specifications for estriol

Estriol		BAC_ES_ROBOX_25°_POS.M				
Injection volume		10 µl				
Flow		1 ml/min				
Solvents		**A**			**B**	
		H_2O - 0.1 % formic acid			acetonitrile (ACN)	
Solvent gradient		**Time [min]**			**ACN %**	
		0.00			20	
		1.00			20	
		4.00			100	
		5.00			100	
		5.01			20	
		6.00			20	
Column		Kinetex 50x4.6 mm; 2.6µ C18; 100 Å (Phenomenex)				
Precolumn		SecurityGuard™ Ulltra Cartridges (AJ0-8775)				
Column temperature		25°C				
Substrate		Estriol (288.38 g/mol)				
Product(s)		no products for the new experiments, older measurements (negative mode) showed metabolites				
Detection	**Trace**	**MSD1**	**MSD2**	**MSD3**	**MSD4**	**VWD1**
	Mode	SCAN	SIM	SIM	SIM	UV
	Signal polarity	pos	pos	pos	pos	pos
	Signal	200 - 500 Da	289 Da (M+1)	305 Da (M+16)	inactive	254 nm
Trace used for evaluation		(negative mode) MSD2, (negative mode) MSD3, (positive mode) UV				
Method for evaluation		Area normalization				
Retention time substrate		(negative mode) 3 min, (positive mode) 2.89 min				
Retention time product(s)		(negative mode): 3.3 min, (positive mode) N/A				

Table 22: HPLC method specifications for famciclovir

Famciclovir		BAC_FAMCICLOVIR_ROBOX.M				
Injection volume		10 µl				
Flow		1 ml/min				
Solvents		**A**		**B**		
		H_2O - 0.1 % formic acid		acetonitrile (ACN)		
Solvent gradient		**Time [min]**		**ACN %**		
		0.00		0		
		1.50		0		
		4.50		100		
		5.50		100		
		5.51		0		
		6.51		0		
Column		Kinetex 50x4.6 mm; 2.6µ C18; 100 Å (Phenomenex)				
Precolumn		SecurityGuard™ Ulltra Cartridges (AJ0-8775)				
Column temperature		25°C				
Substrate		Famciclovir (321.33 g/mol)				
Product(s)		280 g/mol (from esterase activity), 338 g/mol OH-FAM				
Detection	**Trace**	**MSD1**	**MSD2**	**MSD3**	**MSD4**	**VWD1**
	Mode	SCAN	SIM	SIM	SIM	UV
	Signal polarity	pos	pos	pos	pos	pos
	Signal	100 - 500 Da	322 Da (M+1)	338 Da (M+16)	280 Da (M-42)	304 nm
Trace used for evaluation		UV, MSD				
Method for evaluation		Area normalization				
Retention time substrate		(UV) 3.82 min, (MSD) 3.87 min				
Retention time product(s)		(UV): 3.59 min (280 g/mol), (MSD) 3.7 min; 3.8 min; 3.9 min (338 g/mol)				

Table 23: HPLC method specifications for harmine

Harmine		BAC_HARMINE_ROBOX.M				
Injection volume		10 µl				
Flow		1 ml/min				
Solvents		**A**		**B**		
		H_2O - 0.1 % formic acid		acetonitrile (ACN)		
Solvent gradient		**Time [min]**		**ACN %**		
		0.00		10		
		1.00		10		
		4.00		100		
		4.50		100		
		4.51		10		
		6.00		10		
Column		Kinetex 50x4.6 mm; 2.6µ C18; 100 Å (Phenomenex)				
Precolumn		SecurityGuard™ Ulltra Cartridges (AJ0-8775)				
Column temperature		25°C				
Substrate		Harmine (212.25 g/mol)				
Product(s)		no products detected by now				
Detection	**Trace**	**MSD1**	**MSD2**	**MSD3**	**MSD4**	**VWD1**
	Mode	SCAN	SIM	SIM	SIM	UV
	Signal polarity	pos	pos	pos	pos	pos
	Signal	100 - 500 Da	213 Da (M+1)	199 Da (M-14)	229 Da (M-42)	322 nm
Trace used for evaluation		UV				
Method for evaluation		Area normalization				
Retention time substrate		3.0 min				
Retention time product(s)		N/A				

Table 24: HPLC method specifications for hydrocortisone

Hydrocortisone		BAC_HC_ROBOX_25°.M				
Injection volume		10 µl				
Flow		1 ml/min				
Solvents		**A**			**B**	
		H_2O - 0.1 % formic acid			acetonitrile (ACN)	
Solvent gradient		**Time [min]**			**ACN %**	
		0.00			0	
		1.00			0	
		3.50			100	
		4.50			100	
		4.51			0	
		5.50			0	
Column		Kinetex 50x4.6 mm; 2.6µ C18; 100 Å (Phenomenex)				
Precolumn		SecurityGuard™ Ulltra Cartridges (AJ0-8775)				
Column temperature		25°C				
Substrate		Harmine (362.47 g/mol)				
Product(s)		OH-HYD (379 g/mol)				
Detection	**Trace**	**MSD1**	**MSD2**	**MSD3**	**MSD4**	**VWD1**
	Mode	SCAN	SIM	SIM	SIM	UV
	Signal polarity	pos	pos	pos	pos	pos
	Signal	200 - 500 Da	363 Da (M+1)	379 Da (M+16)	inactive	254 nm
Trace used for evaluation		UV				
Method for evaluation		Area normalization				
Retention time substrate		3.59 min				
Retention time product(s)		3.2 min		3.44 min		3.49 min

Table 25: HPLC method specifications for Ibuprofen

Ibuprofen		BAC_IBUPROFEN_ROBOX_POS.M				
Injection volume		10 µl				
Flow		1 ml/min				
Solvents		**A**			**B**	
		H_2O - 0.1 % formic acid			acetonitrile (ACN)	
Solvent gradient		**Time [min]**			**ACN %**	
		0.00			20	
		1.00			20	
		3.00			100	
		5.00			100	
		5.01			20	
		6.00			20	
Column		Kinetex 50x4.6 mm; 2.6µ C18; 100 Å (Phenomenex)				
Precolumn		SecurityGuard™ Ulltra Cartridges (AJ0-8775)				
Column temperature		25°C				
Substrate		Ibuprofen (206.29 g/mol)				
Product(s)		OH-Ibu (223 g/mol)				
Detection	**Trace**	**MSD1**	**MSD2**	**MSD3**	**MSD4**	**VWD1**
	Mode	SCAN	SIM	SIM	SIM	UV
	Signal polarity	neg	pos	pos	neg	pos
	Signal	100 - 500 Da	207 Da (M+1)	223 Da (M+16)	206 Da (M-1)	239 nm
Trace used for evaluation		UV				
Method for evaluation		Area normalization				
Retention time substrate		3.76 min				
Retention time product(s)		2.92 min		3.01 min		3.13 min

Table 26: HPLC method specifications for lidocaine

Lidocaine		BAC_LIDOCAINE_ROBOX_25°C.M				
Injection volume		10 µl				
Flow		1 ml/min				
Solvents		**A**			**B**	
		H_2O - 0.1 % formic acid			acetonitrile (ACN)	
Solvent gradient		**Time [min]**			**ACN %**	
		0.00			0	
		1.00			0	
		4.00			100	
		5.00			100	
		5.01			0	
		6.00			0	
Column		Kinetex 50x4.6 mm; 2.6µ C18; 100 Å (Phenomenex)				
Precolumn		SecurityGuard™ Ulltra Cartridges (AJ0-8775)				
Column temperature		25°C				
Substrate		Lidocaine (234.34 g/mol)				
Product(s)		OH-Lid (251 g/mol)				
Detection	**Trace**	**MSD1**	**MSD2**	**MSD3**	**MSD4**	**VWD1**
	Mode	SCAN	SIM	SIM	SIM	UV
	Signal polarity	pos	pos	pos	pos	pos
	Signal	100 - 500 Da	235 Da (M+1)	251 Da (M+16)	inactive	230 nm
Trace used for evaluation		UV				
Method for evaluation		Area normalization				
Retention time substrate		3.24 min				
Retention time product(s)		3.10 min				

Table 27: HPLC method specifications for moclobemide

Moclobemide		BAC_MOCLOBEMIDE_ROBOX_25°C.M				
Injection volume		5 µl				
Flow		1.1 ml/min				
Solvents		**A**			**B**	
		H_2O - 0.1 % formic acid			acetonitrile (ACN)	
Solvent gradient		**Time [min]**			**ACN %**	
		0.00			0	
		1.00			0	
		3.00			28	
		3.01			100	
		3.50			100	
		3.51			15	
		5.50			15	
Column		Kinetex 50x4.6 mm; 2.6µ C18; 100 Å (Phenomenex)				
Precolumn		SecurityGuard™ Ulltra Cartridges (AJ0-8775)				
Column temperature		25°C				
Substrate		Moclobemide (268.739 g/mol)				
Product(s)		no products detected by now				
Detection	**Trace**	**MSD1**	**MSD2**	**MSD3**	**MSD4**	**VWD1**
	Mode	SCAN	SIM	SIM	SIM	UV
	Signal polarity	pos	pos	pos	pos	pos
	Signal	100 - 450 Da	269 Da (M+1)	285 Da (M+16)	287 Da (M+18)	254 nm
Trace used for evaluation		UV				
Method for evaluation		Area normalization				
Retention time substrate		3.45 min				
Retention time product(s)		N/A				

Table 28: HPLC method specifications for naphthol

Naphthol		BAC_NAPHTOL_ROBOX.M				
Injection volume		10 µl				
Flow		1 ml/min				
Solvents		**A**			**B**	
		H_2O - 0.1 % formic acid			acetonitrile (ACN)	
Solvent gradient		**Time [min]**			**ACN %**	
		0.00			0	
		1.00			0	
		4.00			100	
		5.00			100	
		5.01			0	
		6.00			0	
Column		Kinetex 50x4.6 mm; 2.6µ C18; 100 Å (Phenomenex)				
Precolumn		SecurityGuard™ Ulltra Cartridges (AJ0-8775)				
Column temperature		25°C				
Substrate		2-Naphtol (144.17 g/mol)				
Product(s)		Acetominaphen (152 g/mol), OH-Phe (196 g/mol)				
Detection	**Trace**	**MSD1**	**MSD2**	**MSD3**	**MSD4**	**VWD1**
	Mode	SCAN	SIM	SIM	SIM	UV
	Signal polarity	neg	pos	pos	neg	pos
	Signal	100 - 500 Da	145 Da (M+1)	161 Da (M+16)	177 Da (M+16)	232 nm
Trace used for evaluation		UV				
Method for evaluation		Area normalization				
Retention time substrate		4.17 min				
Retention time product(s)		3.37 min		3.6 min		3.90 min

Table 29: HPLC method specifications for phenacetin

Phenacetin		BAC_PHENACETIN_ROBOX_MS_25°C2.M				
Injection volume		10 µl				
Flow		1 ml/min				
Solvents		**A**			**B**	
		H_2O - 0.1 % formic acid			acetonitrile (ACN)	
Solvent gradient		**Time [min]**			**ACN %**	
		0.00			0	
		1.00			0	
		3.00			100	
		3.01			0	
		5.00			0	
Column		Kinetex 50x4.6 mm; 2.6µ C18; 100 Å (Phenomenex)				
Precolumn		SecurityGuard™ Ulltra Cartridges (AJ0-8775)				
Column temperature		25°C				
Substrate		Phenacetin (179.216 g/mol)				
Product(s)		Acetominaphen (152 g/mol), OH-Phe (196 g/mol)				
Detection	**Trace**	**MSD1**	**MSD2**	**MSD3**	**MSD4**	**VWD1**
	Mode	SCAN	SIM	SIM	SIM	UV
	Signal polarity	neg	pos	pos	pos	pos
	Signal	100 - 500 Da	180 Da (M+1)	152 Da (M-28)	196 Da (M+16)	245 nm
Trace used for evaluation		UV				
Method for evaluation		Area normalization				
Retention time substrate		3.40 min				
Retention time product(s)		3.06 min			3.09 min	

Table 30: HPLC method specifications for piperine

Piperine		BAC_PI_ROBOX_25°.M				
Injection volume		10 µl				
Flow		1 ml/min				
Solvents		**A**			**B**	
		H_2O - 0.1 % formic acid			acetonitrile (ACN)	
Solvent gradient		**Time [min]**			**ACN %**	
		0.00			20	
		1.00			20	
		4.00			100	
		5.00			100	
		5.01			20	
		6.00			20	
Column		Kinetex 50x4.6 mm; 2.6µ C18; 100 Å (Phenomenex)				
Precolumn		SecurityGuard™ Ulltra Cartridges (AJ0-8775)				
Column temperature		25°C				
Substrate		Piperine (285.34 g/mol)				
Product(s)		OH-PIP (302 g/mol)				
Detection	**Trace**	**MSD1**	**MSD2**	**MSD3**	**MSD4**	**VWD1**
	Mode	SCAN	SIM	SIM	SIM	UV
	Signal polarity	neg	pos	pos	neg	pos
	Signal	200 - 500 Da	286 Da (M+1)	302 Da (M+16)	274 Da (M-12)	254 nm
Trace used for evaluation		UV				
Method for evaluation		Area normalization				
Retention time substrate		4.38 min				
Retention time product(s)		3.97 min				

Table 31: HPLC method specifications for progesterone

Progesterone		BAC_PROGESTERON_ROBOX_25°C.M				
Injection volume		10 µl				
Flow		1 ml/min				
Solvents		**A**			**B**	
		H_2O - 0.1 % formic acid			acetonitrile (ACN)	
Solvent gradient		**Time [min]**			**ACN %**	
		0.00			20	
		2.50			75	
		4.50			75	
		4.60			20	
		6.00			20	
Column		Kinetex 50x4.6 mm; 2.6µ C18; 100 Å (Phenomenex)				
Precolumn		SecurityGuard™ Ulltra Cartridges (AJ0-8775)				
Column temperature		25°C				
Substrate		Progesterone (314.47 g/mol)				
Product(s)		OH-PRO (331 g/mol)				
Detection	**Trace**	**MSD1**	**MSD2**	**MSD3**	**MSD4**	**VWD1**
	Mode	SCAN	SIM	SIM	SIM	UV
	Signal polarity	pos	pos	pos	pos	pos
	Signal	100 - 500 Da	315 Da (M+1)	331 Da (M+16)	349 Da (M+35)	290 nm
Trace used for evaluation		MSD2, MSD3				
Method for evaluation		Area Normalization				
Retention time substrate		4.8 min				
Retention time product(s)		3.5 min		3.8 min		4.0 min

Table 32: HPLC method specifications for propranolol

Propranolol		BAC_PROPRANOLOL_ROBOX_25°C.M				
Injection volume		10 µl				
Flow		1 ml/min				
Solvents		**A**			**B**	
		H_2O - 0.1 % formic acid			acetonitrile (ACN)	
Solvent gradient		**Time [min]**			**ACN %**	
		0.00			0	
		5:00			100	
		5.50			100	
		5.51			0	
		7.00			0	
Column		Kinetex 50x4.6 mm; 2.6µ C18; 100 Å (Phenomenex)				
Precolumn		SecurityGuard™ Ulltra Cartridges (AJ0-8775)				
Column temperature		25°C				
Substrate		Propranolol (259.34 g/mol)				
Product(s)		OH-PPL (276 g/mol)				
Detection	**Trace**	**MSD1**	**MSD2**	**MSD3**	**MSD4**	**VWD1**
	Mode	SCAN	SIM	SIM	SIM	UV
	Signal polarity	pos	pos	pos	pos	pos
	Signal	100 - 600 Da	260 Da (M+1)	276 Da (M+16)	172 Da (M-88)	260 nm
Trace used for evaluation		UV				
Method for evaluation		Area Normalization				
Retention time substrate		3.04 min				
Retention time product(s)		2.90 min				

Table 33: HPLC method specifications for salbutamol

Salbutamol		BAC_SALBUTAMOL_ROBOX_25°C.M				
Injection volume		10 µl				
Flow		1 ml/min				
Solvents		**A**			**B**	
		H_2O - 0.1 % formic acid			acetonitrile (ACN)	
Solvent gradient		**Time [min]**			**ACN %**	
		0.00			0	
		1.00			0	
		4.00			100	
		5.00			100	
		5.01			0	
		6.00			0	
Column		Kinetex 50x4.6 mm; 2.6µ C18; 100 Å (Phenomenex)				
Precolumn		SecurityGuard™ Ulltra Cartridges (AJ0-8775)				
Column temperature		25°C				
Substrate		Salbutamol (239.311 g/mol)				
Product(s)		No products detected by now				
Detection	**Trace**	**MSD1**	**MSD2**	**MSD3**	**MSD4**	**VWD1**
	Mode	SCAN	SIM	SIM	SIM	UV
	Signal polarity	pos	pos	pos	pos	pos
	Signal	100 - 500 Da	240 Da (M+1)	256 Da (M+16)	inactive	277 nm
Trace used for evaluation		UV				
Method for evaluation		Area Normalization				
Retention time substrate		3.06 min				
Retention time product(s)		N/A				

Table 34: HPLC method specifications for testosterone

Testosterone		BAC_TESTOSTERONE_MATIC_25°C.M				
Injection volume		10 µl				
Flow		1 ml/min				
Solvents		**A**			**B**	
		H_2O - 0.1 % formic acid			acetonitrile (ACN)	
Solvent gradient		**Time [min]**			**ACN %**	
		0.00			20	
		1.00			20	
		3.00			100	
		5.00			100	
		5.01			20	
		6.00			20	
Column		Kinetex 50x4.6 mm; 2.6µ C18; 100 Å (Phenomenex)				
Precolumn		SecurityGuard™ Ulltra Cartridges (AJ0-8775)				
Column temperature		25°C				
Substrate		Testosterone (288.43 g/mol)				
Product(s)		OH-TES (305 g/mol)				
Detection	**Trace**	**MSD1**	**MSD2**	**MSD3**	**MSD4**	**VWD1**
	Mode	SCAN	SIM	SIM	SIM	UV
	Signal polarity	pos	pos	pos	pos	pos
	Signal	200 - 400 Da	289 Da (M+1)	305 Da (M+16)	287 Da (M-2)	240 nm
Trace used for evaluation		UV				
Method for evaluation		Area normalization				
Retention time substrate		3.48 min				
Retention time product(s)		2.76 min		3.16 min		

Table 35: HPLC method specifications for tolbutamide

Tolbutamide		BAC_TOLBUTAMIDE_ROBOX_25°C.M				
Injection volume		10 µl				
Flow		1 ml/min				
Solvents		**A**			**B**	
		H_2O - 0.1 % formic acid			acetonitrile (ACN)	
Solvent gradient		**Time [min]**			**ACN %**	
		0.00			10	
		1.00			10	
		3.00			100	
		4.00			100	
		4.01			10	
		5.50			10	
Column		Kinetex 50x4.6 mm; 2.6µ C18; 100 Å (Phenomenex)				
Precolumn		SecurityGuard™ Ulltra Cartridges (AJ0-8775)				
Column temperature		25°C				
Substrate		Tolbutamide (270.35 g/mol)				
Product(s)		OH-TOL (287 g/mol)				
Detection	**Trace**	**MSD1**	**MSD2**	**MSD3**	**MSD4**	**VWD1**
	Mode	SCAN	SIM	SIM	SIM	UV
	Signal polarity	pos	pos	pos	pos	pos
	Signal	200 - 400 Da	271 Da (M+1)	287 Da (M+16)	inactive	230 nm
Trace used for evaluation		UV				
Method for evaluation		Area normalization				
Retention time substrate		3.16 min				
Retention time product(s)		2.78 min				